Production of High-Value-Added Chemicals and High-performance Catalysts from Lignin

Irwan Kurnia

A Dissertation Submitted in Partial Fulfillment of the Requirements for the Degree of Doctor of Philosophy in Engineering

GRADUATE SCHOOL OF SCIENCE AND TECHNOLOGY

HIROSAKI UNIVERSITY

2020

Abstract

The growing global population leads to an increasing demand for fossil-based fuels and chemicals, resulting in many societal problems, including energy security and environmental pollutions. Therefore, development of environmentally friendly fuels, chemical feedstocks, and materials becomes more and more important. Lignin is the largest natural and renewable source of aromatics. Industrial lignin is largely produced as the byproduct, especially in paper and pulping industries and in biorefinery processes. Utilization of lignin wastes would solve the issues related to the reduction of environmental impacts of the paper-making process and other delignification processes on the environmental burden. To date, many researches have focused on the production of high-value-added chemicals and development of lignin-derived functional materials, catalyst support, and carbon-based catalysts. In this dissertation work, a kind of zeolite-based catalyst was found to be effectively catalytic upgrading of lignin-derived bio-oils, and meanwhile, the lignosulfonate lignin was successfully applied as a precursor to prepare high-performance catalysts for hydrogen production from decomposition of formic acid and weak-acid carbon-based catalysts for the hydrolysis of cellulose and woody biomass as well as for the cyclization citronellal to produce p-menthane-3,8-diol. It includes 6 Chapters.

Firstly, *in-situ* catalytic upgrading of bio-oil during the fast pyrolysis of lignin over five types of high aluminum zeolites, i.e., H-Ferrierite, H-Mordenite, H-ZSM-5, H-Beta and H-USY zeolites, were performed. It is found that the channel structure, pore sizes and acidity of zeolite had great effect on the product distribution, coke formation, and deoxygenation. The highest yield of light oil was obtained by using H-ZSM-5 zeolite and the highest selectivity toward monoaromatic hydrocarbons was achieved by H-Beta zeolite. This study could provide

a guidance for the selection of suitable zeolite for the *in-situ* catalytic deoxygenation of bio-oil derived from fast pyrolysis of lignin.

Secondly, based on the high char product produces in fast pyrolysis of lignin (52.2 wt%), dealkaline lignin (DAL) was used as a carbon and sulfur source to prepare MoS_2/Mo_2C based catalysts (Mo-DAL) with a facile impregnation-pyrolysis two-step process for the hydrogen production from the formic acid decomposition. Comparison of the catalytic performance of the Mo-DAL catalyst with the carbon black-based one (Mo_2C-CB) revealed that the Mo-DAL catalyst exhibited superior activity to the Mo_2C-CB catalyst. When 20 wt% of Mo was loaded on DAL, the catalyst produced hydrogen quite selectively (99.2%) with almost complete conversion of formic acid (97.4%) at 220 °C. In addition, the catalyst showed stable activity for at least 50 hours in these conditions. These catalytic activity and hydrogen selectivity are superior to the other reported non-precious metal catalysts. Since DAL contains not only carbon but also sodium and sulfur species, multiple kinds of active sites such as Na-intercalated MoS_2, MoS_2, and β-Mo_2C were formed on the Mo-DAL catalysts. Investigation of additional effects of sulfur and sodium species on the Mo-CB catalyst revealed that both activity and selectivity for H_2 production was improved by adding those elements. Thus, this study provides a new viewpoint to utilize waste dealkaline lignin as a precursor of sustainable and selective precious metal-free hydrogen production catalysts for formic acid decomposition.

Thirdly, since the original structure of neutralized lignosulfonate lignin (alkaline lignin, pH 10) contains the phenolic hydroxyl groups, carboxyl groups, and SO_3H groups. Alkaline lignin (AL) can be utilized as low-cost and sustainable weak-acid carbon catalysts which is prepared by pyrolysis of AL followed by an acid solution treatment process, and applied for the hydrolysis of cellulose and woody biomass. The effect of pyrolysis temperature on the acidity

of the final carbon catalyst was investigated. It is found that the AL-derived carbon catalysts at the pyrolysis temperature of 450 °C (denoted as AL-Py-450) exhibited the highest activity in the hydrolysis of ball-milled cellulose with a cellulose conversion of 70.8% and a glucose yield of 46.3% in a neat water reaction system. Furthermore, with the addition of 0.012 wt% hydrochloric acid (HCl) in the above reaction system, the cellulose conversion was increased to 96.1% with a glucose yield of 69.8%. In the same reaction conditions, the AL-Py-450 carbon catalyst also exhibited good catalytic activity for the hydrolysis of lignocellulosic biomass, i.e., Japanese cedar wood, with yields of glucose and xylose of 47.1% and 40.3%, respectively. Therefore, this study could provide a new perspective to utilize the wasted alkaline lignin as a source for the preparation of sustainable weak-acid carbon catalysts for the hydrolysis of cellulose and lignocellulosic biomass.

Finally, the AL-derived carbon catalysts were also applied for cyclization citronellal to produce p-menthane-3,8-diol(PMD), which is a natural mosquito repellent with lower toxicity than the widely-used *N*,*N*-diethyl *m*-toluamide (DEET). Especially, the carbon catalysts obtained by pyrolysis at 500 °C showed 97 % high conversion of (±) citronellal with a 86 % high PMD yield. In addition, it is found that the citronellal cyclization-hydration reaction via carbocation-hydration pathway rather than isopulegol hydration route over such an AL-derived carbon catalyst.

Acknowledgments

Firstly, the most profound gratitude is expressed to my supervisor, Professor Dr. Guoqing Guan, for giving an opportunity to do doctoral researches and as the member of his research group. The sincere gratitude to him for providing full support with his advices and guidance both academically and personally.

I also would like thank to Professor Dr. Abuliti Abudula, Graduate School of Science and Technology, Hirosaki University, for all the comments and advices during our discussion in group meetings.

Sincere appreciation is expressed to Associate Professor Dr. Akihiro Yoshida for providing supports, advices, and guidance on experiments and scientific paper writing.

I would like to acknowledge the scholarship from the Ministry of Education, Culture, Sport, Science, and Technology (MEXT) of Japan (Monbukagakusho) for providing the scholarship during my PhD study in Hirosaki University, Japan.

Special thanks to my parents for their support and supplication in every prayer. This work also dedicated to my beloved father that passed away when I was studying Ph.D. in the second year. Deep regret that I did not accompany him while in his struggling situation. The sincere gratitude and appreciation to my wife, Siti Prita Fitrianti, for her patience and always motivate me to give my best effort in every moment, especially in research activities. To my beloved son, Alfahiro Yusuf Kurnia, thank you for teaching me to appreciate the quality time with family, even it is in a short time.

Finally, I gratefully acknowledge to The Only One, for guiding me in every decision in my life, and for inviting local people friends to my family that support us during the stay in Aomori, Japan, which made it feels like home.

Irwan Kurnia

March 2020

Aomori, Japan

Table of Content

List of Tables

List of Figures

List of Schemes

List of Equations

Chapter 1 Introduction

1.1 High-Value Added Chemicals and Materials from Lignin

1.1.1 Lignin as a prospect of fuel, chemical, and material

The high dependency of society toward petroleum industry and the associated environmental impact such as arising of global climate change, and environmental pollution, have made us pay more attentions to develop environmentally friendly fuels, chemicals, and materials. The lignocellulosic biomass has been acknowledged as the most logical and abundant carbon-based feedstock to substitute fossil-based raw materials. Lignocellulosic biomass consists of three primary components, i.e., cellulose, hemicellulose, and lignin. Among them, Lignin is the second-largest renewable source (15–30%) after cellulose (30–50%). Unlike cellulose and hemicellulose, the use of lignin has no effect on food supply since it is non-edible. Moreover, lignin is the largest natural sources of aromatics and the only scalable and renewable feedstock composed of aromatic monomers [1-3]. Annually, about 5–36 10^8 tons of lignin were produced, in which about 70 million tons of it is commercial lignin. Mostly, industrial lignin is produced as byproduct in paper and pulping and biorefinery industries. Therefore, the utilization of lignin waste would be related to problem-solving to reduce environmental impacts of the paper-making process and other delignification processes [3-5].

Lignin is inexpensive and possesses numerous attractive properties, such as high carbon content, high thermal stability, biodegradability, antioxidant activity and favorable stiffness [6-8]. These advantages have motivated interest in converting lignin into value-added products for various applications. However, the brittle nature of lignin and its incompatibility with other polymer systems have led to little success in creating lignin-based high performance materials [6,9]. Furthermore, it is also an attractive feedstock for the production of biofuels and chemicals. Notably,

the aromatic structure of lignin gifts the potential for the direct preparation of aromatic specialty and fine chemicals. For example, benzene, toluene, and xylenes (BTX) can be produced from it, which can be further rebuilt to the desired platform chemicals. Nevertheless, owing to challenges associated with effective separation of oxygenated aromatics via distillation or other means, full defunctionalization to aromatic hydrocarbon and alkanes will also be of importance for the production of chemicals and fuel components from lignin and its products [10]. On the other hand, a great deal of researches focused on the development of lignin-derived functional materials, catalyst supports, and carbon catalysts, and these have been received growing attention as alternative ways to use the lignin residues in the lignin refinery processes.

1.1.2 Lignin structure

Lignin has a large and complex polymer structure containing methoxyl groups, phenolic hydroxyl groups, and aldehyde functional groups in the side structures of lignin. The differences among the structures of lignin in various plants are based on the linkages formed between the phenylpropanoid lignin monomers. Especially, three aromatic alcohols units, i.e., *p*-coumaryl, coniferyl, and sinapyl (Figure 1.1) existed in it. In the lignin macromolecule, these monomeric units are linked by variety of carbon-oxygen and carbon-carbon bonds such as aryl ether (α-O-4′ and β-O-4′), resinol (β-β′), phenylcoumaran (β-5′), biphenyl (5-5′), and 1,2- diaryl propane (β-1′), as shown in Figure 1.2 [11]. The main lignin linkages are differently distributed according to the type of wood: the β-O-4 ether linkage is the most important one in softwood (50%) and in hardwood (60%). The 4-O-5 and α-O-4 aryl ether bonds are less predominant (around 5 and 8% for both types of wood, respectively). Biphenyl linkages 5-5 (18%), phenylcoumaran β-5 (11%), diarylpropane β-1 (7%) and β– β (2%) are also present with less amounts [12]. The bond

dissociations enthalpies in lignin structure had been calculated, and it is found that the ether linkages are easier to cleave when compared to C-C bonds [13].

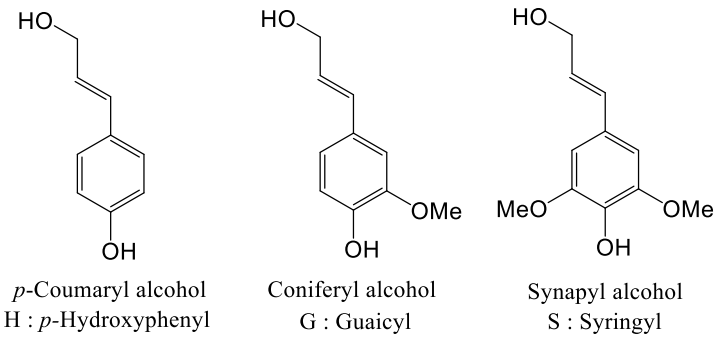

Figure 1.1 Three standard monolignol monomers.

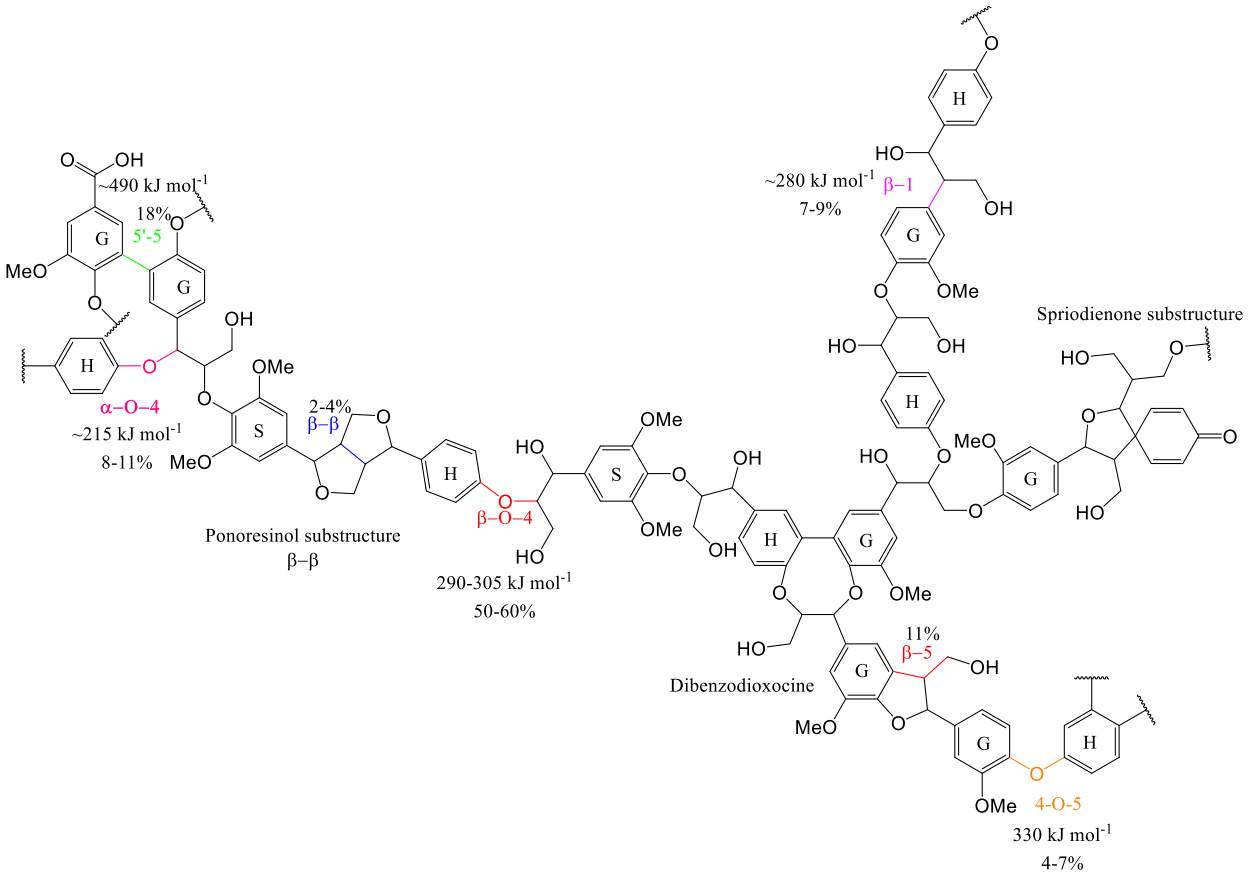

Figure 1.2 Structure and energy bonding of lignin [14].

1.1.3 Lignin fractionation

To date, either industrial or lab-scaled processes for the isolating of lignin from lignocellulosic biomass have been developed. All the isolation methods have the same purpose. That is to degrade the polymeric lignin structure until the resulting fragments become soluble in the pulping media by chemical treatment. Depending on the method, the properties of the isolated lignin would be different. The main factors in the success of each process include the pH of the system, the ability of the solvent and/or solute to participate in lignin fragmentation, the ability of the solvent and/or solute to prevent lignin recondensation, and the ability of the solvent to dissolve lignin fragments [15]. Currently, there are four industrial processes are used to isolate lignin, which can be divided into two categories based on the fact whether the resulting product contains sulfur or not. Lignin isolated from the sulfite and kraft processes usually contains sulfur whereas no sulfur is contained in the lignin isolated from the soda and organosolv process (Figure 1.3) [16].

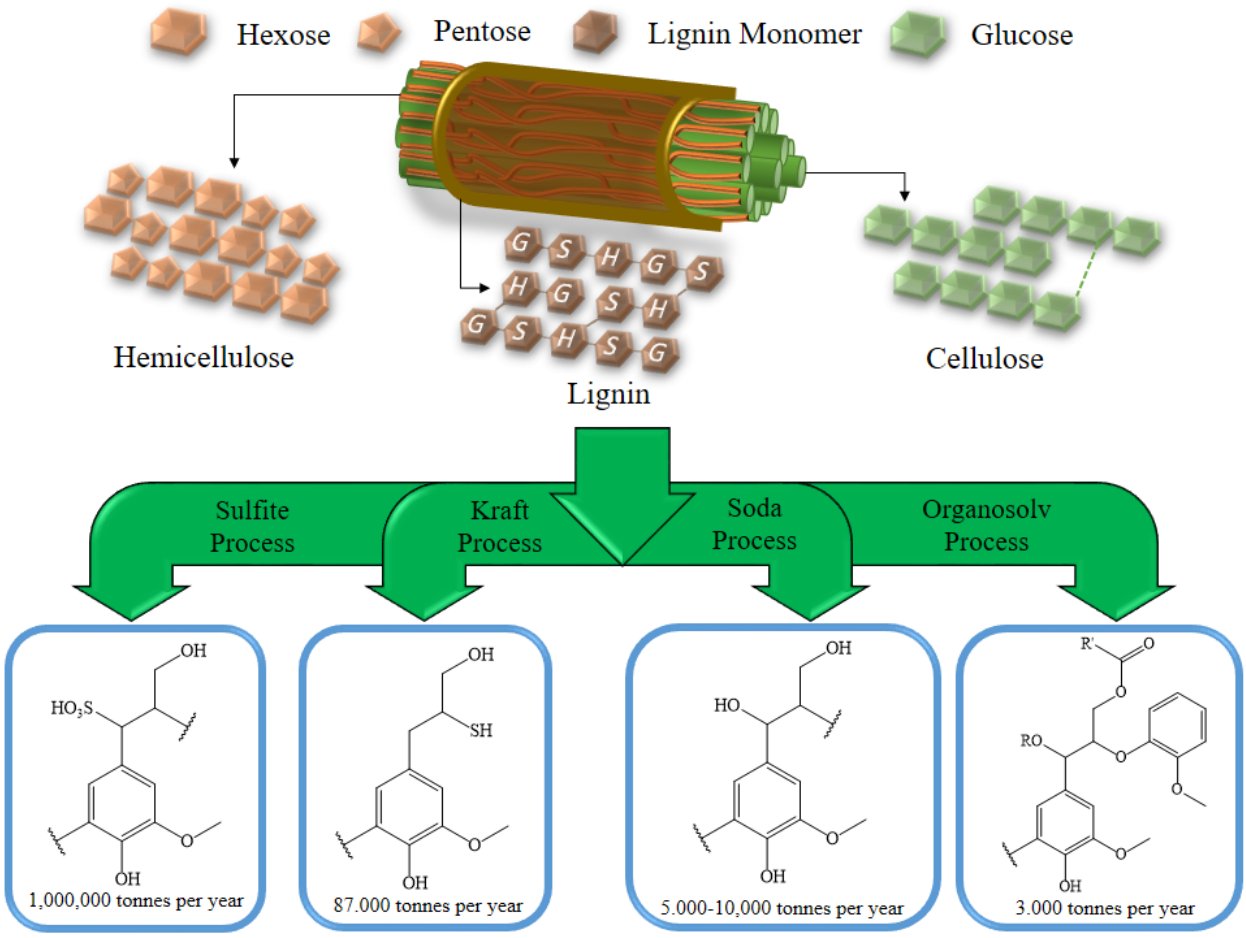

Figure 1.3 Extraction processes and commercial production of lignin.

1.1.3.1 Sulfite process

Approximately one million ton of lignin is produced by a sulfite process every year [16]. Sulfite pulping is a process that uses a heated aqueous solution of a sulfite or bisulfite salt with countercations such as sodium, ammonium, magnesium, or calcium [17]. Depending on the cation and its solubility in aqueous solutions, the resulting pH of the solution varies in the range of 1-13.5, which can be a criterion for the choice of either cation or anion. The reaction purpose of the sulfite process is the sulfonation of the aliphatic lignin chain, which occurs in different locations depending on the pH of the pulping solution. Furthermore, the resulting lignosulfonate is water-soluble and could be dissolved in the aqueous pulping liquor with hemicellulose. To isolate lignin

from this aqueous mixture, other techniques such as precipitation, ultrafiltration, chemical destruction of sugars, or alcohol fermentation of sugars followed by distillation of fermentation product must be used [18].

1.1.3.2 Kraft process

The kraft process also generates sulfated lignin, and its products are rarely used in chemical or material production but burned as energy for pulping mills. Approximately 60 kilotons of the kraft lignin is produced every year [16]. In this process, the biomass feedstock is added to a mixture of sodium hydroxide and sodium sulfide and heated in the range of 150-180 °C. Lignin is depolymerized by cleaving of α and β ether bonds to increase solubility of the fragments. Herein, the mechanism is the same as the soda process. In the presence of hydrosulfide anions, only a small portion of the resulting lignin would be sulfated, allowing isolation of the lignin through acidification and precipitation. Isolation of lignin from this process has been enhanced by a LignoBoost technology [19], in which CO_2 was used as an acid for precipitation and a double slurry and washing process with H_2SO_4 to maximize the quantity and purity of lignin isolated from the black liquor. Every year, about 87 kilotons of lignin is produced by these two processes [16].

1.1.3.3 Soda process

The soda process is typically for nonwood-based biomass sources such as sugar cane or flax. During the soda process, the biomass is added to an aqueous solution of sodium hydroxide and then heated to 160 °C. The depolymerization of lignin occurs with the cleavage of α and β ether bonds, resulting in the generation of free phenolic groups. The resulting lignin fragments are water-soluble and easily to be isolated from the pulping liquor through precipitation by acidified the solution. Lignin isolated by this method has a higher purity than that obtained by the sulfite process

but is much lower in molecular weight [18]. Annually, about 5-10 kilotons of lignin is produced by this process [16]

1.1.3.4 Organosolv process

The organosolv process has emerged in the recent year as an industrial-scale method for lignin isolation. This method utilizes an aqueous-organic solvent mixture such as ethanol, acetone, methanol, or organic acids (acetic or formic acid), then heated it to the desired temperature for the isolating streams of hemicellulose, cellulose, and lignin [20]. This acidic method is more advantageous since the isolation of all three components would be realized simultaneously. It is also seen as environmentally friendly way due to no sulfur involving with no high temperature, and no high pressure. While the organosolv process has yet led the market in production, this method would be possible to replace the kraft lignin production method, and especially it can yield each biomass component in relatively high purity. However, the recovery of spent solvent is still not optimized in the organosolv process, making the cost of this approach relatively high compared to other methods. Thus, only approximately 3 kilotones of lignin is produced every year, which is relatively lower than other isolation methods [16].

1.1.4 Thermochemical process

Degradation and conversion of lignin can be achieved by thermochemical treatments, which include the thermal treatment of lignin in the presence or absence of some solvents, chemical additives and catalysts. Figure 1.4 summarizes the major thermochemical lignin conversion processes. Pyrolysis represents the thermal treatment of the biomass or lignin in the absence of oxygen, with or without any catalyst [21]. Pyrolysis converts lignin to solid char, liquid oil, and gases, and the proportion of which depends primarily on temperature and heating rate [21]. The

composition of the product and the yield of individual compounds depend on the lignin source and the isolation methods. Softwood lignin contains a dominance of guaiacyl units while hardwood lignin has the similar amounts of guaiacyl and syringyl units [22]. Hydrogenolysis or hydrocracking involves thermal treatment in the presence of hydrogen so that the cleavage of bonds is assisted by the addition of hydrogen [23]. Hydrolysis is the process in which water is used to break down the large molecules [24]. Hydrogenolysis is generally accomplished at lower temperatures and, hence, favors higher yields of liquid including monomeric phenols. Gasification converts lignin or biomass to gases [21]. The major products from lignin gasification include H_2, CO, CO_2, and CH_4 [25]. Oxidation represents thermal treatment in the presence of oxygen and is primarily important for the conversion of lignin to aldehydes [26]. Yields and composition of degradation products vary based on the process type and the conditions applied. In addition, the nature of lignin, its composition and various functional groups also have significant effects on the lignin conversion and the yield of product.

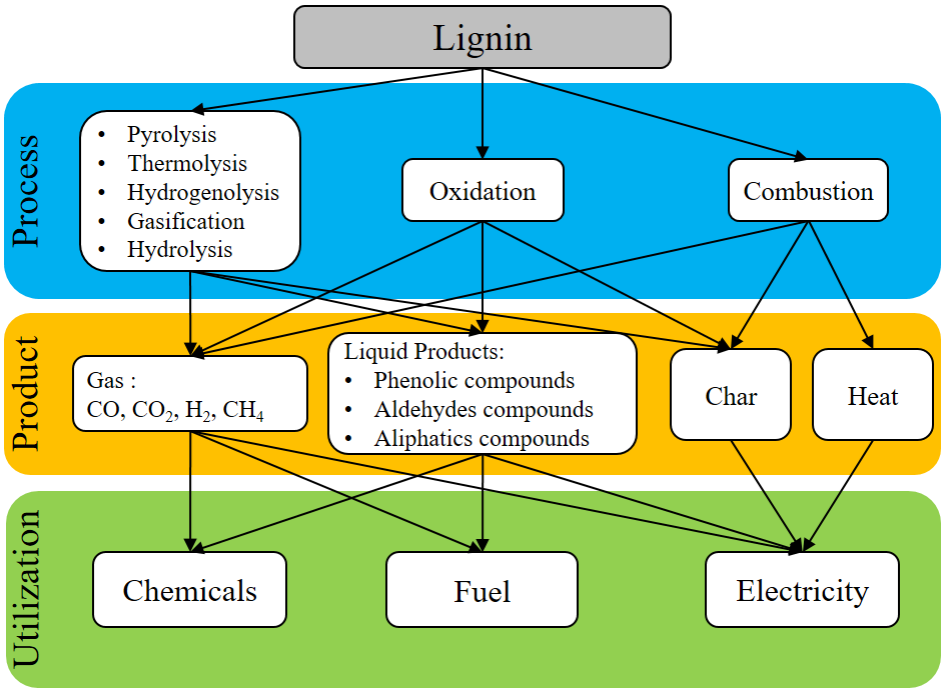

Figure 1.4 Thermochemical lignin conversion processes and their potential products [27].

1.1.4.1 Pyrolysis

Pyrolysis is one of the primary thermochemical methods for producing bio-oil directly from lignocellulosic biomass [28]. The rapid heating of biomass at temperatures in the range of 450-600 °C in the absence of oxygen with or without any catalysts can generate a mixture of non-condensable gases, liquid oil, and solid [29]. It represents a straight forward strategy to break down lignin molecule into smaller fragments. Fast pyrolysis of biomass with the rapid heating rate (above 100 °C/s) has received growing attention since a high yield of a liquid product called a pyrolysis oil or bio-oil can be produced [23]. Pyrolysis of lignin generally produces CO and CO_2 (by reformation of C=O and COOH functional groups), and H_2O, gaseous hydrocarbons (CH_4,C_2H_4,C_2H_2,C_3H_6, etc.), volatile liquids (benzene and alkyl substituted derivatives, methanol, acetone, and acetaldehyde), monolignols, monophenols (such as phenol, syringol, guaiacol, and catechol), and other polysubstituted phenols [27], as well as the thermally stable products char and

coke. The composition of each fraction and the yield of individual compounds are also strongly dependent on the lignin source and the isolation methods [30,31]. The proportion of each pyrolysis product is dependent on the process variables, particularly the temperature and heating rate [32]. At low temperatures, ether bonds and hydroxyl groups attached to β or γ carbons are readily cleaved to form condensable volatile products and water. A large fraction of methoxyl phenols, such as syringol and guaiacol, are contained in the condensable volatile products due to the fact that the methoxyl groups are more resistant than the ether linkages against thermal degradation. C-C is the strongest bond in all chemical transformations, which can be only broken at very high temperatures [33].

1.14.1.1 Thermal pyrolysis

The introduction of other gases in the pyrolyzer could change the reactions. For example, when comparing the pyrolysis of lignin in N_2 and in 4% O_2 in N_2 [34], it is found that the majority of products from the conventional pyrolysis without O_2 peaked in the range of 400-500 °C while the pyrolysis in the presence of O_2 peaked in the range of 200-400 °C. It is interesting to note that the presence of oxygen could not clearly change the type and distribution of the products. In both cases, the phenolic compounds contributed over 40% of the total products detected, and the principal products were guaiacol (2-methoxy phenol), syringol (2,6-dimethoxy phenol), phenol, and catechol. Electron paramagnetic resonance analysis results suggested that methoxyl, phenoxy, and substituted phenoxy radicals were the precursors of the major products. Moreover, an appropiate solvent addition could also enhance the pyrolysis efficiency. Thring et al. [35] proposed that the presence of ethanol could increase the solubility of lignin and thus increase the amount of ether-soluble phenols. Using ethanol-water binary solvent, Ye et al. [36] developed a process for the

hydrothermal depolymerization of cornstalk lignin, and phenolics with the yield of ca.70 wt % were obtained.

1.1.4.1.2 Catalytic pyrolysis

The addition of a catalyst to the pyrolyzer is in favor of controlling the lignin pyrolysis product distribution with the valuable aromatic hydrocarbon compounds (AHCs) via dehydration, decarboxylation, demethoxylation, and so on. Practically, many reseaches employed *Py*-GC–MS to investigate the manner of catalytic fast pyrolysis of lignin and in-situ catalytic upgrading of lignin oil. *Py*-GC-MS is a pyrolysis process performed in micropyrolyzer and the obtained volatile products are directly analyzed by GC–MS. Furthermore, it is a convenient way for the catalyst screening and for understanding the light-oil distribution of different lignin source, as summarized in Table 1.1. However, the ratio of catalyst-to-biomass in *Py*-GC-MS is always too high and the coke and char products cannot be distinguished since they are mixed with the catalyst together in the final product [37]. Moreover, the composition distribution of liquid product, including water and bio-oil (heavy oil and light oil), were unknown in the previous work.

Table 1.1 Several researches employing *Py*-GC-MS to study catalytic pyrolysis and catalytic upgrading of lignin derived oils

No	Pyrolysis Method	C/L Ratio[a], Pyrolysis condition	Catalyst	Result	Ref.
1	Single-shot micro-furnace pyrolyzer	C/L = 0.01; 300-700 °C	NaCl; KCl; $MgCl_2$ & $CaCl_2$	The yield of methoxylated phenols: 22% at 600°C	[38]

	(Model 2020iS, Frontier Laboratories, Japan).				
2	Pyroprobe pyrolzer (CDS 5250, CDS, USA)	C/L = 4; 700°C	Mo_2O/γ-Al_2O_3; Mo_2N/γ-Al_2O_3	Liquid Yield: ~25% (Main Product: monoaromatic hydrocarbon; selectivity: 85%)	[39]
3	Platinum coil pyrolyzer (5150, CDS Analytical)	C/L = 4; 650°C	Na-ZSM 5; ASA; Silicate; H-ZSM 5; H-beta; H-USY	H-USY (yield of liquid product: 74.9%; yield of aromatic hydrocarbon: 40%)	[40]
4	coil-type CDS Pyroprobe 5000	C/L = 0.6-2; 500-700 °C	H-ZSM-5 (Si/Al = 30; 50; 80; 100; 280)	H-ZSM-5 (Si/Al = 30) (Aromatic hydrocarbons yields: 2.62 wt%)	[41]
5	Quartz reactor loosely packed with quartz wool	C/L = 4; 650°C	MCM-41; Al-MCM-41(50); Al-MCM-41(50)-nano; MSU-J; Al-MSU-J(50)-1; SBA-15; Al-SBA-15(20)-1; ASA(35); γ-Al_2O_3; silica; H-ZSM 5(25)	Al-MCM 41-nano & H-ZSM 5 (liquid yield: ~50%; selectivity to aromatic hydrocarbon: ~80%)	[42]
6	Platinum coil pyrolyzer (5150, CDS Analytical)	C/L = 4; 650°C	Co_3O_4; NiO; MoO_3; Fe_2O_3; MnO_2; CuO; Na-ZSM 5; ASA; Silicate; H-ZSM5; H-beta; H-USY;	Co/H-ZSM 5 and Ni/H-ZSM5, (main product: aromatic hydrocarbons; selectivity: ~55%)	[43]

			Me-H-ZSM 5; Me-Na ZSM 5; Me-H USY; Me-Na-USY	Copper oxide (main product: vanillin; selectivity ~35%) Nickel oxide (main product: guaiacol; selectivity: ~25%)	

[a]Ratio of catalyst to lignin

Patwardan et al., [38] investigated the chemical composition of bio-oil derived from the fast pyrolysis of corn stover lignin by using a micro-pyrolyzer with a gel-permeation technique. The analysis results indicated that the monomeric compounds of the primary pyrolysis products would be recombined by the secondary reaction to form oligomeric compounds. Furthermore, they investigated the additional effect of alkali and alkali earth chloride salts (NaCl, KCl, $MgCl_2$, and $CaCl_2$), however, no change was found to increase the primary pyrolysis product. Transition metal nitrides especially Mo_2N are attracting increased interest as catalysts for various reactions since they have favorably high activities toward alkane isomerization, hydrodenitrogenation, and other conversion reactions [39]. Zheng et al. [39] found that the metal nitride catalyst played a critical role in the catalytic cracking of the lignin fast pyrolysis vapors. The use of Mo_2N catalyst supported on γ-Al_2O_3 remarkably decreased the oxygenated volatile organic products and significantly increased the aromatic hydrocarbons (mostly benzene and toluene) compared to MoO_3/γ-Al_2O_3 catalyst. Meanwhile, zeolites are usually used for the catalytic pyrolysis of lignin to aromatic hydrocarbons [40,42], which always play two roles in the lignin pyrolysis process (Scheme 1.1.) [40]. Firstly, in the presence of porous materials without acidic sites, such as Na-ZSM-5 and silicalite, the intermediates are stabilized by adsorption in the porous materials; thus, the yield of solid is decreased with the increasing of the liquid yield. Socondly, the addition of acid functionality results in the cleavage of C-O and C-C bonds. The strong acid sites in zeolites can

induce decarboxylation, dehydration, dealkylation, isomerization, cracking, and oligomerization reactions. In all the above processes, the gases mainly consist of CO_2, CO, and CH_4, which are probably generated from cracking of different side-chain structures and the methoxy groups on aromatic ringvia a direct hydrogen-transfer mechanism or via a radical coupling mechanism or from pyrogallol via an o-quinone intermediate [44]. Furthermore, the framework acidity, and pore size distribution of zeolites can be tuned, which always have great effect on the conversion of lignin to aromatic chemicals. To date, H-ZSM-5, H-USY, H-Mordenite, and H-Beta zeolites, silica, γ-Al_2O_3, macropore materials such as MCM-41, SBA-15, MSU-J have been investigated to improve liquid hydrocarbon products from the fast pyrolysis of lignin [40-42,45,46]. However, the yields of liquid hydrocarbon products are always low even though the zeolite has been involved. Therefore, the modification of zeolite by metal is needed to improve its performance. The loading of cobalt and nickel on ZSM-5 promoted the formation of aromatic hydrocarbons when compared to that of the blank zeolite. Moreover, the high yields in aromatic products can be obtained in the catalytic fast pyrolysis of lignin over the Na-form of the nickel-doped zeolites [43].

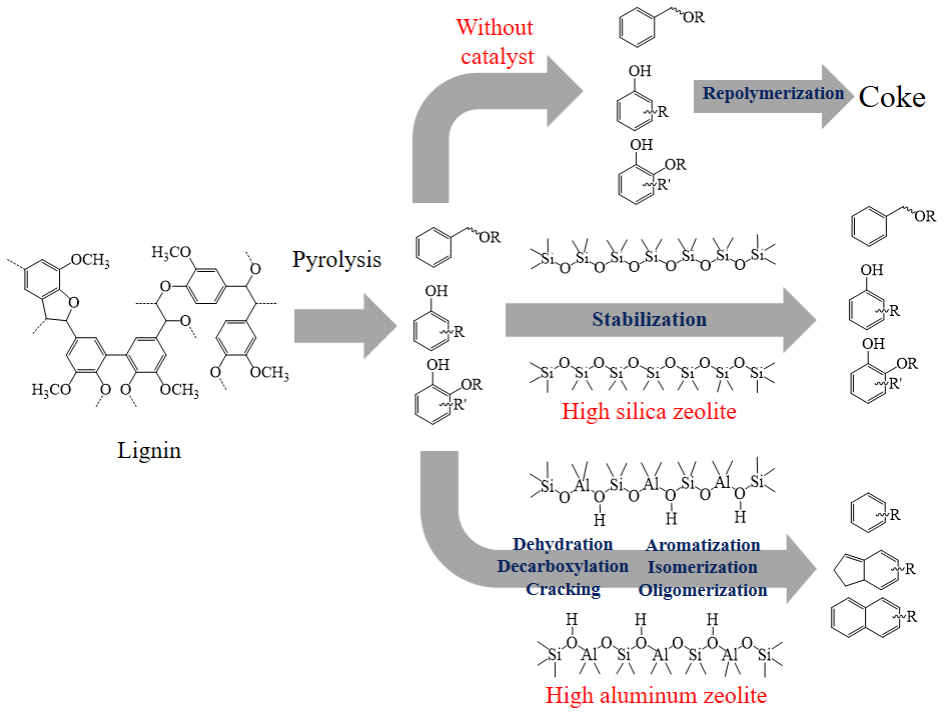

Scheme 1.1 Reaction pathway for non-catalytic/catalytic fast pyrolysis of lignin [40].

1.1.4.2 Gasification

Gasification of lignin can produce synthesis gas (syngas), which is a mixture of hydrogen and carbon monoxide [47,48]. The synthesis gas can then be converted into liquid fuels by two different commercial processes: Fischer-Tropsch synthesis or methanol/dimethyl ether synthesis [49,50]. Supercritical water (374 °C, 218 atm) was also used for the gasification of lignin [48,51]. In terms of thermal efficiency, this process offers the advantage of eliminating the need to dry the biomass, which is especially important for lignin with high moisture content. Four main processing units are needed for the above two routes: a lignin gasifier, a gas cleanup unit, a water-gas shift reactor in certain cases to produce hydrogen with the co-generation of carbon dioxide, and finally a syngas converter. By optimization of the reaction conditions and the catalysts, numerous products, ranging from synthetic natural gas, olefins, and alcohols to various transportation fuels, such as gasoline, jet fuel, and diesel, can be produced through the gasification[52]. In this case,

catalysts are always required in the several downstream processes, including (1) cracking of tars; (2) steam reforming of gas in order to increase H_2 content; and (3) synthesis-gas conversion [53].

Although syngas routes for the production of chemicals are well established for coal and natural gas conversion, there are still huge challenges regarding lignin gasification. One possible opportunity for future application is process intensification, which focuses on hybrid/combining processes to reduce cost [52]. Biomass gasifiers are still in the developmental stage with relation to producing a clean synthetic gas. Among the few reported attempts at lignin gasification at the pilot scale, Cerone and co-workers [54] carried out autothermal gasification of lignin-rich fermentation residues to evaluate the performance of a pilot plant with a feeding rate of 20−30 kg h^{-1}. The core reactor of the plant is an autothermal fixed bed updraft gasifier, operated slightly above atmospheric conditions. The average production of raw syngas was 1.94 kg per kg of dry residue, of which H_2 and CO were 27.2 and 696 g, respectively. The efficiency of energy conversion from solid to cold gas was 64% and reached about 81%, including the contribution of the condensable organic fraction. It should be noted that the lignins from different plants and isolation methods represent significantly different structures and reactivity and as such, adequate assessment of the specific lignin types in a given gasification system is needed. Venkitasamy and co-workers [55] have shown that the thermodynamic state changes in gasification are functions of elemental composition, rather than biomass species.

1.1.4.3. Hydrothermal way

In recent years, hydrothermal liquefaction (HTL) has been widely studied in biomass conversion with water as the reaction medium. HTL is efficient in lignin conversion for producing low-molecular-weight compounds [56], during which hydrolysis and pyrolysis occur simultaneously and the degraded products are basically phenolic compounds. It is considered as

an environmentally friendly and sustainable technology, with the advantages of short holding time, high conversion rate, and less secondary pollution.

Under the subcritical conditions (≤374.15 °C and 22.13 MPa), water can promote the ionic reactions, while the free-radical reactions mainly occur under the supercritical conditions (> 374.15 °C and 22.13 MPa) [56]. The variation trend of water viscosity is similar to that of dielectric constant, which decreases with the increase of temperature, while the diffusion coefficient increases with the increase of temperature. Therefore, hot pressured water can simultaneously serve as a reactant and catalyst in the conversion of lignin [57]. Understanding the degradation mechanisms of lignin is of great significance for the production of value-added aromatic derivatives (Figure 1). The cleavage of C-O-C bonds between aromatic rings is easier than that of C-C bonds, hence the lignin is hydrolyzed into methoxy phenolics first and then further hydrolyzed to phenolics [58]. During the HTL process of lignin, hydrolysis, fracture of ether bonds (C-O-C) and carbon–carbon bonds (C-C), demethoxylation, alkylation, and condensation can occur and compete against each other [59]. Monomeric and bipolymeric phenolics can be obtained through the most thermodynamically favorable cleavage of β-O-4 ether bond and C_α-C_β bond under mild conditions. With the increase in reaction temperature, other phenolic compounds can be generated through demethoxylation and alkylation [60]. The HTL degradation of lignin can be divided into three steps: hydrolysis of lignin, fracture of ether bonds and carbon–carbon bonds amongst monomers, and the cleavage and degradation of methoxy group on benzene ring as well as the alkylation of the groups on benzene ring [61]. Under the supercritical conditions, the HTL of lignin is fast and phenolic compounds can be obtained in a short duration, but re-polymerization also proceeds immediately with the increase of temperature, which is the major hurdle for obtaining phenolic compounds [62]. Although lignin has a massive natural reserve with high potential for

aromatics production, the HTL degradation of lignin has not reached the industrial scale (or not even the pilot-scale) because of the difficulty in depolymerization and products separation. Many laboratory scale studies have been performed for the lignin conversion, in which 60 wt% low-molecular-weight aromatics from oxidized lignin [63] or near theoretical yields of guaiacyl and syringyl monomers from a soluble lignin fraction [64] were obtained. However, the studied reaction conditions are difficult to be applied for industrialization. Furthermore, improvements in current chemical methods are needed for providing effective, environmentally sound, and simple strategies for the separation and recovery of aromatic monomers [56,65].

1.1.4.4. Hydrogenolysis

Although the traditional thermochemical transformation of lignin allows rapid breakdown of lignin, it is difficult to purify the oil-phase products by distillation because of their high boiling points and great tendency towards polymerization at elevated temperature [66,67]. More importantly, the high oxygen content and high viscosity of obtained products cannot be directly used as fuel for the energy terminal customers. In comparison to the thermochemical method, lignin hydrogenolysis offers the advantages of yielding products with high selectivity, high calorific value, and less coke formation. Hydrogenolysis refers to the cleavage reaction of carbon–carbon and carbon miscellaneous bonds in the reduction condition and the substitution of the released atoms or groups with hydrogen atoms [68]. The linkage between the structural units of lignin is mainly ether bonds, accounting for about 60–75% of total bonding [69], and the β-O-4 type ether bond is the most common one that accounts for 45–62% of all connection modes. Therefore, most research studies on the mechanisms of catalytic depolymerization of lignin are carried out to fracture the β-O-4 bond [70]. Other ether bonds include the α-O-4 and 4-O-5 types.

The second major lignin unit is carbon–carbon bonds, accounting for about 20–35%, which mainly include β-β', β-5′, and 5–5′ types [71,72].

The research progress of lignin hydrogenolysis can be divided into three levels. The first one is to partially reduce the functional groups of lignin macromolecules, such as reducing ether and carbonyl groups into hydroxyl groups, without breaking the molecular structure of lignin and its benzene rings. The second level is to break down lignin macromolecules into small molecules of phenolics and arenes. The third one is to further reduce the small molecules to alkanes as gasoline components. The application of the first level is limited and uneconomical, while the products from the second level are too complex and require higher separation cost compared to that of petroleum industry. Products from the third level can be used as low-value fuel, and more preferably, as feedstock for the production of aromatic compounds and high-value derivatives. To reduce the cost of separation, it is critical to improve the selectivity of the target products by selecting suitable raw materials (mainly wood lignin at present) and efficient catalysts with high selectivity and stability. Based on the types of catalysts used, the hydrogenolysis of lignin can be divided into heterogeneous catalytic hydrogenolysis, homogeneous catalytic hydrogenolysis, and electrocatalytic hydrogenolysis processes [73].

1.1.5 Functional material, catalyst support, and carbon-based catalyst.

As described in the previous section, various thermochemical conversion processes such as pyrolysis, hydrogenolysis, and hydrothermal processing ways have been tried to convert it to high value-added chemicals [74-76]. However, a large amount of char and high-molecular weight product are always produced finally since the lignin is a kind of thermo-stable polymeric

compound and hardly to be decomposed. Consequently, many researchers considered to transfer the lignin derivatives to functional materials as shown in Table 1.2:

Table 1.2 Utilization lignin as functional materials

No.	Lignin source	Treatment	Application	Ref.
1	Hydrolysis lignin of poplar hydrolysate	Pyrolysis at 600-900 ℃; 6 h Ball-milling 6-48 h	Carbon black	[77]
2	Sodium lignosulfonate	Pyrolysis at 600-1000 ℃; 1-4 h	Supercapacitor	[78]
3	Kraft lignin	Fractionation by Laccase-Mediator System Fractionation by Formic Acid/Fenton (Iron Ion and Hydrogen Peroxide)	Asphalt binder	[79]
4	Softwood kraft lignin	Oxidation with H_2O_2 (60-100 ℃)	Dispersant of kaolin suspensions	[80]
5	Kraft lignin	$ZnCl_2$ activation in Microwave oven 2.45 GHz at 600 ℃ for 4 min	Cu(II) adsoption	[81]
6	Soda lignin	Pyrolysis at 800 ℃ for 6 h then Air oxidation at 150-350 ℃ for 1 h	4-Nitrophenol removal	[82]
7	Alkali lignin	Amidation: hexamethylene diisocyanate, Poly ε-caprolactame catalyzed with $Sn(Oct)_2$	Bioplastic	[83]

Due to the high carbon content in lignin, Snowdon et al. [77] have tried to convert waste lignin from bioethanol productuction process to carbon black material. The obtained carbon showed low electrical conductivity but had superior thermal conductivity. In contrast, the electrical conductivity decreased when the lignin was ball milled before the carbonization due to the increase of oxygen content on the surface of the obtained carbon black. Nevertheless, the thermal conductivity of the ball-milled-lignin-derived carbon black was much higher than that of untreated one. As such, the obtained carbon black can be used in non-conductive black ink, toner, paint, thermal paste, and thermally conductive filler.

Further, carboneous lignin has been applied in energy storage material field. Pang et al. [78] synthesized interconnected hierarchical porous carbon for supercapacitor application from industrial waste sodium lignosulfonate via carbonization. The obtained carbon materials showed a superior energy density of 8.4 Wh L^{-1} (at 13.9 W L^{-1}) with a high power density of 5573.1 W L^{-1} (at 3.5 Wh L^{-1}) in 7 M KOH electrolyte, and a remarkable cycling stability even after 20000 cycles. Herein, the contribution of the reversible Faradic redox reactions of the surface oxygen- and nitrogen-containing groups on lignosulfonate-derived carbon material played an important role in the high capacitve performance in alkaline electrolyte. These functional groups can modify the acid-basic feature and electron donor-acceptor characteristic of carbon materials as pseudocapacitance-active sites, further introducing extra pseudocapacitance and enhancing specific capacitance.

Lignin utilization as functional materials also can be found in the construction field. Xie et al. [79] demonstrated the potential of lignin as high-performance asphalt binder via formic acid-H_2O_2 treatment. The addition of asphalt binder modifier derived from lignin can stand hotter summer temperatures without rutting problem and cracking in the low temperature. The similarity in

molecular structures of asphaltene in asphalt binder and oxidized lignin makes it possible for lignin to cross-link through dipolar−dipolar interactions to improve the high temperature performance. Furthermore, the improvement of asphalt binder's low temperature performance could be resulted from the increase of oxygenated groups in lignin structure. In addition, He et al. [80] prepared kaolin dispersant by oxidized kraft lignin (OKL) with hydrogen peroxide under alkaline conditions to generate carboxylate group, which could stabilize the dispersion a of particles. The addition of OKL would decrease the zeta potential and introduce a more intensive repulsion force between particles. This repulsion force prevented clay particles from self-agglomeration and produced particles that were smaller with a higher surface area.

In environmental application, lignin derived carbon material has been widely used as the adsorbent of pollutant. Maldhure et al. [81] prepared activated carbons by zinc chloride activation by using different impregnation methods with and without microwave treatment at 500–800 °C for adsorption of Cu^{2+} metal contaminant. Integration of microwave technique to conventional impregnation method has shown the beneficial effects in terms of porous structure, relatively greater surface area, reduction of time and energy towards effectiveness of impregnation. Furthermore, it has clearly shown the formation of a larger number of active surface functional groups than those obtained by conventional thermal process and shown higher capacity for adsorption of Cu^{2+} compared to conventional process. The adsorption on the samples could be favorably described by Langmuir isotherm, and the adsorption kinetics was found to be well fitted by the pseudo-second-order model. Martin-Martinez et al. [82] synthesized softwood lignin derived carbon for elimination of 4-nitrophenol. Herein, carbonization of lignin was conducted at 800 C under N_2 atmosphere and further activated under oxidative atmosphere at four different temperatures (150, 200, 300 and 350 °C). The contents of acidic functionalities increased with the

activation temperature, suggesting the incorporation of more acidic oxygenated groups during the treatment under air atmosphere. The materials prepared at higher activation temperatures (300 and 350 °C) have proven their potential in the elimination of 4-nitrophenol (4-NP) from aqueous model solutions (5 g L^{-1}) when using catalytic wet peroxide oxidation (CWPO).

Recently, utilization of lignin as a precursor of bioplastics was reported to substitute the petroleum-based plastics which are difficult to be degradated. Zhang et al. [83] synthesized a novel lignin-poly(ε-caprolactone)-based polyurethane bioplastics with high performance. The poly(ε-caprolactone) was incorporated as a biodegradable soft segment to the lignin by the bridge of hexamethylene diisocyanate (HDI) with long flexible aliphatic chains and high reactivity. The effects of -NCO/-OH molar ratio, content of lignin, and molecular weight of the PCL on the properties of the resultant polyurethane plastics were thoroughly evaluated. It is important that the polyurethane film still possessed high performance in the tensile strength, breaking elongation, and tear strength. Moreover, it was very stable at 340.8 °C and presented excellent solvent-resistance. The results demonstrated that the modification of the lignin based on the urethane chemistry represents an effective strategy for developing lignin-based high-performance sustainable materials.

Besides functional materials, lignin can be used as the promising lignin-based carbon catalyst or catalyst support due to its aromatic units and three-dimensional interpenetrating polymer network structure, which is responsible to its high stability and excellent performance. Generally, the transformation of lignin-to-catalyst requires acid treatment and surface modification to increase the catalytic activity of lignin-based carbon catalyst. Table 1.3 shows the application resume of catalyst support and carbon catalyst from lignin.

Table 1.3 The application resume of catalyst support and carbon catalyst from lignin.

No.	Lignin source	Catalyst	Application	Ref.
1	Kraft lignin	K_2CO_3 activation carbon-based lignin	Transesterification catalyst	[84]
2	Alkali lignin	Sulfonated carbon-based alkaline lignin	Cellulose hydrolysis	[85]
3	Sodium lignosulfonate	Sulfonated carbon-based lignin	Hemicellulose hydrolysis	[86]
4	Enzymatic hydrolysis lignin residue	Sulfonated Fe_3O_4-lignin	Fructose dehydration	[87]
5	Kraft lignin	TiO_2-lignin	Lignin depolymerization	[88]
6	Alkali lignin	Co/Mn-lignin	Oxidation of 5-HMF to 2,5-furandicarboxylic acid	[89]

Alkali metal "anchoring" properties of oxygenated functional group from lignin derived carbon catalyst has been reported for transesterification of rapeseed oil with methanol. Li et al. [84] prepared K_2CO_3 supported on Kraft lignin derived activated carbon by simply mixing and subsequently activating at 800 °C under N_2 atmosphere. The biodiesel yield of 99.6% was achieved by using the catalyst prepared by 0.6 of K_2CO_3/KL mass ratio and activation at 800 °C, under the transesterification condition of 65 °C, 2 h, methanol to rapeseed oil molar ratio of 15:1 and 3.0 wt.% catalyst (relative to the weight of rapeseed oil). The solid catalyst was reused for 4 times and biodiesel yield remained over 82.1% for the fourth time.

Meanwhile, generating acid functional groups on lignin derived carbon has been popular in biorefinery of lignocellulosic biomass. Hu et al. [85] synthesized 1D lignin based solid acid catalysts for direct hydrolysis of highly crystalline rice straw cellulose (CrI=72.2 %), via sulfonation and hydrothermal treatment of lignin based activated carbon with a mesoporous structure and 0.56 mmol/g sulfonic and 0.88 mmol/g total acid. Under optimal hydrothermal condition of 150 °C and 5 atm, 77.9 % of cellulose was hydrolyzed in three consecutive runs, yielding 64 % glucose with 91.7% selectivity as well as 8.1 % cellulose nanofibrils. These 1D acid catalysts could be used repetitively to fully hydrolyze the remaining cellulose as well as be easily separated from products for hydrolysis of additional cellulose. Li et al [86] utilized lignosulfonate lignin derived carbon acid catalyst for the hydrolysis of hemicellulose in corncob which was prepared by carbonization, followed by sulfonation with H_2SO_4 and oxidation with H_2O_2. The catalyst exhibited high selectivity and produced a relatively high xylose yield of up to 84.2% (w/ w) with a few by-products. Under these conditions, the retention rate of cellulose was 82.5%, and the selectivity reached 86.75%. After 5 cycles of reuse, the catalyst still showed high catalytic activity, with slightly decreased yields of xylose from 84.2% to 70.7%.

In addition, magnetic material was doped on lignin derived carbon acid catalyst in order to simplify the separation process by using an external magnet. Hu et al. [87] prepared a magnetic lignin-derived carbon acid catalyst by a simple and inexpensive impregnation–carbonization sulfonation process. A high surface area of Fe_3O_4 carbon which contains of -SO_3H, -COOH and phenolic -OH groups, exhibited a good catalytic activity for the dehydration of fructose into 5-hydroxymethylfurfural (HMF). Full conversion of fructose and a high HMF yield of 81.1% was achieved in the presence of dimethylsulfoxide (DMSO) at 130 °C for 40 min. Furthermore, these catalysts exhibited excellent catalytic stability for at least 5 reused times.

The utilization of lignin as support catalyst to promote catalytic activity of the metal oxide also have been reported. Srisasiwimon et al. [88] utilized lignin wastes to modify TiO_2 and form the composite photocatalyst (TiO_2/lignin) by a sol-gel microwave technique to enhance the photoabsorption. Evaluation of photocatalytic performance was investigated from lignin conversion to high-value added chemicals such as vanillin. It is reported that carbon from lignin could improved photocatalytic performance of TiO_2/lignin composite compared with the pristine. Zhou et al. [89] reported a novel catalyst of cobalt nanoparticles (NPs) encapsulated in lignin derived graphitic carbon with manganese and nitrogen heteroatoms (Co-Mn/N@C) which was synthesized by pyrolyzing a mixture of Co/Mn-lignin complex and dicyandiamide. Co-Mn/N@C catalyst exhibited excellent activity and recyclability for oxidizing 5-hydroxymethylfurfural (HMF) into 2,5-furandicarboxylic acid (FDCA) in aqueous system using O_2 as oxidant. It is found that Mn/N- doped carbon can activate the reactivity of Co NPs for HMF oxidation by tuning the electronic structure of embedded metal NPs.

1.2 Motivation and Objectives

As discussed in the previous section, lignin from lignosulfonate process is the largest commercial byproduct from the pulp and paper industries. Various methods for converting lignosulfonate lignin into high-value-added chemical and material have been proposed since lignin is considered as a promising aromatic platform resource for the production of aromatic hydrocarbons. Meanwhile, catalytic upgrading of bio-oil derived from lignin is always required in order to improve its quality. Many researches employed *Py*-GC-MS as a convenient way to study catalytic pyrolysis and catalytic upgrading process for catalyst screening. However, the ratio of catalyst-to-biomass in *Py*-GC-MS was too high and the coke and char products cannot be distinguished since they were mixed with the catalyst together in the final product. In addition, a few researches concentrate to utilize the original structure of the lignosulfonate lignin containing hydroxyl functional group, sulfonate functional group, and impurities in the form of sodium salt to produce some functional materials and catalysts. Thus, it is interesting to develope new strategies on the utilization of lignosulfonate lignin as the precursor of catalyst or carbon-based catalysts. In this study, the main objectives are limited in the scope of:

a. To provide guidance for the selection of a suitable zeolite for the *in-situ* catalytic deoxygenation of bio-oil derived from fast pyrolysis of lignin. It is expected to obtain more information than *Py*-GC-MS, especially the amounts of light-oil, coke, gas, and water for scaling up the catalytic upgrading process

b. To develop a new application of lignosulfonate lignin as a catalyst precursor material and lignin-derived carbon catalyst for the biorefinery process.

1.3 Organization and Ouline of This Dissertation.

In this dissertation, catalytic upgrading of lignin bio-oil to obtain BTX products and utilization of lignin as the catalyst precursor were investigated in details. Particularly, the studies are focused on developing preliminary study of catalytic upgrading of lignin bio-oil in a fix-bed reactor with high aluminum zeolite types. Furthermore, the utilization of lignosulfonate lignin with the original properties as a precursor catalyst material and lignin-derived carbon acid catalysts was also explored.

Chapter 1 briefly introduces the recent progress of biorefinery process of lignin for the productions of fuels, chemicals, and catalyst materials. Furthermore, the fractionation of lignocellulosic bimass to lignin was reviewed. Based on the literature survey, the motivation, objectives and outlines of this research are given.

Chapter 2 provides a guidance for the selection of suitable zeolite for the *in-situ* catalytic deoxygenation of bio-oil derived from fast pyrolysis of lignin to obtain BTX products. Five types of high aluminum zeolites, i.e., H-Ferrierite, H-Mordenite, H-ZSM-5, H-Beta and H-USY zeolites, were investigated in this study. It is found that the channel structure, pore sizes and acidity of zeolite had significant effect on product distribution, coke formation, and deoxygenation.

Chapter 3 presents a new viewpoint to utilize waste dealkaline lignin as a precursor of sustainable and selective precious metal-free hydrogen production catalysts for formic acid decomposition. Dealkaline lignin (DAL) was used as a carbon and sulfur source to prepare MoS_2/Mo_2C based catalysts (Mo-DAL) with a facile impregnation-pyrolysis two-step process for the hydrogen production from the formic acid decomposition. The 20% Mo-DAL catalyst produced hydrogen quite selectively (99.2%) with almost complete conversion of formic acid (97.4%) at 220 °C. The catalyst showed stable activity for at least 50 hours in these conditions.

Chapter 4 demostrates a new application of alkaline lignin (AL) as low-cost and sustainable carbon acid catalysts via a pyrolysis process followed by an acid solution treatment process. The obtained catalysts were applied for the hydrolysis of cellulose and woody biomass for the production of monomeric sugars such as glucose and xylose. The AL-Py-450 carbon catalyst exhibited good catalytic activity for the hydrolysis of lignocellulosic biomass, i.e., Japanese cedar wood, with yields of glucose and xylose of 47.1% and 40.3%, respectively.

Chapter 5 exhibits another new application of the AL-derived carbon acid catalyst for the cyclization citronellal to produce *p*-menthane-3,8-diol. By application such a catalyst, the conversion of (±) citronellal reached as high as 97 % with a high PMD yield of 86 %.

Chapter 6 summarizes the main results in this dissertation and the perspectives of the possible future works related with the lignin coversions and applications.

References

[1] J.S. Luterbacher, D. Martin Alonso, J.A. Dumesic, Targeted chemical upgrading of lignocellulosic biomass to platform molecules, Green Chemistry, 16 (2014) 4816-4838.

[2] C.O. Tuck, E. Perez, I.T. Horvath, R.A. Sheldon, M. Poliakoff, Valorization of Biomass: Deriving more value from waste, Science, 337 (2012) 695−699.

[3] C. Li, X. Zhao, A. Wang, G.W. Huber, T. Zhang, Catalytic Transformation of Lignin for the Production of Chemicals and Fuels, Chemical Reviews, 115 (2015) 11559-11624.

[4] J. Lora, Industrial Commercial Lignins: Sources, Properties and Applications, in: M.N. Belgacem, A. Gandini (Eds.) Monomers, Polymers and Composite from Renewable Resources, Elsevier, Amsterdam, 2008, pp. 225– 241.

[5] T.Saito, R.H. Brown, M.A. Hunt, D.L. Pickel, J.M. Pickel, J.M. Messman, F.S. Baker, M. Keller, A.K. Naskar, Turning renewable resources into value-added polymer: development of lignin-based thermoplastic, Green Chemistry, 14 (2012) 3295–3303.

[6] V.K. Thakur, M.K. Thakur, P. Raghavan, M.R. Kessler, Progress in Green Polymer Composites from Lignin for Multifunctional Applications: A Review, ACS Sustainable Chemistry & Engineering, 2 (2014) 1072-1092.

[7] V.K. Thakur, M.K. Thakur, Recent advances in green hydrogels from lignin: a review, International Journal of Biological Macromolecules, 72 (2015) 834-847.

[8] E. Ten, W. Vermerris, Recent developments in polymers derived from industrial lignin, Journal of Applied Polymer Science, 132 (2015) 1-13.

[9] S. Laurichesse, L. Avérous, Chemical modification of lignins: Towards biobased polymers, Progress in Polymer Science, 39 (2014) 1266-1290.

[10] R. Rinaldi, R. Jastrzebski, M.T. Clough, J. Ralph, M. Kennema, P.C.A. Bruijnincx, B.M. Weckhuysen, Paving the Way for Lignin Valorisation: Recent Advances in Bioengineering, Biorefining and Catalysis, Angewandte Chemie International Edition, 55 (2016) 8164-8215.

[11] D. Kai, M.J. Tan, P.L. Chee, Y.K. Chua, Y.L. Yap, X.J. Loh, Towards lignin-based functional materials in a sustainable world, Green Chemistry, 18 (2016) 1175-1200.

[12] D. Dimmel, Overview, in: C. Heitner, D.R. Dimmel, J.A. Schmidt (Eds.) Lignins and Lignans: Advances in Chemistry, CRC Press, Boca Raton, 2010, pp. 1-10.

[13] R. Parthasarathi, R.A. Romero, A. Redondo, S. Gnanakaran, Theoretical study of the remarkably diverse linkages in lignin, Journal of Physical Chemistry Letters, 2 (2011) 2660-2666.

[14] B. Joffres, D. Laurenti, N. Charon, A. Daudin, A. Quignard, C. Geantet, Thermochemical Conversion of Lignin for Fuels and Chemicals: A Review, Oil & Gas Science and Technology – Revue d'IFP Energies nouvelles, 68 (2013) 753-763.

[15] T.J. McDonough, The chemistry of organosolv deligninification, Institute of Paper Science and Technology, 76 (1993) 186-193.

[16] Z. Strassberger, S. Tanase, G. Rothenberg, The pros and cons of lignin valorisation in an integrated biorefinery, RSC Advances, 4 (2014) 25310-25318.

[17] J. Lora, Industrial Commercial Lignins: Sources, Properties and Applications, in: M.N. Belgacem, A. Gandini (Eds.) Monomers, Polymers and Composites from Renewable Resources, Elsevier, New York, 2008, pp. 225−241.

[18] B.M. Upton, A.M. Kasko, Strategies for the conversion of lignin to high-value polymeric materials: Review and perspective, Chemical Reviews, 116 (2016) 2275-2306.

[19] F. Oehman, H. Theliander, P. Tomani, P. Axegard, Method for separating lignin from black liquor, a lignin product, and use of a lignin product for production of fuels or materials, in, 2010.

[20] P. Kumar, D.M. Barrett, M.J. Delwiche, P. Stroeve, Methods for Pretreatment of Lignocellulosic Biomass for Efficient Hydrolysis and Biofuel Production, Industrial & Engineering Chemistry Research, 48 (2009) 3713-3729.

[21] G.W. Huber, S. Iborra, A. Corma, Synthesis of Transportation Fuels from Biomass: Chemistry, Catalysts, and Engineering, Chemical Reviews, 106 (2006) 4044-4098.

[22] D.J. Gardner, T.P. Schultz, G.D. McGinnis, The pyrolytic behavior of selected lignin preparations, Journal of Wood Chemistry and Technology, 5 (1985) 85-110.

[23] M. Windt, D. Meier, J.H. Marsman, H.J. Heeres, S. de Koning, Micro-pyrolysis of technical lignins in a new modular rig and product analysis by GC-MS/FID and GC × GC-TOFMS/FID, Journal of Analytical and Applied Pyrolysis, 85 (2009) 38-46.

[24] M. Saisu, T. Sato, M. Watanabe, T. Adschiri, K. Arai, Conversion of Lignin with Supercritical Water−Phenol Mixtures, Energy & Fuels, 17 (2003) 922-928.

[25] V. Sricharoenchaikul, Assessment of black liquor gasification in supercritical water, Bioresource Technology, 100 (2009) 638-643.

[26] J.C. Villar, A. Caperos, F. García-Ochoa, Oxidation of hardwood kraft-lignin to phenolic derivatives with oxygen as oxidant, Wood Science and Technology, 35 (2001) 245-255.

[27] M.P. Pandey, C.S. Kim, Lignin Depolymerization and Conversion: A Review of Thermochemical Methods, Chemical Engineering and Technology, 34 (2011) 29-41.

[28] D. Mohan, C.U. Pittman, P.H. Steele, Pyrolysis of wood/ biomass for bio-oil: A critical review, Energy Fuels, 20 (2006) 848−889.

[29] H.B. Goyal, D. Seal, R.C. Saxena, Bio-Fuels from Thermochemical Conversion of Renewable Resources: A Review, Renewable and Sustainable Energy Reviews, 12 (2008) 504-517.

[30] M. Zhang, F.L.P. Resende, A. Moutsoglou, D.E. Raynie, Pyrolysis of lignin extracted from prairie cordgrass, aspen, and Kraft lignin by Py-GC/MS and TGA/FTIR, Journal of Analytical and Applied Pyrolysis, 98 (2012) 65-71.

[31] V. Mendu, A.E. Harman-Ware, M. Crocker, J. Jae, J. Stork, S. Morton, A. Placido, G. Huber, S. Debolt, Identification and thermochemical analysis of high-lignin feedstocks for biofuel and biochemical production, Biotechnology for Biofuels, 4 (2011) 1-13.

[32] J. Cho, S. Chu, P.J. Dauenhauer, G.W. Huber, Kinetics and reaction chemistry for slow pyrolysis of enzymatic hydrolysislignin and organosolv extracted lignin derived from maplewood, Green Chemistry, 14 (2012) 428-439.

[33] G. Jiang, D.J. Nowakowski, A.V. Bridgwater, Effect of the Temperature on the Composition of Lignin Pyrolysis Products, Energy Fuels, 24 (2010) 4470−4475.

[34] J. Kibet, L. Khachatryan, B. Dellinger, Molecular Products and Radicals from Pyrolysis of Lignin, Environmental Science & Technology, 46 (2012) 12994−13001.

[35] R.W. Thring, S.P.R. Katikaneni, N.N. Bakhshi, Production of gasoline range hydrocarbons from Alcell lignin using HZSM-5 catalyst, Fuel processing technology, 62 (2000) 17-30.

[36] Y. Ye, J. Fan, J. Chang, Effect of reaction conditions on hydrothermal degradation of cornstalk lignin, Journal of Analytical and Applied Pyrolysis, 94 (2012) 190-195.

[37] D.A. Ruddy, J.A. Schaidle, J.R. Ferrell Iii, J. Wang, L. Moens, J.E. Hensley, Recent advances in heterogeneous catalysts for bio-oil upgrading via “ex situ catalytic fast pyrolysis”: catalyst development through the study of model compounds, Green Chem., 16 (2014) 454-490.

[38] P.R. Patwardhan, R.C. Brown, B.H. Shanks, Understanding the fast pyrolysis of lignin, ChemSusChem, 4 (2011) 1629-1636.

[39] Y. Zheng, D. Chen, X. Zhu, Aromatic hydrocarbon production by the online catalytic cracking of lignin fast pyrolysis vapors using Mo2N/γ-Al2O3, Journal of Analytical and Applied Pyrolysis, 104 (2013) 514-520.

[40] Z. Ma, E. Troussard, J.A. Van Bokhoven, Controlling the selectivity to chemicals from lignin via catalytic fast pyrolysis, Applied Catalysis A: General, 423-424 (2012) 130-136.

[41] J.Y. Kim, J.H. Lee, J. Park, J.K. Kim, D. An, I.K. Song, J.W. Choi, Catalytic pyrolysis of lignin over HZSM-5 catalysts: Effect of various parameters on the production of aromatic hydrocarbon, Journal of Analytical and Applied Pyrolysis, 114 (2015) 273-280.

[42] V.B.F. Custodis, S.A. Karakoulia, K.S. Triantafyllidis, J.A. Van Bokhoven, Catalytic Fast Pyrolysis of Lignin over High-Surface-Area Mesoporous Aluminosilicates: Effect of Porosity and Acidity, ChemSusChem, 9 (2016) 1134-1145.

[43] Z. Ma, V. Custodis, J.A. Van Bokhoven, Selective deoxygenation of lignin during catalytic fast pyrolysis, Catalysis Science and Technology, 4 (2014) 766-772.

[44] M. Asmadi, H. Kawamoto, S. Saka, Thermal reactivities of catechols/pyrogallols and cresols/xylenols as lignin pyrolysis intermediates, Journal of Analytical and Applied Pyrolysis, 92 (2011) 76-87.

[45] D. Shen, J. Zhao, R. Xiao, Catalytic transformation of lignin to aromatic hydrocarbons over solid-acid catalyst: Effect of lignin sources and catalyst species, Energy Conversion and Management, 124 (2016) 61-72.

[46] Y. Yu, X. Li, L. Su, Y. Zhang, Y. Wang, H. Zhang, The role of shape selectivity in catalytic fast pyrolysis of lignin with zeolite catalysts, Applied Catalysis A: General, 447-448 (2012) 115-123.

[47] A. Farzaneh, T. Richards, E. Sklavounos, A. van Heiningen, A Kinetic Study of CO2 and Steam Gasification of Char from Lignin Produced in the SEW Process, BioResources, 9 (2014) 3052-3063.

[48] A. Yamaguchi, N. Hiyoshi, O. Sato, M. Shirai, Gasification of Organosolv-lignin Over Charcoal Supported Noble Metal Salt Catalysts in Supercritical Water, Topics in Catalysis, 55 (2012) 889-896.

[49] G.P. van der Laan, A. Beenackers, Kinetics and Selectivity of the Fischer−Tropsch Synthesis: A Literature Review, Catalysis Reviews - Science and Engineering, 41 (1999) 255-318.

[50] P.J.A. Tijm, F.J. Waller, D.M. Brown, Methanol technology developments for the new millennium, Applied Catalysis A: General, 221 (2001) 275-282.

[51] F.L.P. Resende, S.A. Fraley, M.J. Berger, P.E. Savage, Noncatalytic gasification of lignin in supercritical water, energy Fuels, 22 (2008) 1328-1334.

[52] Y.C. Lin, G.W. Huber, The critical role of heterogeneous catalysis in lignocellulosic biomass conversion, Energy & Environmental Science, 2 (2009) 68-80.

[53] D. Ferdous, A.K. Dalai, S.K. Bej, R.W. Thring, Production of H_2 and medium heating value gas via steam gasification of lignins in fixed-bed reactors, The Canadian Journal of Chemical Engineering, 79 (2001) 913-922.

[54] N. Cerone, F. Zimbardi, L. Contuzzi, E. Alvino, M.O. Carnevale, V. Valerio, Updraft Gasification at Pilot Scale of Hydrolytic Lignin Residue, Energy Fuels, 28 (2014) 3948-3956.

[55] C. Venkitasamy, D. Hendry, N. Wilkinson, L. Fernando, W.A. Jacoby, Investigation of thermochemical conversion of biomass in supercritical water using a batch reactor, Fuel, 90 (2011) 2662-2670.

[56] L. Cao, C. Zhang, H. Chen, D.C.W. Tsang, G. Luo, S. Zhang, J. Chen, Hydrothermal liquefaction of agricultural and forestry wastes: state-of-the-art review and future prospects, Bioresource Technology, 245 (2017) 1184-1193.

[57] T. Belkheiri, S.-I. Andersson, C. Mattsson, L. Olausson, H. Theliander, L. Vamling, Hydrothermal Liquefaction of Kraft Lignin in Subcritical Water: Influence of Phenol as Capping Agent, Energy & Fuels, 32 (2018) 5923-5932.

[58] H.S. Lee, J. Jae, J.M. Ha, D.J. Suh, Hydro- and solvothermolysis of kraft lignin for maximizing production of monomeric aromatic chemicals, Bioresource Technology, 203 (2016) 142-149.

[59] C.Y. Jeong, S.K. Dodla, J.J. Wang, Fundamental and molecular composition characteristics of biochars produced from sugarcane and rice crop residues and by-products, Chemosphere, 142 (2016) 4-13.

[60] Q. Li, D. Liu, X. Hou, P. Wu, L. Song, Z. Yan, Hydro-liquefaction of microcrystalline cellulose, xylan and industrial lignin in different supercritical solvents, Bioresource Technology, 219 (2016) 281-288.

[61] L. Cao, C. Zhang, S. Hao, G. Luo, S. Zhang, J. Chen, Effect of glycerol as co-solvent on yields of bio-oil from rice straw through hydrothermal liquefaction, Bioresource Technology, 220 (2016) 471-478.

[62] T. Yang, J. Wang, B. Li, X. Kai, W. Xing, R. Li, Behaviors of rice straw two-step liquefaction with sub/supercritical ethanol in carbon dioxide atmosphere, Bioresource Technology, 258 (2018) 287-294.

[63] A. Rahimi, A. Ulbrich, J.J. Coon, S.S. Stahl, Formic-acid-induced depolymerization of oxidized lignin to aromatics, Nature, 515 (2014) 249–252.

[64] L. Shuai, M.T. Amiri, Y.M. Questell-Santiago, F. Héroguel, Y. Li, H. Kim, R. Meilan, C. Chapple, J. Ralph, J.S. Luterbacher, Formaldehyde stabilization facilitates lignin monomer production during biomass depolymerization, Science, 354 (2016) 329-333.

[65] H. Prajitno, J. Park, C. Ryu, H.Y. Park, H.S. Lim, J. Kim, Effects of solvent participation and controlled product separation on biomass liquefaction: A case study of sewage sludge, Applied Energy, 218 (2018) 402-416.

[66] Z. Jiang, P. Zhao, C. Hu, Controlling the cleavage of the inter- and intra-molecular linkages in lignocellulosic biomass for further biorefining: A review, Bioresource Technology, 256 (2018) 466-477.

[67] J. Wang, W. Li, H. Wang, Q. Ma, S. Li, H.M. Chang, H. Jameel, Liquefaction of kraft lignin by hydrocracking with simultaneous use of a novel dual acid-base catalyst and a hydrogenation catalyst, Bioresource Technology, 243 (2017) 100-106.

[68] R. Shu, Q. Zhang, L. Ma, Y. Xu, P. Chen, C. Wang, T. Wang, Insight into the solvent, temperature and time effects on the hydrogenolysis of hydrolyzed lignin, Bioresource Technology, 221 (2016) 568-575.

[69] M. Zaheer, R. Kempe, Catalytic Hydrogenolysis of Aryl Ethers: A Key Step in Lignin Valorization to Valuable Chemicals, ACS Catalysis, 5 (2015) 1675-1684.

[70] C. Espro, B. Gumina, E. Paone, F. Mauriello, Upgrading Lignocellulosic Biomasses: Hydrogenolysis of Platform Derived Molecules Promoted by Heterogeneous Pd-Fe Catalysts, Catalysts, 7 (2017) 78-113.

[71] M. Luo, H. Lin, B. Li, Y. Dong, Y. He, L. Wang, A novel modification of lignin on corncob-based biochar to enhance removal of cadmium from water, Bioresource Technology, 259 (2018) 312-318.

[72] R. Shu, J. Long, Y. Xu, L. Ma, Q. Zhang, T. Wang, C. Wang, Z. Yuan, Q. Wu, Investigation on the structural effect of lignin during the hydrogenolysis process, Bioresource Technology, 200 (2016) 14-22.

[73] L. Cao, I.K.M. Yu, Y. Liu, X. Ruan, D.C.W. Tsang, A.J. Hunt, Y.S. Ok, H. Song, S. Zhang, Lignin valorization for the production of renewable chemicals: State-of-the-art review and future prospects, Bioresource Technology, 269 (2018) 465-475.

[74] I. Kurnia, S. Karnjanakom, A. Bayu, A. Yoshida, J. Rizkiana, T. Prakoso, G. Guan, A. Abudula, *In-situ* catalytic upgrading of bio-oil derived from fast pyrolysis of lignin over high aluminum zeolites, Fuel Processing Technology, 167 (2017) 730-737.

[75] S.F. Hashmi, H. Meriö-Talvio, K.J. Hakonen, K. Ruuttunen, H. Sixta, Hydrothermolysis of organosolv lignin for the production of bio-oil rich in monoaromatic phenolic compounds, Fuel Processing Technology, 168 (2017) 74-83.

[76] M. Niu, Y. Hou, W. Wu, R. Yang, Degradation of lignin in $NaVO_3$-H_2SO_4 aqueous solution with oxygen, Fuel Processing Technology, 161 (2017) 295-303.

[77] M.R. Snowdon, A.K. Mohanty, M. Misra, A study of carbonized lignin as an alternative to carbon black, ACS Sustainable Chemistry and Engineering, 2 (2014) 1257-1263.

[78] J. Pang, W. Zhang, J. Zhang, G. Cao, M. Han, Y. Yang, Facile and sustainable synthesis of sodium lignosulfonate derived hierarchical porous carbons for supercapacitors with high volumetric energy densities, Green Chemistry, 19 (2017) 3916-3926.

[79] S. Xie, Q. Li, P. Karki, F. Zhou, J.S. Yuan, Lignin as Renewable and Superior Asphalt Binder Modifier, ACS Sustainable Chemistry and Engineering, 5 (2017) 2817-2823.

[80] W. He, W. Gao, P. Fatehi, Oxidation of kraft lignin with hydrogen peroxide and its application as a dispersant for kaolin suspensions, ACS Sustainable Chemistry and Engineering, 5 (2017) 10597-10605.

[81] A.V. Maldhure, J.D. Ekhe, Preparation and characterizations of microwave assisted activated carbons from industrial waste lignin for Cu(II) sorption, Chemical Engineering Journal, 168 (2011) 1103-1111.

[82] M. Martin-Martinez, M.F.F. Barreiro, A.M.T. Silva, J.L. Figueiredo, J.L. Faria, H.T. Gomes, Lignin-based activated carbons as metal-free catalysts for the oxidative degradation of 4-nitrophenol in aqueous solution, Applied Catalysis B: Environmental, 219 (2017) 372-378.

[83] Y. Zhang, J. Liao, X. Fang, F. Bai, K. Qiao, L. Wang, Renewable High-Performance Polyurethane Bioplastics Derived from Lignin-Poly(ε-caprolactone), ACS Sustainable Chemistry and Engineering, 5 (2017) 4276-4284.

[84] X.-f. Li, Y. Zuo, Y. Zhang, Y. Fu, Q.-x. Guo, In situ preparation of K_2CO_3 supported Kraft lignin activated carbon as solid base catalyst for biodiesel production, Fuel, 113 (2013) 435-442.

[85] S. Hu, F. Jiang, Y.-L. Hsieh, 1D Lignin-Based Solid Acid Catalysts for Cellulose Hydrolysis to Glucose and Nanocellulose, ACS Sustainable Chemistry & Engineering, 3 (2015) 2566-2574.

[86] X. Li, F. Shu, C. He, S. Liu, N. Leksawasdi, Q. Wang, W. Qi, M.A. Alam, Z. Yuan, Y. Gao, Preparation and investigation of highly selective solid acid catalysts with sodium lignosulfonate for hydrolysis of hemicellulose in corncob, RSC Advances, 8 (2018) 10922-10929.

[87] L. Hu, X. Tang, Z. Wu, L. Lin, J. Xu, N. Xu, B. Dai, Magnetic lignin-derived carbonaceous catalyst for the dehydration of fructose into 5-hydroxymethylfurfural in dimethylsulfoxide, Chemical Engineering Journal, 263 (2015) 299-308.

[88] N. Srisasiwimon, S. Chuangchote, N. Laosiripojana, T. Sagawa, TiO_2/Lignin-Based Carbon Composited Photocatalysts for Enhanced Photocatalytic Conversion of Lignin to High Value Chemicals, ACS Sustainable Chemistry and Engineering, 6 (2018) 13968-13976.

[89] H. Zhou, H. Xu, Y. Liu, Aerobic oxidation of 5-hydroxymethylfurfural to 2,5-furandicarboxylic acid over Co/Mn-lignin coordination complexes-derived catalysts, Applied Catalysis B: Environmental, 244 (2019) 965-973.

Chapter 2 *In-situ* catalytic upgrading of bio-oil derived from fast pyrolysis of lignin over high aluminum zeolites

2.1. Introduction

As described in **Chapter 1**, the high dependency of society to fossil-based industry has resulted in serious problems such as depletion petroleum resource and environmental pollution. The development of environmental friendly fuels, chemical feestocks, and materials has attracted many researchers to find the alternative resouces. One of the most logical and abundant carbon-based feedstock to replace petroleum-based materials is lignocellulosic biomass which consists of cellulose, hemicellulose, and lignin. Lignin is considered as the abundance of renewable aromatic resource in the world. It is mainly produced in pulp and paper industry as by-product [1]. Unlike cellulose and hemicellulose, the use of lignin has no effect on food supply since it is non-edible [2]. Nowadays, the depletion of fossil fuels and its impact on environment make lignin as a promising aromatic platform resources for the production of aromatic hydrocarbons [3].

Pyrolysis is one of classical thermochemical process for cleavage of lignin to liquid products, i.e., bio-oil [4]. However, such a bio-oil contains a large amount of oxygenated aromatic functional groups so that it cannot be directly used as fuel and must be upgraded prior to use [5,6]. Catalytic upgrading of bio-oil is one of processes to remove oxygen in the oxygenated compounds and improve its quality [7]. Zeolite catalyst is widely applied for the upgrading of bio-oil by deoxygenation, in which the strong acid sites in zeolites are responsible for the dehydration, decarboxylation, demethoxylation, and so on to convert oxygenated components to aromatic hydrocarbons as shown in Scheme 2.1 [8]. It is reported that the Si/Al molar ratio determined the number of Brønsted acid sites, and H-ZSM-5 zeolite with high Al/Si molar ratio exhibited high performance for the catalytic pyrolysis of various lignin feedstock such as alkaline lignin [9],

milled wood lignin [10], Chinese fir lignin, and rice straw lignin [11]. Jae *et al.* [12] found that the framework and pore size distribution in the zeolite also had great effect on the conversion of glucose to aromatic chemicals after testing 13 different kinds of zeolites. To date, H-ZSM-5, H-USY, H-Mordenite, and H-Beta zeolites, silica, γ-Al_2O_3, macropore materials such as MCM-41, SBA-15, MSU-J have been investigated for the fast pyrolysis of lignin by using pyrolysis-gas chromatography-mass spectrometry (*Py*-GC-MS), in which the catalyst was mixed with lignin [9-11,13,14]. *Py*-GC-MS is a pyrolysis process performed in micropyrolyzer and the obtained volatile products are directly analyzed by GC-MS. It is a convenient way for the catalyst screening. However, the ratio of catalyst-to-biomass in *Py*-GC-MS was too high and the coke and char products cannot be distinguished since they were mixed with the catalyst together in the final product [15].

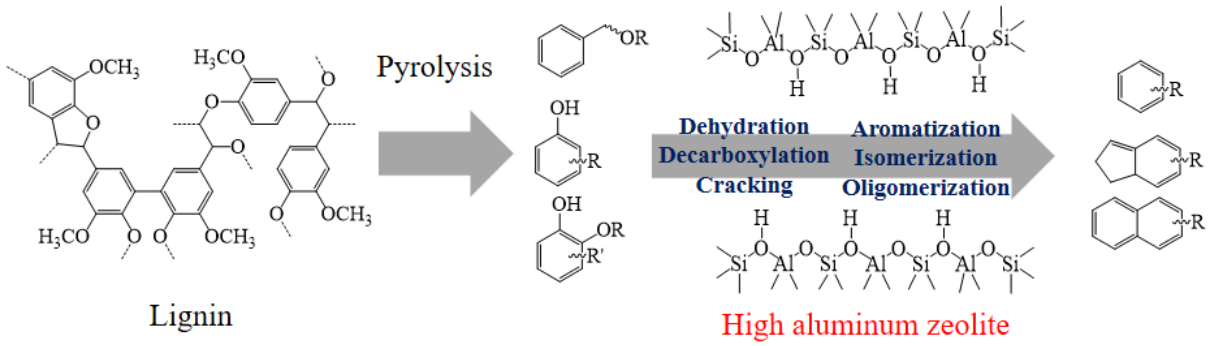

Scheme 2.1 Reaction pathway on catalytic upgrading of bio-oil derived from fast pyrolysis of lignin

Thring *et al.* [16] reported that the highest yield of liquid from pyrolysis of Alcell® lignin was 43 wt.% by using H-ZSM-5 zeolite at 550 °C and the main products were benzene, toluene, and xylene (BTX) with toluene dominating. Ma *et al.* [9] claimed that the liquid yield reached 74.9 wt.% by using a H-USY zeolite, but a high catalyst-to-lignin ratio was used. However, the composition distribution of liquid product, including water and bio-oil (heavy oil and light oil),

were unknown in these works. To solve this problem, *in-situ* catalytic upgrading of bio-oil in which the catalyst was separately placed with biomass and only contacted with pyrolysis vapors was suggested [17]. As such, the real amount of coke on the catalyst and the product distribution, i.e., char, coke, gas, bio-oil and water, can be easily determined [18-20].

In this work, in order to find suitable high aluminum zeolites for the deoxygenation of bio-oil derived from the fast pyrolysis of lignin, *in-situ* catalytic upgrading of bio-oil during the fast pyrolysis of lignin over five types of high aluminum zeolites, i.e., H-Ferrierite, H-Mordenite, H-ZSM-5, H-Beta and H-USY zeolites, were performed in a fixed bed reactor placed in a rapid heating infrared furnace. The zeolite was characterized by BET, XRD and NH_3-TPD, and the upgraded bio-oil was analyzed by GC-MS and Karl-Fisher analyzer. It is expected to provide a guidance for the selection of a suitable zeolite for the *in-situ* catalytic deoxygenation of bio-oil derived from fast pyrolysis of lignin with more information than *Py*-GC-MS, especially the amounts of light-oil, coke, gas, and water for scaling up the catalytic upgrading process. Moreover, it is expected to clarify mechanism of deoxygenation of bio-oil derivatives from pyrolysis of lignin over different framework structures in high aluminum zeolites via *in-situ* catalytic upgrading method.

2.2. Materials and Methods

2.2.1. Materials

Dealkaline lignin from Tokyo Chemical Industry Co., Ltd., Japan (TCI) was used as the feedstock, which was dried overnight at 110 °C prior to use. As shown in Table 2.1, the dried lignin had a moisture content of 0.3 wt.% determined by moisture balance and an ash content of 15.2 wt.% determined from the residual weight after calcination at 800 °C for 2 h in air with an

elemental composition of C (63.0 wt.%), H (5.5 wt.%), O (24.9 wt.%), S (6.4 wt.%) and N (0.2 wt.%).

Table 2.1. Proximate and ultimate analysis of dried lignin

Feedstock	Proximate Analysis (wt.%)				Ultimate Analysis[a] (wt.%)				
	Moisture	Volatile Matter	Fixed Carbon	Ash	C	H	N	S	O
Dried Lignin	0.3	42	42.5	15.2	63.0	5.5	0.2	6.4	24.9

[a] dry basis

High aluminum zeolites with cation type-H, i.e., H-USY (HSZ-330; Si/Al 6), H-Mordenite (HSZ-620; Si/Al 15), H-Ferrierite (HSZ-722; Si/Al 18), H-ZSM-5 (HSZ-822; Si/Al 24) and H-Beta (HSZ-931; Si/Al 28) were purchased from TOSOH Corp., Japan. These selected zeolites had the highest aluminum content for each type. All zeolites were calcined at 650 °C for 2 h in air with a heating rate of 10 °C/min to remove the remaining impurities, and thereafter pressed to tablet form and then crushed and sieved to a 0.1-1.0 mm of particle size.

2.2.2. Lignin characterization

Thermal degradation of the dried lignin was analyzed by thermogravimetric analyzer (DTG-60H, Shimadzu, Japan). Less than 10 mg of dried lignin was heated with a heating rate of

20 °C/min in a temperature range of 50-700 °C (ΔT = 50 °C) [21]. High purity of nitrogen was used as carrier gas with a flow rate of 50 cm^3/min.

2.2.3. Zeolite characterization

Surface area and pore distribution of the zeolites were determined by nitrogen adsorption measurement (Nova 4200e, Quantachrome, USA). Before measurement, the calcined zeolite was vacuum-degassed at 200 °C for 2 h. Brunauer-Emmet-Teller method (BET) was used for determination of the total surface area and t-plot method was used for determination of micropore volume. Distribution of acid sites on the zeolite was analyzed by ammonia desorption measurement (NH_3-TPD) (BELCAT, Japan). The crystalline structure of the zeolite was characterized by using X-ray diffractometry (Smartlab, Rigaku, Japan) in the 2θ-range of 10-70 °.

2.2.4. In-situ catalytic upgrading of bio-oil

Figure 2.1 shows the equipment configuration of *in-situ* catalytic upgrading of bio-oil from the fast pyrolysis of lignin. A quartz fixed bed reactor was set in an infrared furnace (RHL-E210P, Ulvac-Rico, Inc., Japan), by which the heating rate can be set as high as 1000 °C/min so that the feedstock is rapidly heated up. The weight ratio of zeolite to the dried lignin was 1:1 [18], which were separated by a thin layer of quartz wool. Nitrogen was passed through the reactor with a flow rate of 100 cm^3/min for about 15 min before pyrolysis starting. For the *in-situ* catalytic upgrading of bio-oil during the fast pyrolysis, the reactor was rapidly heated up to 650 °C with a heating rate of 1000 °C/min and then held at 650 °C for 5 min, in which the generated bio-oil was carried by nitrogen gas from the lignin layer to the catalyst layer and deoxygenated. The upgraded bio-oil was collected by acetone in a bottle with cold bath. The non-condensable gases were passed

through a gas dryer and collected in a gas bag. Each experiment was performed at least 2 times with an error less than 10 %.

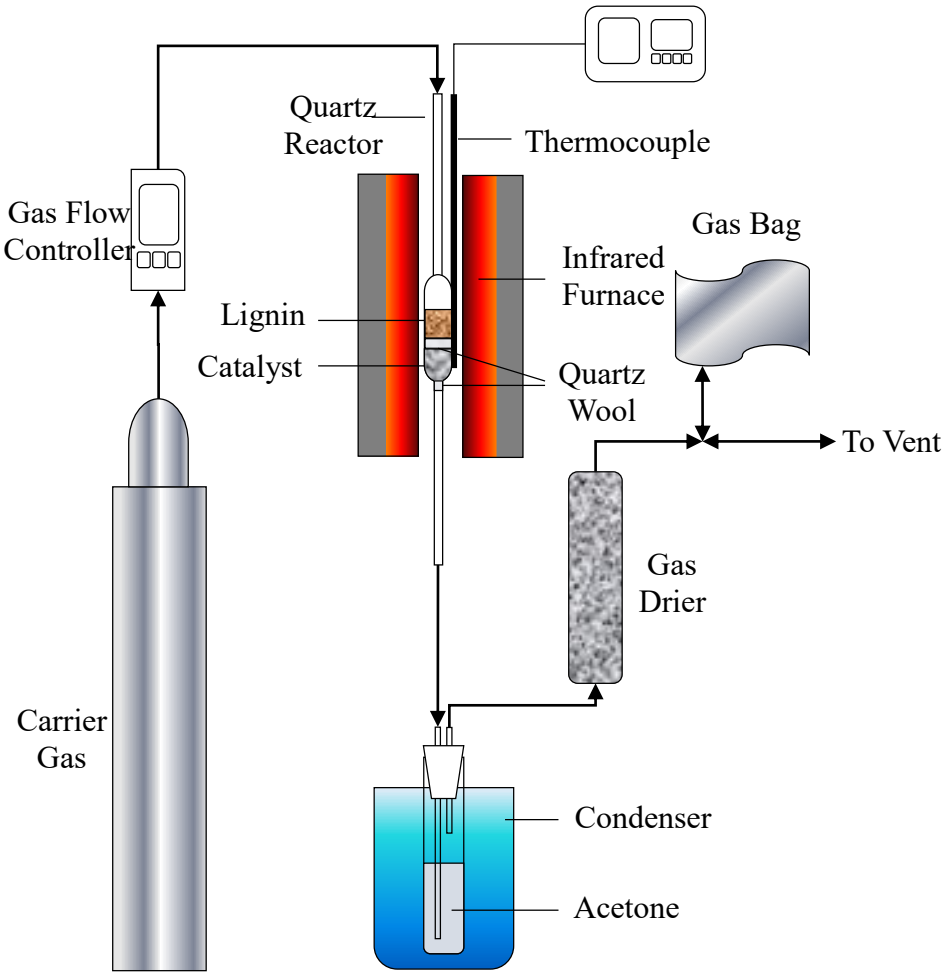

Figure 2.1 Schematic equipment configuration of in-situ catalytic upgrading of bio-oil derived from the fast pyrolysis of lignin.

The collected bio-oil was analyzed by GC-MS (GC-2010 Plus for GC, QP-2010 Ultra for MS, Shimadzu Japan) with an Ultra ALLOY+-5 capillary column. One microlitre of the bio-oil in acetone was injected into GC-MS using an auto-injector with an injection temperature of 300 °C. The column temperature was increased from 50 to 300 °C with a heating rate of 10 °C/min and hold at 300 °C for 10 min. In this analysis, only the light bio-oil with boiling point below 300 °C

can be detected. For identification of the compositions of the light bio-oil, all mass spectra were compared with those data in the NIST 08 mass spectrum library. As shown in Figure 2.2, the light oil in this study was classified into seven groups: monoaromatic hydrocarbons (MAHs), polyaromatic hydrocarbons (PAHs), aromatic oxygenated, phenol, phenol ether, thiol & sulfur, and furan & other. Moreover, for quantitative analysis, aromatic hydrocarbons were classified into six groups: benzene, monosubstituted benzene, disubstituted benzene, trisubstituted benzene, indene and naphthalene groups. The amount of aromatic hydrocarbons was determined by curve fitting of similar backbone structure of standard chemicals, i.e., benzene, toluene, *p*-xylene, mesitylene, indene and naphthalene, which were purchased from Wako Chemicals Co., Ltd., Japan.

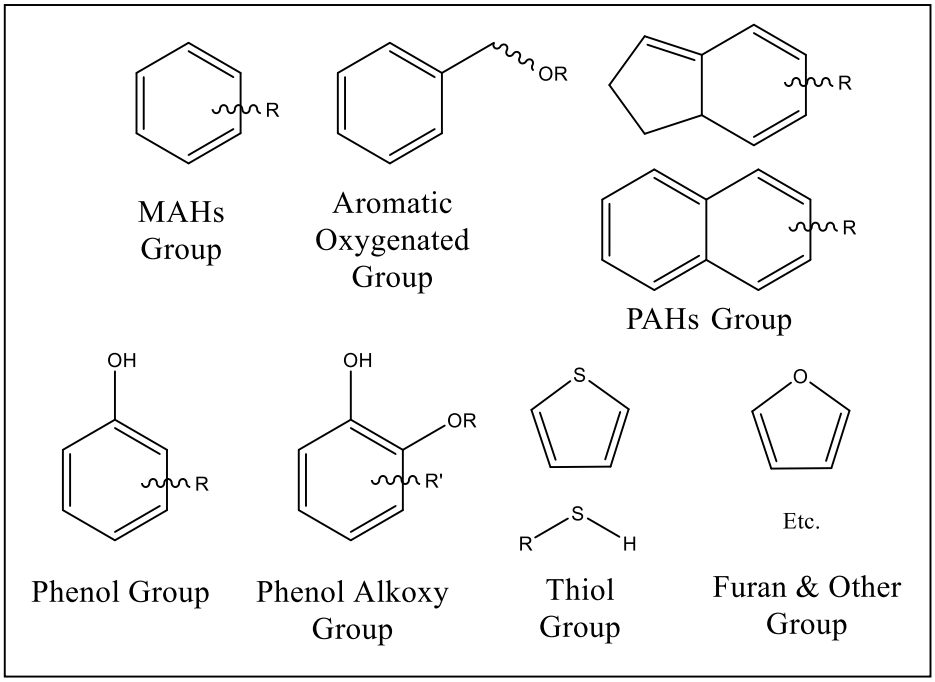

Figure 2.2 Classification of the product in light bio-oil.

The non-condensable gases were analyzed by GC-TCD (GC-TCD, Agilent 7890, USA). To quantify non-condensable gases, GC-TCD was also calibrated by the standard gas CO_2, CH_4, CO,

and H_2, which were provided by Japan Fine Product Co., Ltd., Japan. The amount of deposited coke on zeolite was determined by measuring the weight loss of the spent zeolite calcined at 650 °C for 2 h in air. Karl-Fisher titration (MKS-500, KEM, Japan) was applied to determine the water content in the bio-oil. In this study, since the lignin and zeolite were separately placed in the reactor for the catalytic upgrading of bio-oil, the yield of char can be assumed as the same as that obtained by pyrolysis of lignin without catalyst [18-20].

2.3. Results and discussion

2.3.1. Characteristics of lignin

In this work, the dried lignin was used as a feedstock in order to avoid the effect of moisture content on the pyrolysis of lignin. Table 2.1 shows the proximate and ultimate properties of the dried dealkaline lignin. One can see that a high amount of fixed carbon (42.5 wt.%) and a high mass ratio of carbon-to-hydrogen, and a high oxygen content were contained in the lignin. As shown in Figure 2.3, thermal decomposition of lignin occurred in a wide range of temperature. It is reported that the structure of lignin contains stable aryl ether linkages and the maximum decomposition rate of aryl ether bonding occurs at 376 °C [22]. Due to the decomposition of aryl ether linkages, lignin is generally decomposed to the aromatic oxygenated monomers and aromatic hydrocarbon derivatives [21,22].

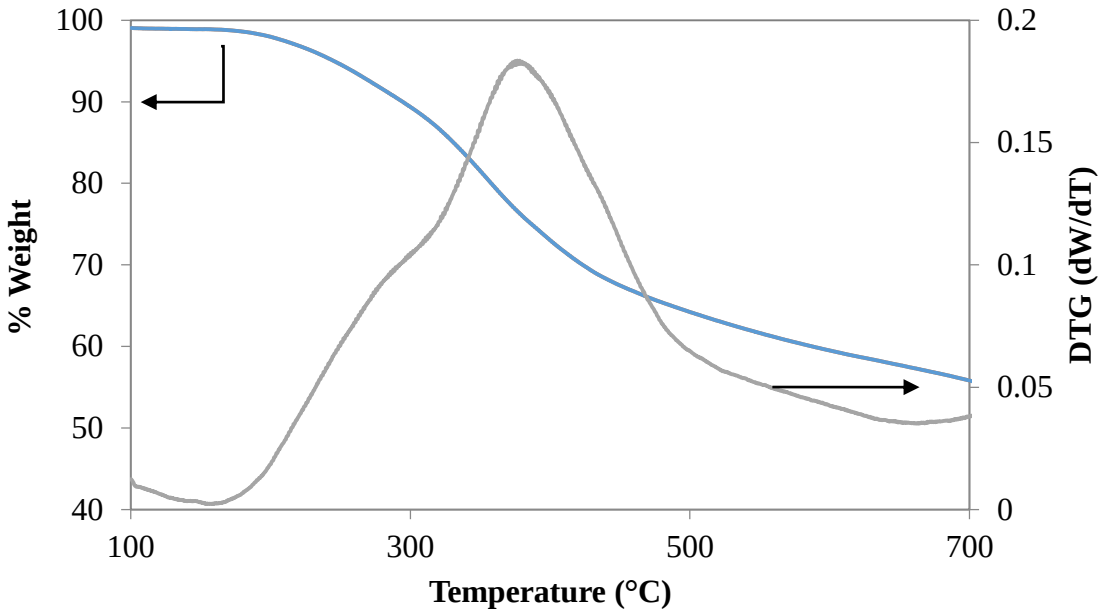

Figure 2.3 TG/DTG profile of dried lignin.

2.3.2. Catalyst characterization

As shown in Table 2.2, H-Ferrierite and H-Mordenite have two-dimensional channels and orthorombic structures. H-Ferrierite has ten-membered ring apertures of 4.2 × 5.4 Å interconnected with eight-membered rings apertures 3.5 × 4.8 Å while H-Mordenite has twelve-membered ring apertures of 6.5 × 7.0 Å interrelated with eight-ring apertures of 2.6 × 5.7 Å. H-ZSM-5, H-Beta and H-USY zeolites have three-dimensional structure. H-ZSM-5 zeolite has orthorombic structure with straight ten-membered ring apertures of 5.1 × 5.5 Å interconnected perpendicularly by channels with the corrugated ten-membered ring apertures of 5.3 × 5.6 Å. H-Beta and H-USY zeolites have twelve- and twelve-membered ring channel structure, respectively. Moreover, H-Beta zeolite has tetragonal structure with two parallel straight channel apertures of 6.6 × 6.7 Å linked to the corrugated channel ring apertures 5.6 × 5.6 Å while H-USY has cubic structure with twelve-membered ring apertures of 7.4 × 7.4 Å interconnected perpendicularly with each other

[23]. As shown in Table 2.2, BET surface areas of all zeolites are mainly contributed by micropores although external surface areas are also included in small portion, providing activities in the catalytic upgrading of bio-oil derived from lignin [14]. In contrast, H-Mordenite, H-Beta and H-USY zeolites with twelve-membered rings have higher surface areas than ten-membered ring zeolites, H-Ferrierite and H-ZSM-5, indicating that the channel and pore size of the zeolite contribute to its surface area.

Table 2.2. Characteristics of high aluminum zeolites used in this study.

Catalyst	H-Ferrierite	H-Mordenite	H-ZSM-5	H-Beta	H-USY
IZA code [23]	FER	MOR	MFI	BEA	FAU
Channel system [23]	10-8	12-8	10-10	12-12	12-12
Pore dimension [23]	2	2	3	3	3
Channel dimension (Å) [23]	[001] 4.2 × 5.4 [010] 3.5 × 4.8	[001] 6.5 × 7.0 [001] 2.6 × 5.7	[100] 5.1 × 5.5 [010] 5.3 × 5.6	<100> 6.6 × 6.7 [001] 5.6 × 5.6	<111> 7.4 × 7.4
Average pore sizes (Å) [24]	4.8	7	5.8	6.5	9
Si/Al molar ratio [24]	18	15	24	28	6
Total amount of acid sites (mmol NH_3/g catalyst)	1.44	1.22	1.23	0.75	0.93
S BET (m^2/g)[a]	260.2	368.4	333.3	414.2	494.1
S micro (m^2/g)[b]	209.9	345.9	265.0	316.1	402.4
S external (m^2/g)[b]	50.3	22.5	68.3	98.1	91.7
V total (cm^3/g)[b]	0.220	0.203	0.259	0.428	0.391
V micro (cm^3/g)[b]	0.102	0.168	0.130	0.112	0.200
CI Index	4.5 [25]	0.5 [26]	6.9 [27]	0.6 [28]	0.4 [28]

a BET method

b t-plot method

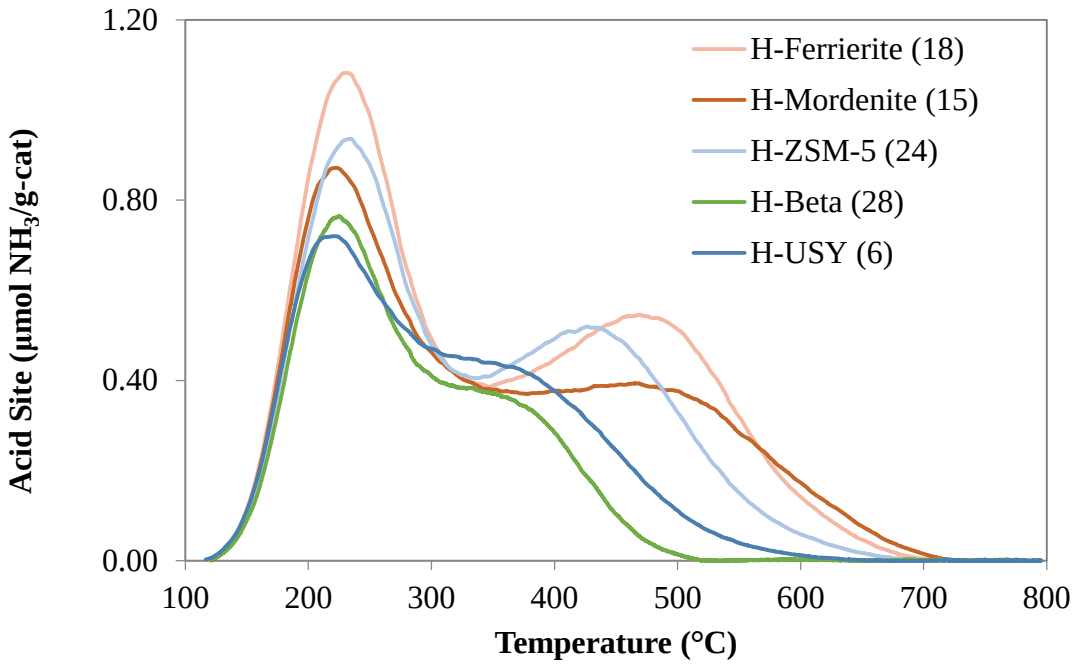

Figure 2.4 NH_3-TPD profiles of zeolites

Figure 2.4 shows NH_3-TPD profiles of all zeolites. One can see that the largest peak in each profile was observed at relatively low temperature range of 215-220 °C, and H-Ferrierite zeolite exhibited the highest total amount of acid sites among these zeolites. H-Beta zeolite has the lowest total peak area corresponding to acid sites, especially in the range of 400-600 °C which correspond to the strong acid sites. H-Ferrierite and H-ZSM-5 zeolites with ten-membered ring structures have strong high temperature acid sites at 470 °C and 420 °C, respectively. In contrast, H-Beta and H-USY zeolites with twelve-membered rings have low peak areas of acid site at high temperature. It indicates that the amount of acid sites is related to the channel structure in zeolite. Here, it should be noted that Si/Al molar ratio had no obvious effect on the total amount of acid sites although it was reported that the lowest Si/Al molar ratio had the highest acidity for H-ZSM-5 zeolite type [9-11]. In this study, the order of total amount of acid sites was H-Ferrierite > H-ZSM 5 ≈ H-Mordenite > H-USY > H-Beta as shown in Table 2.2.

2.3.3. Bio-oil derived from lignin without catalyst

It is reported that the highest bio-oil yield from lignin is generally obtained at 650 °C [9,13,14]. In the present study, the pyrolysis temperature was also selected at this temperature. Here, the amounts of the generated char, gas, and water during the pyrolysis process were determined directly by the instruments, but the bio-oil yield was determined by mass balance calculation as reported in the literature [29].

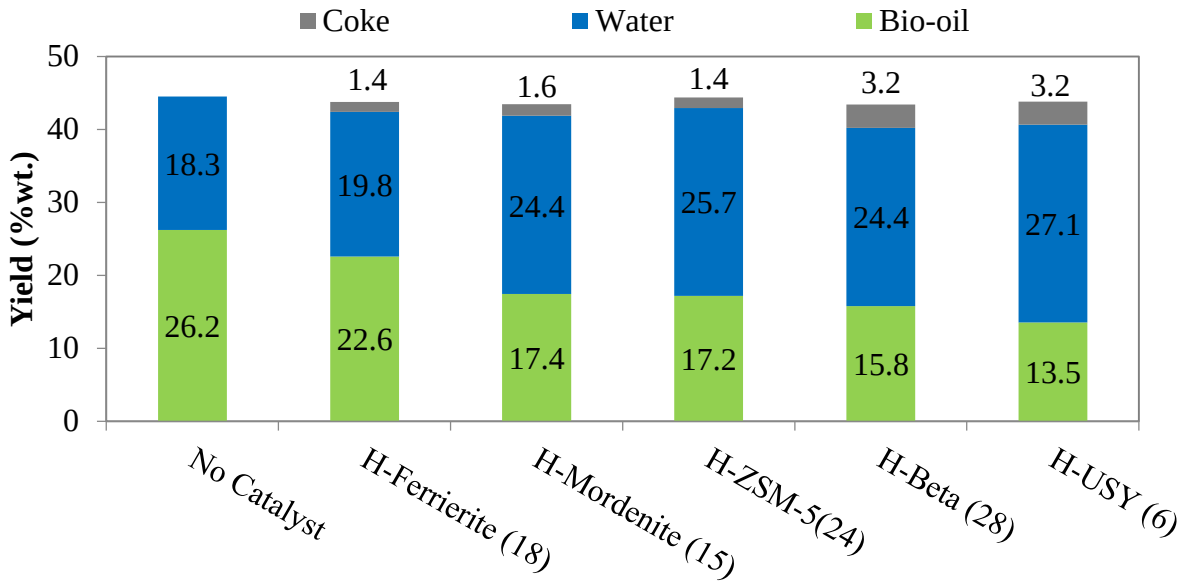

Figure 2.5 Yields of liquid products and coke from fast pyrolysis without catalyst and *in-situ* catalytic upgrading process.

Figure 2.5 shows the product distributions. One can see that the fast pyrolysis resulted in 52.2 wt.% char, 3.3 wt.% gas, 18.3 wt.% water and 26.2 wt.% bio-oil. It should be noted that the yield of char produced by pyrolysis experiment at 650 °C was lower than that from thermogravimetry

analysis (57.7 wt.%) with a slow pyrolysis, indicating that the fast pyrolysis was benefit for getting more decomposition product. Here, the obtained bio-oil included light oil and heavy oil. The compositions on the light oil with boiling points lower than 300 °C were detected by GC-MS. It is reported that oligomer structure of aryl ether existed in the heavy bio-oil since the thermal decomposition of lignin can produce reactive radicals of phenolic compounds which can be easily to be re-polymerized to the oligomer structure of aryl ether. Also, the strongest C-C linkage of aryl structure was found in the heavy bio-oil [29-33]. In this study, the analysis results of light oil were used to evaluate the performance of zeolites on the upgrading of bio-oil.

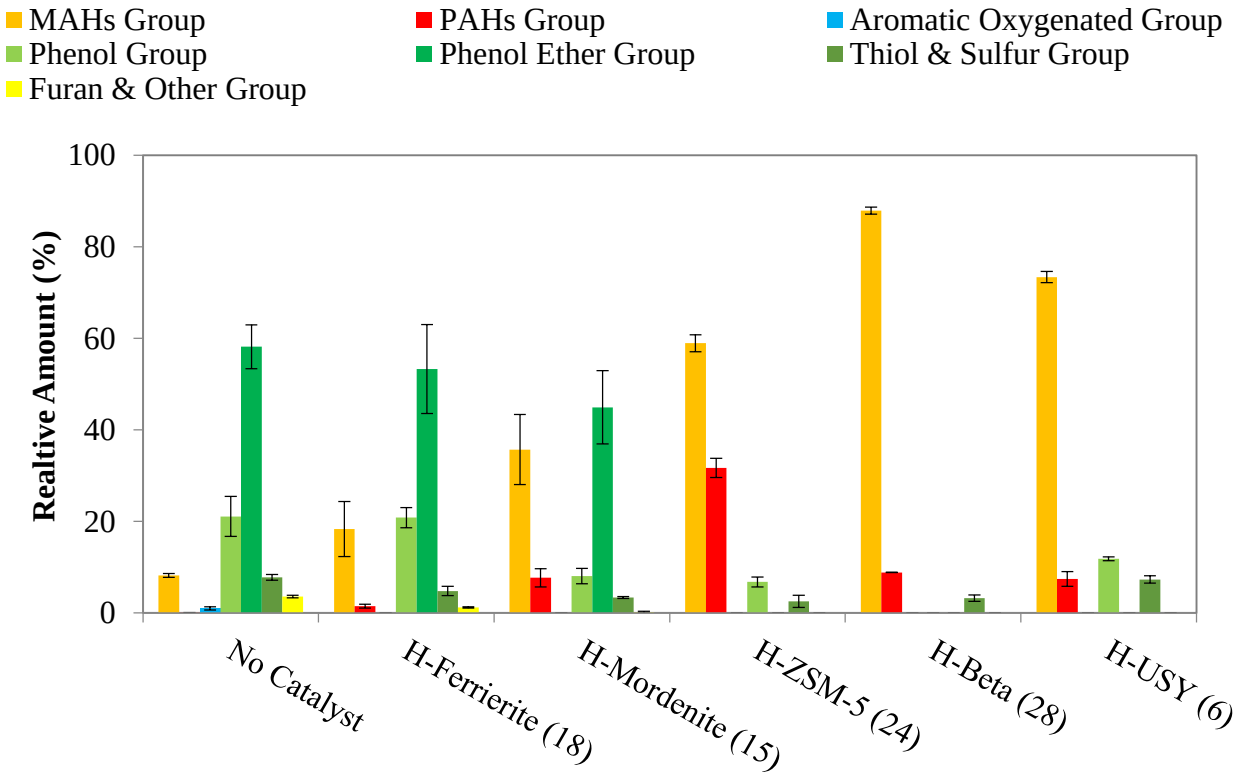

Figure 2.6 Chemical compositions in the light bio-oil from fast pyrolysis without catalyst and *in-situ* catalytic upgrading process.

Figure 2.6 shows the compositions of light oil in the bio-oil derived from lignin without a catalyst. One can see that phenol groups (phenol, cresol, dimethyl phenol, and so on), and phenol-ether groups (guaiacol, creosol, vanillin, and so on) were the main products with the selectivities of 21.1% and 58.2%, respectively. Here, these products should be derived from the decomposition of aryl ether linkages in the main structure. Thiol groups (dimethyl disulfide, dimethyl trisulfide, thiophene, and so on) were also included with a selectivity of 7.8%. In addition, furan and other groups (furan, propionic acid methyl ester, and so on) with a selectivity of 3.6% were contained in the light bio-oil and only a trace of aromatic oxygenated (anisole, benzofuran, cinnamaldehyde, and so on) and polyaromatic hydrocarbons (indene and naphatalene) were existed. It should be noted that the selectivity of monoaromatic hydrocarbons (benzene, toluene, xylene, and so on) was only 8.2%, and as shown in Figure 2.7, the yield of aromatic hydrocarbons including monosubstituted, disubstituted benzene and indene was approximately 4.0 mg/g-bio-oil. Moreover, Figure 2.8 indicates that the total yield of carbon dioxide, methane, carbon monoxide and hydrogen was about 2.08 mmol/g-lignin. Thus, a deoxygenation process should be performed in order to get higher yield of aromatic hydrocarbons.

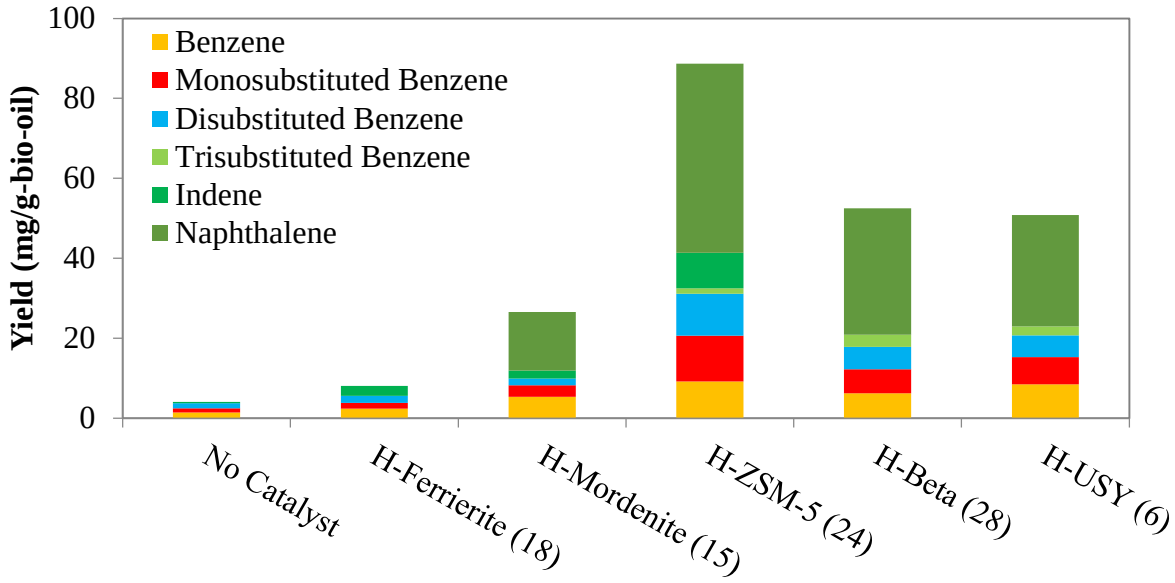

Figure 2.7 Yields of aromatic hydrocarbons in the light bio-oil from fast pyrolysis without catalyst and *in-situ* catalytic upgrading process.

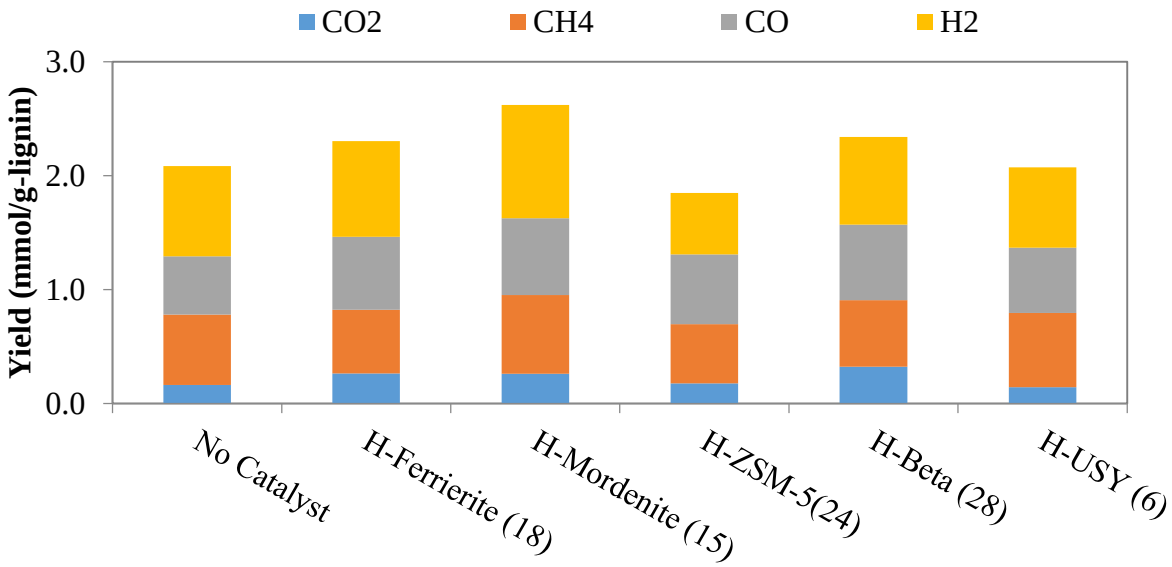

Figure 2.8 Yields of gas product from fast pyrolysis without catalyst and *in-situ* catalytic upgrading process.

2.3.4. Catalytic performances of various zeolites

Catalytic upgrading of bio-oil involves cracking, hydrogenation, aromatization, dehydration, decarbonylation, decarboxylation, and so on [34]. Deoxygenation from bio-oil could produce water, CO, and CO_2. Figure 2.5 shows the distributions of products. One can see that the yields of water, bio-oil and coke were not changed significantly from non-catalytic pyrolysis process (44.5 wt.%) to catalytic upgrading process (40.2-42.4 wt.%); however, the water yield was increased, indicating that the dehydration reaction occurred during the catalytic upgrading process. As such, the mass fraction of bio-oil derived from lignin with the *in-situ* catalytic upgrading decreased due to the dehydration reaction of oxygenated compounds contained in the liquid product. As shown in Figure 2.5, H-Ferrierrite zeolite, which has the highest amount of total acid sites but the smallest pore size among the tested zeolites, yielded the lowest amount of water. Whereas, H-USY zeolite, which has the second lowest total amount of acid sites but the largest pore size, yielded the largest amount of water. It is inferred from this comparison that the dehydration reaction should be mainly governed by the pore size but not the total amount of acid sites in the zeolite. As shown in Figure 2.6, H-Ferrierite and H-Mordenite with relatively smaller pore sizes (eight-membered rings) had low activity to convert the oxygenated products, while the H-USY, H-Beta, and H-ZSM-5 zeolites with relatively larger pore sizes had higher ability to convert the oxygenated products to the aromatic hydrocarbons product. It is expected that more derivatives in the bio-oil could enter the larger zeolite pores so that more active sites in the zeolite pores can be provided for the dehydration reaction. However, H-Beta zeolite with larger average pore size than H-ZSM-5 zeolite, resulted in a lower water yield than that over H-ZSM-5 zeolite because H-Beta zeolite has lower total amount of acid sites than H-ZSM-5 zeolite to be provided for the dehydration reaction. As shown in Table 2.3, the dimensions of the main oxygenated products are 6.7-8.1 Å on the y-axis, and the

dimensions of the main deoxygenated products, i.e., monoaromatic hydrocarbons and polyaromatic hydrocarbons are also 6.7-8.5 Å on the y-axis. It is reported that y-axis dimension of the oxygenated products determined whether the oxygenated products could enter into the pore of zeolite or not [14]. As shown in Figure 2.6, phenol and phenol ether groups were the main oxygenated products from the fast pyrolysis of lignin without catalyst. Hence, the conversion of oxygenated product should be related with the channel systems and pore sizes. With the increase in the channels and pore sizes, for example, from H-Ferrierite (10-8, 4.8 Å) to H-Beta zeolite (12-12, 6.5 Å), the conversion of oxygenated products increased. It indicates that the oxygenated products were difficult to diffuse into the H-Ferrierite zeolite pores even though it has high acidity. In contrast, H-Beta zeolite with lower acid sites has higher conversion of oxygenated product. It should be due to that the channel and pore sizes provided the access of oxygenated product to the acid sites. Furthermore, as shown in Figure 2.6, H-Beta zeolite almost converted oxygenated products completely into aromatic hydrocarbons even with the weight ratio that zeolite-to-lignin is 1:1. This result indicates that the *in-situ* catalytic upgrading process is more efficient than the catalytic pyrolysis in which the zeolite was mixed with lignin where the weight ratios of zeolite-to-lignin were high, i.e., 4:1 [9,10] and 20:1 [14]. However, it should be noted that the products with phenol groups still remained in the upgraded bio-oil when H-USY (12-12, 9 Å) zeolite was used even though its pore size was larger than H-Beta zeolite.

Table 2.3 Molecular dimension of model compounds in the upgraded bio-oil [14].

Model Compound	x (Å)	y (Å)	z (Å)
Phenol group & Aromatic oxygenated group			
Phenol	8.1	6.7	3.4
m-Cresol	8.1	7.4	4.2
Phenol ether group			
Guaiacol	9.5	8.1	4.2
Phenol, 2,6-dimethoxy	10.7	7.9	4.2
Vanillin	10.2	7.3	4.2
Monoaromatic hydrocarbons group			
Benzene	7.4	6.7	3.4
Toluene	8.3	6.7	4.2
p-Xylene	9.1	6.7	4.2
Mesitylene	9.0	8.5	4.2
Polyaromatic hydrocarbons group			
Indene	9.1	7.4	4.2
Naphthalene	9.2	7.4	3.4

Figure 2.7 shows the yield of aromatic hydrocarbons in the upgraded bio-oil. One can see that H-Ferrierite zeolite had the lowest performance for the conversions of phenol and phenol-ether groups to aromatic hydrocarbons even though it had high amount of acid sites. Here, the channel and pore sizes of H-Ferrierite zeolite (10-8, 4.8 Å) should hinder the phenol (6.7-7.4 Å) and phenol ether groups (7.3-8.1 Å) to enter. As shown in Figure 2.7, the yield of aromatic hydrocarbons by

using H-Ferrierite zeolite was only 8.1 mg/g bio-oil and the main compositions of aromatic hydrocarbons were benzene, monosubstituted benzene, disubstituted benzene and indene with molecular dimensions of 6.7-7.4 Å.

As shown in Figure 2.6, the catalytic performance of H-Mordenite zeolite was higher than that of H-Ferrierite in the conversion of phenol and phenol ether groups products; however, the oxygenated products still remained in the upgraded bio-oil. From Figure 2.7, one can see that the yield of aromatic hydrocarbons by using H-Mordenite zeolite was 26.7 mg/g-bio-oil, which was higher than that when using H-Ferrierite zeolite. Here, it should be noted that phenol and phenol ether groups cannot enter the eight-membered ring pores in H-Mordenite zeolite. Moreover, it is reported that the oxygenated products were highly converted to aromatic hydrocarbons when the zeolites had three-dimensional pore system [12,14]. It indicates that the diffusion of oxygenated products to the acid sites in three-dimensional pore system should be much easier than that in two-dimensional pore system.

Figure 2.7 indicates that the highest yield (88.7 mg/g-bio-oil) of aromatic hydrocarbons in the upgraded oil was achieved when H-ZSM-5 zeolite was used even though H-ZSM-5 had smaller channel and pore sizes (10-10, 5.8 Å). Oxygenated products with dimensions of 6.7-8.1 Å were converted to the aromatic hydrocarbons over this zeolite. It is possible that the channel and pore sizes of H-ZSM-5 were enlarged when the reaction was held at high temperatures [14]. High yields of monoaromatic hydrocarbons and polyaromatic hydrocarbons indicate that the channel and pore sizes of H-ZSM-5 are suitable to stabilize the intermediate structure of aromatic hydrocarbons. Meanwhile, the constraint index, which was observed from the relative reaction rates of n-hexane and 3-methyl pentane cracking [35], should play an important role. Zeolite with a high constraint index should give high steric hindrance effect [12]. Figure 2.9 shows the correlation of aromatic

hydrocarbons yield with the constraint index of zeolite. High constraint index of H-ZSM-5 zeolite resulted in a high yield of aromatic hydrocarbons. However, H-Ferrierite zeolite which has high constraint index, had the lowest catalytic activity because of its smaller dimension of channel and pore sizes. Meanwhile, as shown in Figure 2.10, H-Mordenite, H-Beta and H-USY with larger pore sizes and lower constraint index provided more void space to enhance the coking, resulting in the fast deactivation of zeolite [36].

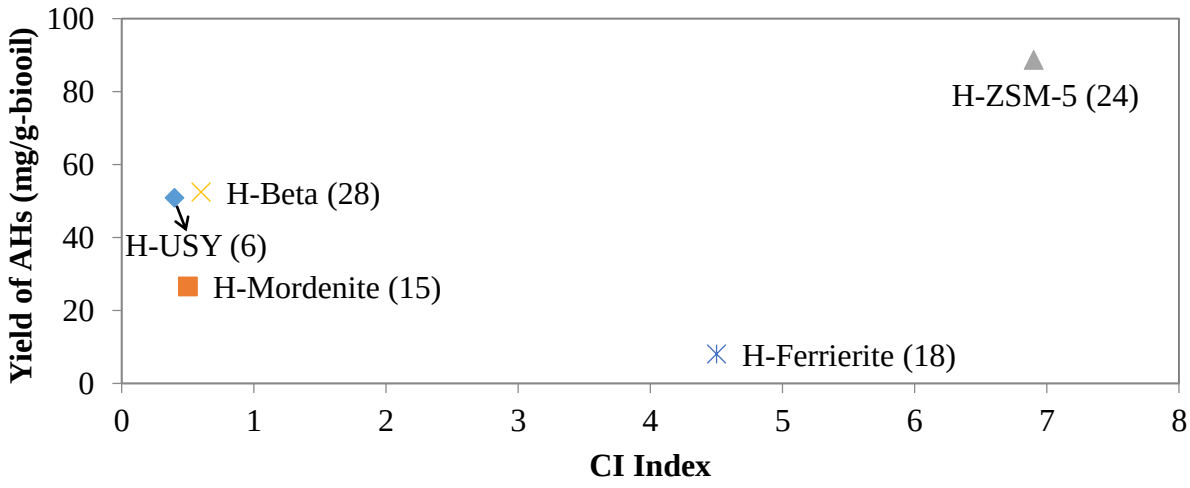

Figure 2.9 Correlation of aromatic hydrocarbons yield with the constraint index of zeolites.

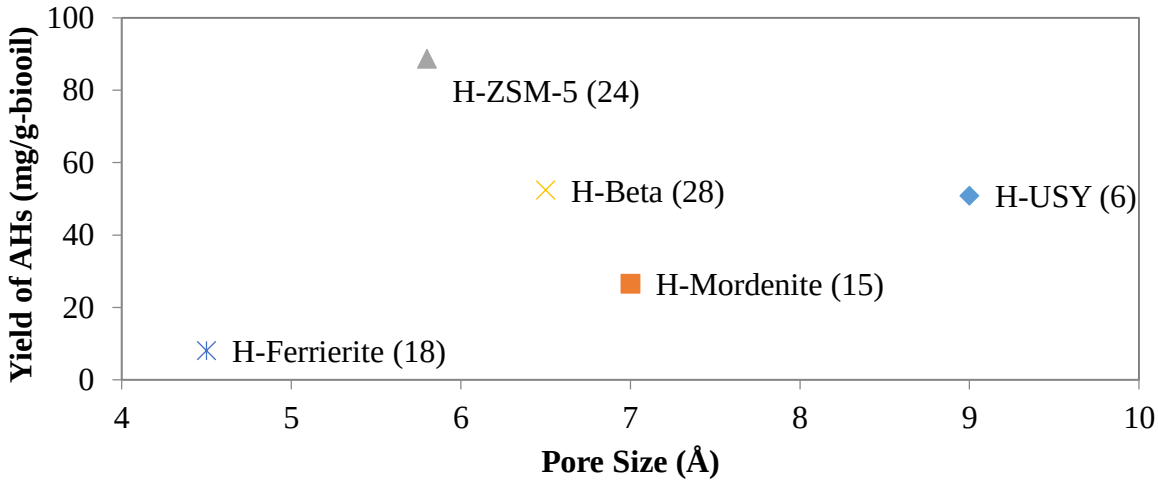

Figure 2.10 Correlation of aromatic hydrocarbons yield with the pore size of zeolites

As shown in Figure 2.7, by using H-Beta and H-USY zeolites, indene was not obtained while the yields of monoaromatic hydrocarbons and naphthalene products decreased. Sometimes, the larger pore could act as the medium for re-polymerization of polyaromatic hydrocarbons, resulting in the formation of larger aromatic molecules, i.e., coke formation [9]. As shown in Figure 2.6, H-USY deactivated much faster than H-Beta zeolite. One can see that all oxygenated products were converted to the aromatic hydrocarbons over H-Beta zeolite, while some phenol groups still remained in the product when H-USY zeolite was used even though the catalytic upgrading processes were performed in the same condition.

Similar to the conversion of oxygenated products, the selectivity of monoaromatic hydrocarbons increased with the increase of the channel and pore sizes (Figure 2.6), especially for H-Beta and H-USY zeolites. That is, H-Beta zeolite had higher selectivity than H-USY, but the yield of light bio-oil was almost the same (Figure 2.7). Figure 2.10 summarizes the correlation between the pore size of zeolite and the yield of aromatic hydrocarbons.

Figure 2.8 shows gas production in deoxygenation reaction. Decarbonylation and decarboxylation reaction produced carbon monoxide and carbon dioxide [34]. Meanwhile, methane was produced from demethylation [37]. Here, the gas yields are expressed as the molar yields. It is found that the gas yield in the catalytic upgrading process increased only a little. Moreover, the yields of methane and hydrogen over H-ZSM-5 zeolite were lower than those over other catalysts and non-catalytic process, which was related with the high light bio-oil yield over H-ZSM-5 zeolite as indicated above. Here, the generated hydrogen could serve as proton donor to stabilize intermediate radicals [38]. Therefore, the produced hydrogen could be consumed to prevent the intermediate radicals to be re-polymerized to the coke. Moreover, the low yield of

methane and high yield of substituted monoaromatic hydrocarbons indicate that the channel and pore sizes of H-ZSM-5 can hinder the demethylation reaction to produce methane.

Figure 2.11a and b show XRD spectra of zeolites before and after catalytic upgrading process. Although it is reported that high temperature can increase the inner pressure of the crystal lattice and break the framework structure [39], as shown in Figure 2.11b, after the regeneration (calcined in air at 650°C for 2 h), one can see that the zeolite crystalline structure remained unchanged, indicating that the zeolite structure can be well regenerated after the catalytic upgrading process at high temperature in the present study.

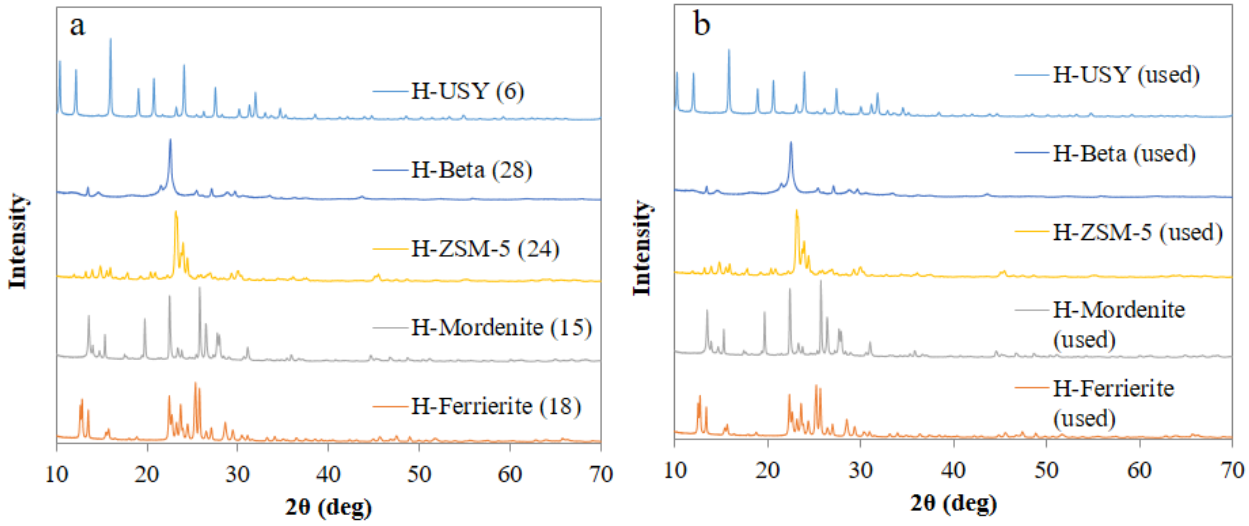

Figure 2.11 XRD spectra of zeolites (a) before reaction; (b) the spent zeolites after regeneration in air at 650°C for 2 h

2.4. Conclusions

Five types of high aluminum zeolites, i.e., H-Ferrierite, H-Mordenite, H-ZSM-5, H-Beta and H-USY zeolites were investigated for *in-situ* catalytic upgrading of bio-oil derived from fast pyrolysis of lignin. It is found that the channel structure, pore sizes and acidity of zeolite had significant effect on the upgrading quality, coke formation, and deoxygenation. H-ZSM-5 zeolite

with ten-membered rings of channel system and 5.8 Å of pore size resulted in the highest yield of aromatic hydrocarbons in the upgraded bio-oil. H-Beta zeolite with twelve-membered rings of channel system and 6.5 Å of pore size showed the highest selectivity towards monoaromatic hydrocarbons. In addition, the *in-situ* catalytic upgrading process is more efficient than the catalytic pyrolysis. It is expected to provide a guidance to select a zeolite for catalytic upgrading of bio-oil derived from lignin.

References

[1] Z. Fang, R.L. Smith, Production of biofuels and chemicals from lignin, vol. 6, Springer, Singapore, 2016.

[2] C. Li, X. Zhao, A. Wang, G.W. Huber, T. Zhang, Catalytic Transformation of Lignin for the Production of Chemicals and Fuels, Chemical Reviews, 115 (2015) 11559-11624.

[3] D. Stewart, Lignin as a base material for materials applications: Chemistry, application and economics, Industrial Crops and Products, 27 (2008) 202-207.

[4] B.V. Babu, Biomass pyrolysis: a state-of-the-art review, Biofuels, Bioproducts and Biorefining, 2 (2008) 393-414.

[5] G.W. Huber, S. Iborra, A. Corma, Synthesis of Transportation Fuels from Biomass: Chemistry, Catalysts, and Engineering, Chemical Reviews, 106 (2006) 4044-4098.

[6] Y.C. Lin, G.W. Huber, The critical role of heterogeneous catalysis in lignocellulosic biomass conversion, Energy and Environmental Science, 2 (2009) 68-80.

[7] S. Wan, Y. Wang, A review on ex situ catalytic fast pyrolysis of biomass, Frontiers of Chemical Science and Engineering, 8 (2014) 280-294.

[8] C. Zhao, Y. Kou, A.A. Lemonidou, X. Li, J.A. Lercher, Highly selective catalytic conversion of phenolic bio-oil to alkanes, Angewandte Chemie - International Edition, 48 (2009) 3987-3990.

[9] Z. Ma, E. Troussard, J.A. Van Bokhoven, Controlling the selectivity to chemicals from lignin via catalytic fast pyrolysis, Applied Catalysis A: General, 423-424 (2012) 130-136.

[10] J.Y. Kim, J.H. Lee, J. Park, J.K. Kim, D. An, I.K. Song, J.W. Choi, Catalytic pyrolysis of lignin over HZSM-5 catalysts: Effect of various parameters on the production of aromatic hydrocarbon, Journal of Analytical and Applied Pyrolysis, 114 (2015) 273-280.

[11] D. Shen, J. Zhao, R. Xiao, Catalytic transformation of lignin to aromatic hydrocarbons over solid-acid catalyst: Effect of lignin sources and catalyst species, Energy Conversion and Management, 124 (2016) 61-72.

[12] J. Jae, G.A. Tompsett, A.J. Foster, K.D. Hammond, S.M. Auerbach, R.F. Lobo, G.W. Huber, Investigation into the shape selectivity of zeolite catalysts for biomass conversion, Journal of Catalysis, 279 (2011) 257-268.

[13] V.B.F. Custodis, S.A. Karakoulia, K.S. Triantafyllidis, J.A. Van Bokhoven, Catalytic Fast Pyrolysis of Lignin over High-Surface-Area Mesoporous Aluminosilicates: Effect of Porosity and Acidity, ChemSusChem, 9 (2016) 1134-1145.

[14] Y. Yu, X. Li, L. Su, Y. Zhang, Y. Wang, H. Zhang, The role of shape selectivity in catalytic fast pyrolysis of lignin with zeolite catalysts, Applied Catalysis A: General, 447-448 (2012) 115-123.

[15] D.A. Ruddy, J.A. Schaidle, J.R. Ferrell Iii, J. Wang, L. Moens, J.E. Hensley, Recent advances in heterogeneous catalysts for bio-oil upgrading via “ex situ catalytic fast pyrolysis”: catalyst development through the study of model compounds, Green Chem., 16 (2014) 454-490.

[16] R.W. Thring, S.P.R. Katikaneni, N.N. Bakhshi, Production of gasoline range hydrocarbons from Alcell lignin using HZSM-5 catalyst, Fuel processing technology, 62 (2000) 17-30.

[17] A. Galadima, O. Muraza, In situ fast pyrolysis of biomass with zeolite catalysts for bioaromatics/gasoline production: A review, Energy Conversion and Management, 105 (2015) 338-354.

[18] J. Rizkiana, G. Guan, W.B. Widayatno, J. Yang, X. Hao, K. Matsuoka, A. Abudula, Mg-modified ultra-stable Y type zeolite for the rapid catalytic co-pyrolysis of low-rank coal and biomass, RSC Advances, 6 (2016) 2096-2105.

[19] W.B. Widayatno, G. Guan, J. Rizkiana, J. Yang, X. Hao, A. Tsutsumi, A. Abudula, Upgrading of bio-oil from biomass pyrolysis over Cu-modified β-zeolite catalyst with high selectivity and stability, Applied Catalysis B: Environmental, 186 (2016) 166-172.

[20] S. Karnjanakom, A. Bayu, X. Hao, S. Kongparakul, C. Samart, A. Abudula, G. Guan, Selectively catalytic upgrading of bio-oil to aromatic hydrocarbons over Zn, Ce or Ni-doped mesoporous rod-like alumina catalysts, Journal of Molecular Catalysis A: Chemical, 421 (2016) 235-244.

[21] D.-l. Guo, S.-b. Wu, B. Liu, X.-l. Yin, Q. Yang, Catalytic effects of NaOH and Na_2CO_3 additives on alkali lignin pyrolysis and gasification, Applied Energy, 95 (2012) 22-30.

[22] M. Brebu, C. Vasile, Thermal degradation of lignin - A review, Cellulose Chemistry and Technology, 44 (2010) 353-363.

[23] C. Baerlocher, L.B. McCusker, D. Olson, W.M. Meier, C. International Zeolite Association. Structure, Atlas of zeolite framework types, Six ed., Elsevier Science, Amsterdam, 2007.

[24] T. Corp, Zeolite, in, 2017.

[25] M.D. Macedonia, E.J. Maginn, Impact of confinement on zeolite cracking selectivity via Monte Carlo integration, AIChE Journal, 46 (2000) 2504-2517.

[26] H.v. Bekkum, E.M. Flanigen, P.A. Jacobs, J.C. Jansen, Introduction to zeolite science and practice, vol. 137, Elsevier Science, Amsterdam, 2001.

[27] S.I. Zones, T.V. Harris, The Constraint Index test revisited: anomalies based upon new zeolite structure types, Microporous and Mesoporous Materials, 35-36 (2000) 31-46.

[28] Y.F. Chu, Catalytic reforming with improved zeolite catalysts, in, United States, 1988.

[29] P.R. Patwardhan, R.C. Brown, B.H. Shanks, Understanding the fast pyrolysis of lignin, ChemSusChem, 4 (2011) 1629-1636.

[30] A.I. Afifi, J.P. Hindermann, E. Chornet, R.P. Overend, The cleavage of the aryl-O-CH_3 bond using anisole as a model compound, Fuel, 68 (1989) 498-504.

[31] R. Bayerbach, D. Meier, Characterization of the water-insoluble fraction from fast pyrolysis liquids (pyrolytic lignin). Part IV: Structure elucidation of oligomeric molecules, Journal of Analytical and Applied Pyrolysis, 85 (2009) 98-107.

[32] G. Jiang, D.J. Nowakowski, A.V. Bridgwater, Effect of the Temperature on the Composition of Lignin Pyrolysis Products, Energy & Fuels, 24 (2010) 4470-4475.

[33] P.F. Britt, A.C. Buchanan, K.B. Thomas, S.-K. Lee, Pyrolysis mechanisms of lignin: surface-immobilized model compound investigation of acid-catalyzed and free-radical reaction pathways, Journal of Analytical and Applied Pyrolysis, 33 (1995) 1-19.

[34] M. Al-Sabawi, J. Chen, S. Ng, Fluid Catalytic Cracking of Biomass-Derived Oils and Their Blends with Petroleum Feedstocks: A Review, Energy & Fuels, 26 (2012) 5355-5372.

[35] V.J. Frillette, W.O. Haag, R.M. Lago, Catalysis by crystalline aluminosilicates: Characterization of intermediate pore-size zeolites by the “Constraint Index”, Journal of Catalysis, 67 (1981) 218-222.

[36] J.R. Carpenter, S. Yeh, S.I. Zones, M.E. Davis, Further investigations on Constraint Index testing of zeolites that contain cages, Journal of Catalysis, 269 (2010) 64-70.

[37] M.A.n. González-Borja, D.E. Resasco, Anisole and Guaiacol Hydrodeoxygenation over Monolithic Pt–Sn Catalysts, Energy & Fuels, 25 (2011) 4155-4162.

[38] M. Kleinert, T. Barth, Phenols from Lignin, Chemical Engineering & Technology, 31 (2008) 736-745.

[39] J. He, X. Yang, D.G. Evans, X. Duan, New methods to remove organic templates from porous materials, Materials Chemistry and Physics, 77 (2002) 270-275.

Chapter 3 Utilization of Dealkaline Lignin as a Source of Sodium-Promoted MoS_2/Mo_2C Hybrid Catalysts for Hydrogen Production from Formic Acid

3.1. Introduction

Conversions of lignin to value-added chemicals or materials are attracting more and more attentions [1]. Various depolymerization processes for lignin such as acid/base catalyzed hydrolysis [2,3], pyrolysis [4,5], hydroprocessing [6], and oxidation [7] have been widely studied. However, in the biorefinery processes, almost half of lignin cannot convert to other chemicals and remain as char in the final product since lignin is a kind of thermo-stable polymeric compound which is difficult to be completely decomposed, as indicated in the **Chapter 2**. Recently, utilization of lignin as functional materials for dispersant [8], emulsifier [9], carbon black [10], carbon fiber [11], and supercapacitor [12] has received growing attention as alternative ways of lignin utilization to lignin refinery. Since carbon (C), sulfur (S), and some alkaline metal species such as Na are contained in lignosulfonate lignin, it can be a promising precursor to produce sulfur and sodium-contained hybrid catalysts. For example, transition metal carbides and sulfides have attracted considerable attentions because they show catalytic activity similar to noble metals in various catalytic reactions such as hydrogenation since the addition of those elements in transition metal (like tungsten or molybdenum) lattices can change the electron distribution on metal elements and affect the electronic negativity of the metal carbides in a desirable direction to improve their activities [13-15]. In the synthesis of transition metal carbides, precursor to provide carbon source is necessary. Thusly, lignin can serve as the carbon precursor for synthesis of catalysts. Moreover, it is expected that doping some other elements on the transition metal carbides such as Mo_2C may improve their catalytic activities. As such, S, and Na in lignosulfonate lignin could be served as the precursors to form MoS_2 and/or Na_2S simultaneously besides the main

catalytic component of Mo_2C, so that the obtained hybrid catalysts are expected to show higher activity for various reactions such as hydrogen production from formic acid, dry reforming of methane, steam reforming of methanol, steam reforming of biomass tar, and water-gas-shift reaction [16]. It is reported that the presence of alkali metal ions can make a significant change in the manner of Pd/C catalyst for the formic acid (a model chemical in biomass-derived bio-oil) decomposition with a liquid-like "solution" mechanism [17], as follows:

$$K_2CO_3 + 2HCOOH \rightarrow 2HCOO^- + 2K^+ + H_2O + CO_2 \quad (1)$$

$$HCOOH \leftrightarrow HCOO^- + H^+ \quad (2)$$

$$HCOO^- + Pd \rightarrow PdH + CO_2 + e^- \quad (3)$$

$$H^+ + Pd + e^- \rightarrow PdH \quad (4)$$

$$2PdH \leftrightarrow 2Pd + H_2 \quad (5)$$

Formic acid has regarded as a potential on-site hydrogen source for fuel cells because its storage and transportation is much easier than gaseous hydrogen [18]. Although gravimetric hydrogen storage capacity of formic acid corresponds only to 4.4 wt%, formic acid has a high density of 1.22 g/cm^3. Hence, the energy density of formic acid equals to 1.77 kW·h/dm^3 which is higher than commercial hydrogen pressure tanks of Toyota Mirai (1.4 kW.h/dm^3, 70 MPa) [19,20]. However, decomposition of formic acid occurs with two reaction pathways; dehydrogenation (CO_2 + H_2) and dehydration (CO + H_2O). Carbon monoxide is harmful for PEFC-type fuel cells, so that development of catalysts which may promote the former reaction quite selectively is a key issue for utilizing formic acid as a hydrogen carrier. Noble metal based catalysts such as Au [21-23], Pd [17], and Pt [24] based ones have been reported intensively for this reaction. However, the high price and scarcity or resources of noble metals limit their large-scale application. Thusly, it is necessary to develop non-precious metal catalysts for formic acid decomposition. To date, only a

few non-precious metal catalysts have been reported such as α-Fe_2O_3 [25], γ-Al_2O_3 [26], MoS_2 [14], and Mo_2C [27,28]. Among them, MoS_2 and Mo_2C are reported to exhibit sufficient activity for achieving over than 90% of formic acid conversion, however, selectivity toward hydrogen is lower than 95% [14,27,28]. Meanwhile, although α-Fe_2O_3 is the cheapest catalyst, the catalytic activity is low.

In the present study, dealkaline lignin (DAL) was used as a carbon and sulfur source to prepare MoS_2/Mo_2C based catalysts (Mo-DAL) with a facile impregnation-pyrolysis two-step process and used for the selective hydrogen production from formic acid. The prepared catalysts were characterized using a scanning electron microscope (SEM) with an energy dispersive X-ray detector (EDX), transmission electron microscope (TEM), X-ray diffraction (XRD), N_2 absorption measurements, and Raman spectroscopy. Moreover, effects of Mo loading amount and the existences of sulfur and sodium species on the catalyst performance were investigated. This study provides a new viewpoint to utilize waste dealkaline lignin as a precursor of low-cost and effective MoS_2/Mo_2C based catalysts with high selectivity for the hydrogen production from formic acid.

3.2. Materials and Methods

3.2.1. Synthesis of Mo-DAL catalysts.

Mo-DAL catalysts were prepared by using a facile impregnation-pyrolysis two-step process. In brief, varying amount of ammonium heptamolybdate tetrahydrate ($(NH_4)_6Mo_7O_{24}.4H_2O$, Wako Pure Chemical Industries, Japan) was dissolved in 20 mL of DI water and then 5 g of dealkaline lignin (DAL) (Tokyo Chemical Industry Co., Ltd., Japan) was added into the solution. The mixture was stirred for two hours to obtain a homogenous suspension followed by drying in an oven at 110°C for 12 h. The obtained solid was ground and filled into a fixed-bed quartz reactor, which

was purged with argon gas at a flow rate of 50 cm^3/min for 30 min before pyrolysis process started. Then, the reactor was heated at 800 °C for 1 h with a heating rate of 5 °C/min and a 50 cm^3/min of argon flow. After the pyrolysis step, the reactor was cooled down to room temperature and the obtained catalyst was passivated in a 1% O_2/Ar gas flow for 12 h at room temperature. In the present study, the catalysts with 5, 10, and 20 wt% of Mo loading were prepared. The loaded amount of molybdenum was determined as follows: the weight of loaded molybdenum calculated from the weight of the molybdenum precursor used was divided by the weight of catalysts after pyrolysis and passivation processes. Hereafter, those catalysts are denoted as 5% Mo-DAL, 10% Mo-DAL, and 20% Mo-DAL.

3.2.2. Synthesis of Mo-CB and sodium loaded Mo-CB catalysts.

For comparison, two kinds of Mo-CB catalysts, i.e., 5% Mo_2C-CB and 5% MoS_2-CB catalysts, were prepared. The 5% Mo_2C-CB catalyst was synthesized with a similar method as the Mo-DAL catalyst by only replacing carbon source from DAL to carbon black (CB) (Vulcan XC 72R, CABOT Corp., USA). In addition, $(NH_4)_6Mo_7O_{24}.4H_2O$ was impregnated using a mixture of 20 mL of DI water and 2 mL of ethanol instead of pure DI water in order to disperse CB into the solution.

The 5% MoS_2-CB catalyst was synthesized according to the reported vulcanization method [29]. Mo_2C-CB and sulfur powder (Wako Pure Chemical Industries, Japan) with a molar ratio of Mo:S = 1:2.1 were ground together for 30 min. The obtained solid was put into a fixed-bed quartz reactor and pyrolyzed at 800 °C. After the pyrolysis step finished, the obtained material was cooled down to room temperature and passivated in 1% O_2/Ar for 12 h at room temperature.

Further, to investigate the addition effect of sodium on Mo-CB catalysts, 5% Mo_2C-CB and 5% MoS_2-CB were mixed with sodium formate (Wako Pure Chemical Industries, Japan) with a molar ratio of Mo:Na = 1:9.

3.2.3. Catalysts characterization.

The crystal structure of the catalysts were analyzed by a X-ray diffractometer (Rigaku Smartlab, Rigaku, Japan) in the 2θ range of 10-90° with a scanning step of 0.02° using Cu Kα radiation (k = 0.1542 nm) in order to identify crystalline material formed on the catalysts. A scanning electron microscope (SU8010, Hitachi, Japan) coupled with an energy dispersive X-ray detector (EMAX x-act, Horiba, Japan) was used to the semi-quantitative determination of a molar ratio of Na, Mo, and S atoms. The informatio[i]n of metal particle distribution and lattice spacing were characterized by using a transmission electron microscope (JEM-2100F, JEOL, Japan). BET surface area was measured through nitrogen adsorption at 77 K by using a surface area and pore size analyzer (NOVA 4200e, Quantachrome, USA). Raman spectroscopy measurement was performed by using a Raman spectrophotometer (NRS 5100, Jasco, Japan) equipping a laser source of 532 nm. Thermal degradation of the dealkaline lignin was analyzed by a thermogravimetric analyzer (DTG-60H, Shimadzu, Japan) with a nitrogen flow rate of 50 cm3/min. The elemental composition (C, H, N, and S) of the dealkaline lignin was analyzed by using an elemental analyzer (Vario EL cube, Elementar, German). Ash composition was analyzed by using an energy dispersive X-ray fluorescence spectrometer (EDX-800HS, Shimadzu, Japan).

ImageJ software, which is open source software, was used to process the TEM image. The sharpen function was used to increase the sharpness of the TEM image. Furthermore, the straight

function was applied to measure the lattice spacing distance which is calibrated by the standard measure bar on the TEM image.

3.2.4. Catalytic dehydrogenation of formic acid.

Catalytic performances were evaluated with a similar reported method [28,30]. Firstly, a catalyst was pressed into tablet form and then crushed and sieved to 0.25-0.5 mm of particle size. 0.25 g of catalyst particles packed in a fixed-bed reactor was activated under a stream of 15% CH_4/H_2 with a flow rate of 100 cm^3/min at 600 °C for 1 h prior to the reaction. Then formic acid vaporized at 120 °C was introduced with a stream of argon with a flow rate of 60 cm^3/min to the catalyst bed (WHSV of 4 h^{-1}; molar ratio of formic acid to argon is 136). The reaction was conducted at a temperature range from 130 to 240 °C. The gaseous product was passed through a gas dryer and collected in a gas bag for 10 min. The collected gas was analyzed by a gas chromatograph (Agilent 7890B, Refinery Gas Analyzer G3445 #526 series) equipped with molecular sieve 5A and hayesep Q columns as well as dual TCD detectors. Produced amounts of H_2, CO_2, CO_2, and CH_4 were quantified by the internal standard technique using the carrier gas of argon as an internal standard. The conversion of formic acid and H_2 selectivity were calculated by using the following equations of (3.1) and (3.2), respectively. For getting the reliable kinetic parameters, most of the data were collected at the condition that the conversion is lower than 15%. The TOFs were determined based on the total loading amount of molybdenum on the catalysts.

Equation 3.1 Conversion calculation of formic acid

$$\text{Conversion}\ (\%) = \frac{\text{mol}\ CO_2(\text{outlet}) + \text{mol}\ CO(\text{outlet})}{\text{mol}\ HCOOH(\text{Inlet})} \times 100$$

Equation 3.2 Selectivity calculation of hydrogen product

$$\mathrm{H_2\ selectivity\ (\%)} = \frac{\mathrm{mol\ H_2\ (outlet)}}{\mathrm{mol\ H_2(outlet) + mol\ CO\ (outlet)}} \times 100$$

3.3. Results and Discussion

3.3.1. Catalyst characterization.

In this work, molybdenum-based dealkaline lignin catalysts were synthesized by wet-impregnation of the molybdenum source on DAL followed by pyrolysis. The high fixed carbon as well as the presence of sodium and sulfur at DAL were confirmed by ultimate, proximate, and ash composition analysis (Table 3.1). Initially, in order to elucidate thermal behavior of DAL itself, both of fresh and pyrolyzed DAL without Mo loading were analyzed by XRD. The XRD pattern of pyrolyzed DAL is presented in Figure 3.1(a). At 2θ of 23.4° and 30.0° (ICDD card 00-003-0933), the peaks ascribable to Na_2S were observed. Considering the fact that Na_2S was not detected on fresh DAL, Na_2S was suggested to be formed by reduction of sulfate or sulfonate groups presented in dealkaline lignin. It is reported that the reduction of sulfate or sulfonate groups takes place at a temperature range of 750-790 °C in an endothermic manner [31]. An apparent weight loss at the same temperature range in an endothermic manner on the TGA-DTA analysis of fresh DAL was observed (Figure 3.2 (a)). Furthermore, the XRD peaks ascribable to Na_2SO_4 (ICDD card 00-005-0631) were observed on the fresh DAL. However, after the pyrolysis, the XRD peaks of Na_2SO_4 were converted to Na_2S (Figure 3.2 (b)). Those results support that the formation of Na_2S occurred by the reduction of sulfate and/or sulfonate with carbon species.

Table 3.1 Proximate, ultimate, and ash compositon of the dried dealkaline lignin.

Feedstock	Proximate Analysis (wt%)				Ultimate Analysis[a] (wt%)				Ash Composition[b] (wt%)			
	Moisture	Volatile Matter	Fixed Carbon	Ash	C	H	N	S	Na	S	Si	K
Dried Dealkaline Lignin	0.3	42	42.5	15.2	63.0	5.5	0.2	6.4	50.4	43.7	3.5	2.4

[a] Dry basis, [b] XRF analysis

The DAL-based catalysts with varying Mo loading amounts of 5 to 20 wt% were analyzed by XRD and TEM. The observation of peaks at 2θ of 23.4° and 30.0° (ICDD card 00-003-0933) clearly indicates the presence of Na_2S in 5% Mo-DAL (Figure 3.1). The TEM analysis also supports the presence of Na_2S since particles with a lattice spacing of 0.23 nm were observed (Figure 3.3 (a) and (c)). In the increase of Mo loading amount, the intensities of XRD peaks corresponding to Na_2S decreased (Figure 3.1). This fact suggests that Na_2S was consumed by the reaction with Mo species probably by forming MoS_2 and sodium intercalated MoS_2. In order to confirm the presence of MoS_2 and sodium intercalated MoS_2, the 5% Mo-DAL catalyst was analyzed by Raman spectroscopy, TEM, and XRD. The Raman spectrum of 5% Mo-DAL is shown in Figure 3.4. Observation of peaks at 389 cm^{-1} (E_{2g}, in-plane vibration of Mo-S) and 416 cm^{-1} (A_{1g}, the out-of-plane vibration of the S atoms) indicates the formation of MoS_2 species on the catalyst [29]. Furthermore, the presence of particles with lattice spacing of 0.61-0.66 nm ascribable to the (002) plane of MoS_2 was observed on TEM (Figure 3.3 (a) and (d)). This result also supports the presence of MoS_2 species [32]. In this analysis, not only the particles of MoS_2 but also the particles with an apparently larger lattice spacing of 0.76-0.82 nm, were also observed (Figure 3.3

(a) and (b)). These larger line spacings are probably caused by intercalation of sodium into the lattice of MoS_2 to form Na_xMoS_2. It is notable that these observed line spacings are quite close to the reported values [32]. The presence of Na_xMoS_2 was also confirmed by observation of a low angle broad peak centered at 2θ of 10.6° (d = 0.83nm) on the XRD pattern of 5% Mo-DAL (Figure 3.1). Although the peaks ascribable to β-Mo_2C were not clearly observed on 5% Mo-DAL by XRD, those were observed at 2θ of 34.4°, 37.9°, and 39.4° (ICDD 00-011-0680) on 10 and 20% Mo-DAL (Figure 3.1). As shown in Table 3.2, the formation of certain amount of β-Mo_2C on those catalysts is due to the lower ratio of S to Mo on those catalysts than 5%Mo-DAL. Therefore, only when excess amount of Mo over S atoms presents on catalysts, Mo species might react with carbon sources to form β-Mo_2C [15].

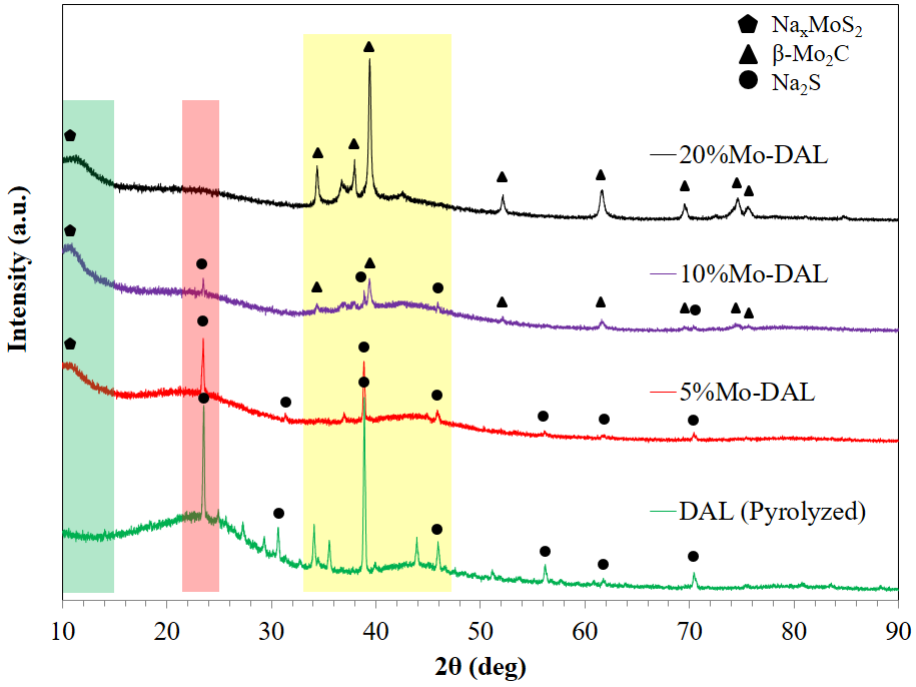

Figure 3.1 XRD patterns of DAL-based catalysts.

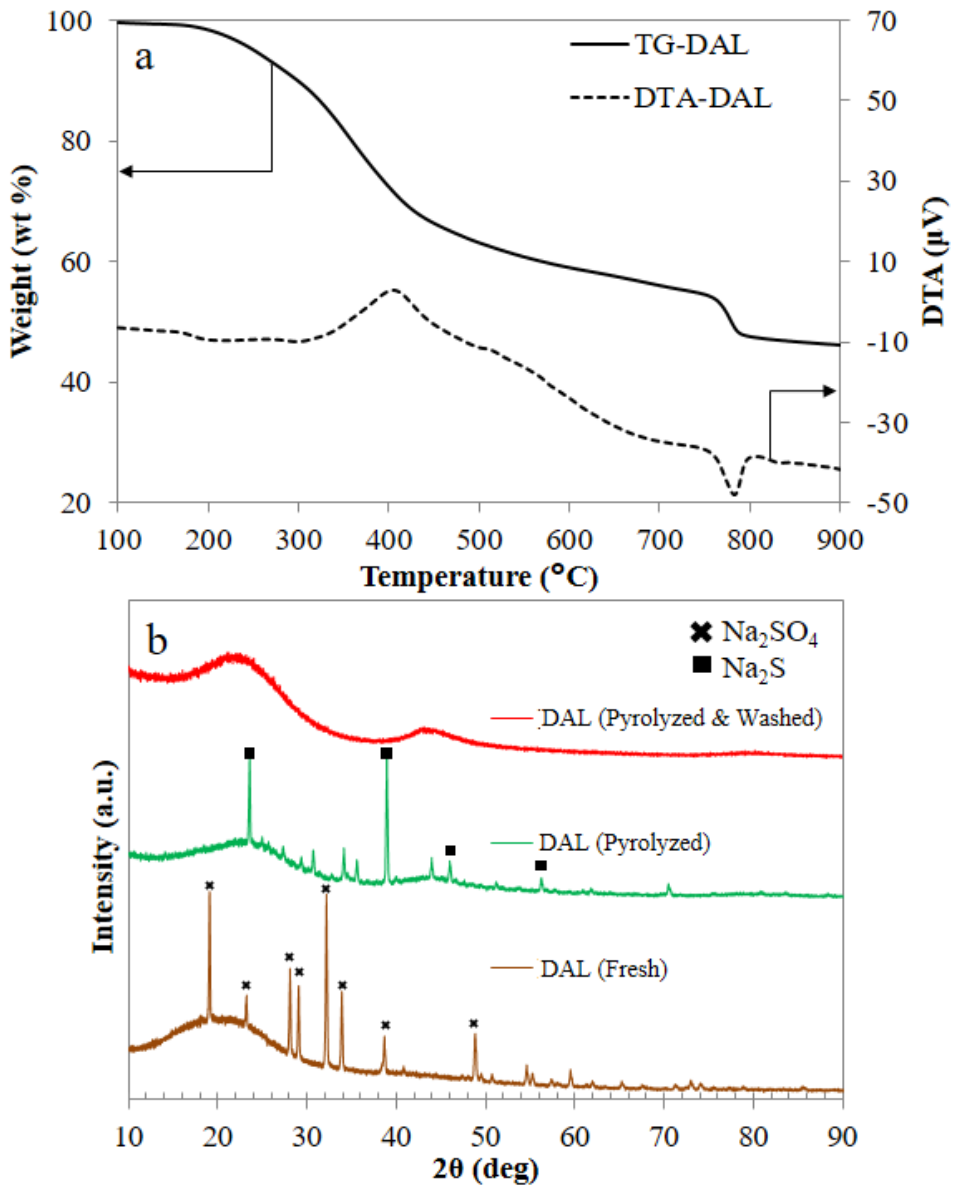

Figure 3.2 Dealkaline lignin characterization. (a) TGA-DTA profiles of DAL (b) XRD patterns of DAL, pyrolyzed DAL, and pyrolyzed-washed DAL.

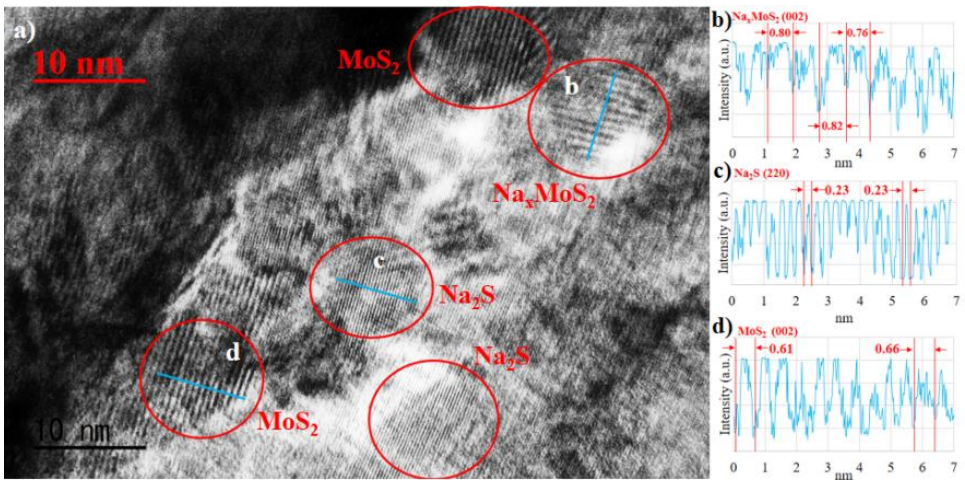

Figure 3.3 (a) TEM image of 5% Mo-DAL catalyst and line profile of (b) Na_xMoS_2, (c) Na_2S, and (d) MoS_2 particles.

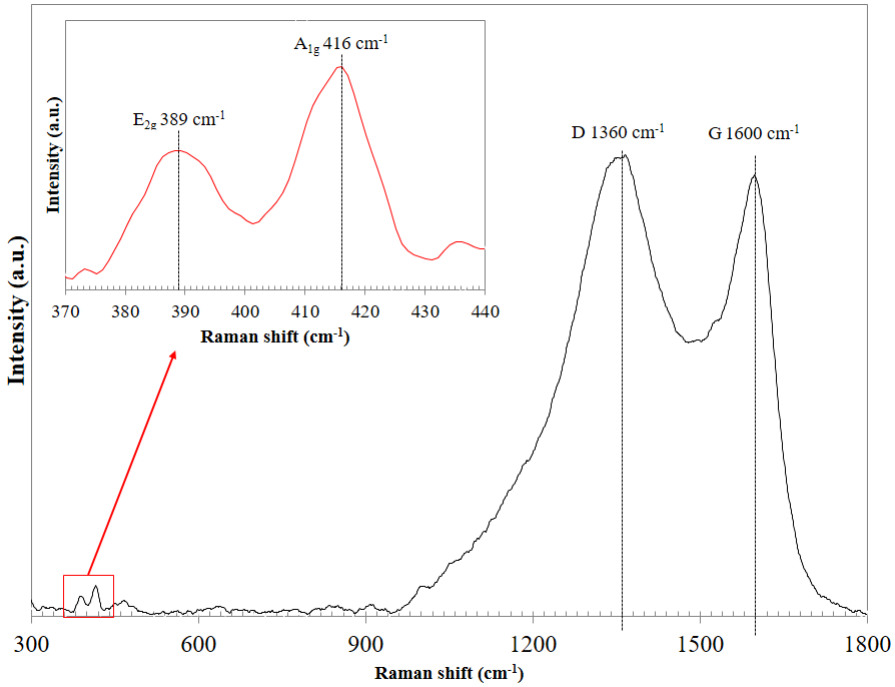

Figure 3.4 Raman spectra of 5% Mo-DAL catalyst. The inset shows the Raman spectra which indicates existence of MoS_2 on 5% Mo-DAL catalyst.

The state of carbon species on the catalysts were also investigated by Raman spectroscopy. Two peaks at 1375 cm^{-1} (D-band) and 1620 cm^{-1} (G-band) were observed on the Raman spectrum of 5% Mo-DAL (Figure 3.4). Generally, the intensity ratio between these two peaks (I_D/I_G) is known to express the degree of graphitization of carbonaceous materials [10]. The high I_D/I_G ratio observed on the 5% Mo-DAL catalyst indicates that carbon is mainly existed as amorphous. In the TEM analysis, the characteristic layered structure of graphite with a lattice spacing of 0.34 nm was not observed. In summary, it is demonstrated that a facile impregnation-pyrolysis two-step process using lignin as a precursor gave the molybdenum-based catalysts which have hybrid active sites composed of β-Mo_2C, MoS_2, and sodium intercalated MoS_2 deposited on the amorphous carbon.

3.3.2. Catalytic performance of the Mo-based DAL catalysts.

Table 3.2. Kinetic parameters for formic acid decomposition over Mo-DAL catalysts.

Entry	Catalysts	S_{BET}[a] (m^2/g)	Na/Mo[b]	S/Mo[b]	Temp. Optimum[c] (° C)	Conv. (%)	H_2 Selectivity (%)	H_2/CO_2 molar ratio	Ea ($kJ.mol^{-1}$)	ln A ($ln\ h^{-1}$)
1	DAL (Pyrolyzed)	< 1	-	-	240	4.2	5.7	0.26	-	-
2	5%Mo-DAL	2.2	8.9	4.6	240	97.3	99.2	1.04	80.0	24.8
3	10%Mo-DAL	12.4	5.3	2.3	230	97.5	98.9	1.03	83.8	25.7
4	20%Mo-DAL	19.7	2.2	0.8	220	98.0	99.4	1.04	75.1	22.9
5	5%Mo_2C-CB	176.5	-	-	240	90.3	88.1	0.94	92.7	26.8
6	5%MoS_2-CB	134.9	-	2.7	240	86.0	96.2	0.69	117.1	35.2
7	5%Mo_2C-CB-Na	104.2	8.6	-	230	99.1	93.7	1.07	76.1	24.1
8	5%MoS_2-CB-Na	100.0	8.5	2.2	230	99.1	97.1	0.98	74.6	23.9

[a]S_{BET} is calculated by using N_2 isotherm data of the multiple point method within P/P_0 lower than 0.3, [b]EDS analysis (mol/mol), [c]Based on the highest yield of H_2 product.

The catalytic decomposition of formic acid by using Mo-DAL with 5, 10, and 20 wt% of Mo loading was conducted at the temperature range of 130-240 °C with a WHSV of 4 h^{-1}. The results are summarized in Figure 3.5 and Table 3.2 (entry 2-4). Formic acid conversion increased by increasing reaction temperature regardless of the loading amount of Mo on the catalysts. In the selected temperature range, all the catalysts produced hydrogen with higher selectivity than 98%. Moreover, the ratio of H_2/CO_2 is close to 1 on those catalysts, suggesting the main reaction is dehydrogenation of formic acid. However, the trends of selectivity in temperature were slightly different for the catalysts. On the 10 and 20% Mo-DAL catalysts, the selectivity to hydrogen reached the maximum at 210 °C and then decreased at higher temperature, while the selectivity

constantly increased on 5% Mo-DAL. As discussed in the previous section, the Mo-DAL catalysts with 10 and 20 wt% of Mo loading mainly consist of β-Mo_2C, MoS_2, and sodium intercalated MoS_2, while 5% Mo-DAL catalyst consists of only MoS_2 and sodium intercalated MoS_2. The different components of catalytic active sites on these catalysts were supposedly reflected on the trends of selectivity in reaction temperature. In order to confirm that the catalytic activity of Mo-DAL catalysts was provided by Mo species, the reaction with the pyrolyzed DAL was also conducted (Table 3.2, entry 1). Even at 240 °C, the conversion of formic acid and selectivity to hydrogen were only 4.2 and 5.7%, respectively. These results clearly show that the catalytic activity of Mo-DAL was not provided by carbonaceous species, sulfide or basic sodium species but by Mo species. However, this fact does not mean that those sulfide and sodium species did not participate in the reaction at all. In the following sections, the support effects of DAL including additional effects of sulfur and sodium species are discussed.

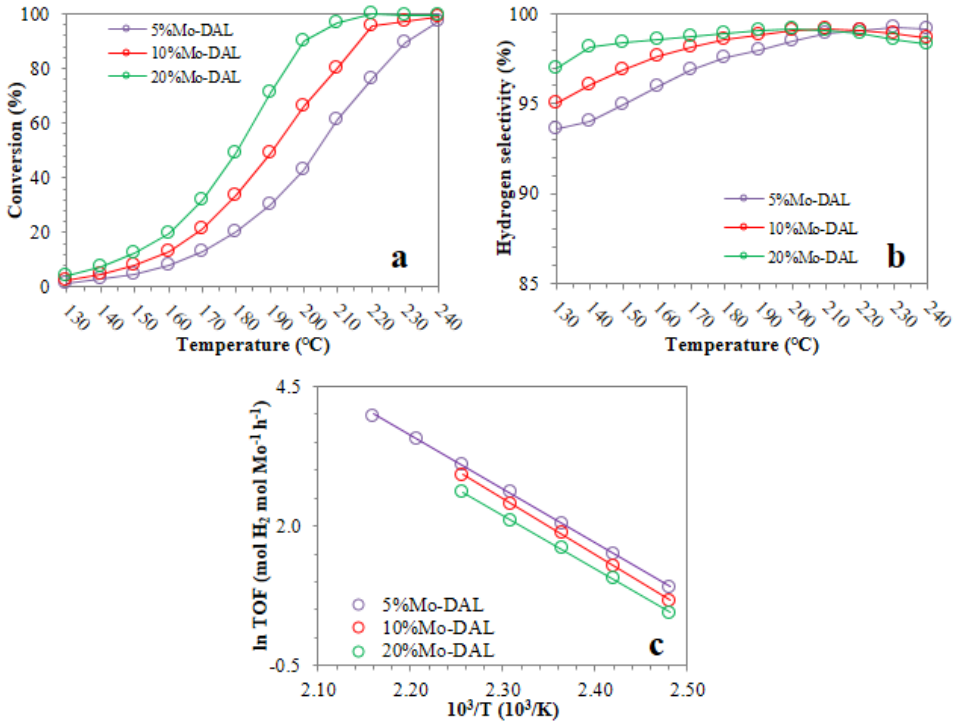

Figure 3.5 (a) The conversion profile (b) Hydrogen selectivity (c) Arrhenius plots of Mo-DAL catalysts.

3.3.3. Demonstration of the addition effects of sulfur and sodium.

In order to clarify the effects of coexisting elements on DAL, i.e. sulfur and sodium, the additional effects of those elements were investigated on the catalysts prepared with a pure carbon support as models. Here, carbon black was selected as the support and carbon source because other conventional carbon materials such as graphite and activated carbon are unsuitable by the following reasons: the former has insufficient surface area due to its high crystallinity and the latter usually contains alkaline metal elements that make unable to evaluate additional effects of those elements.

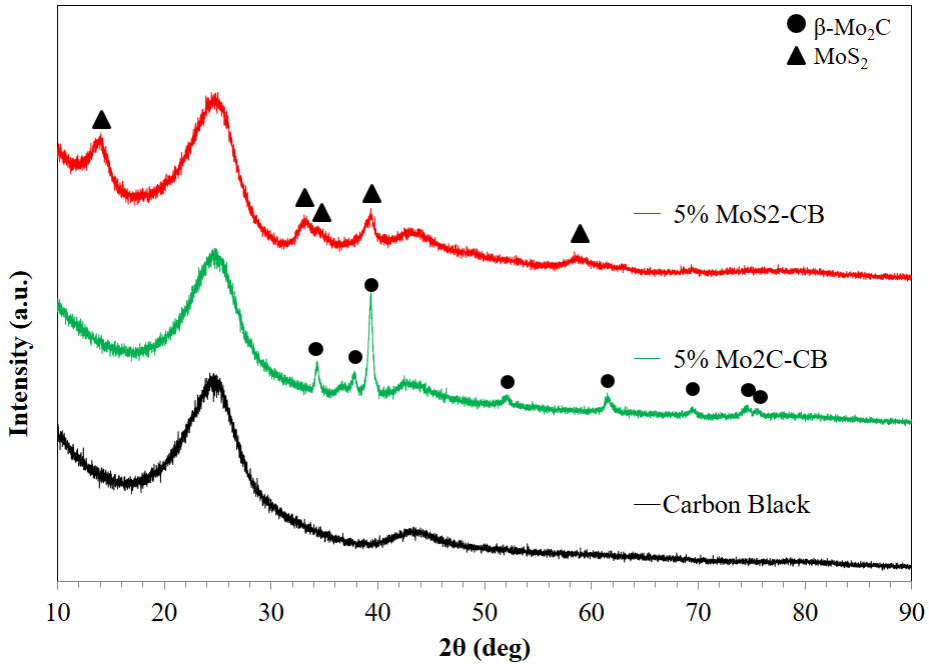

Figure 3.6 XRD patterns of carbon black (CB), 5% Mo_2C-CB, and 5% MoS_2-CB catalysts.

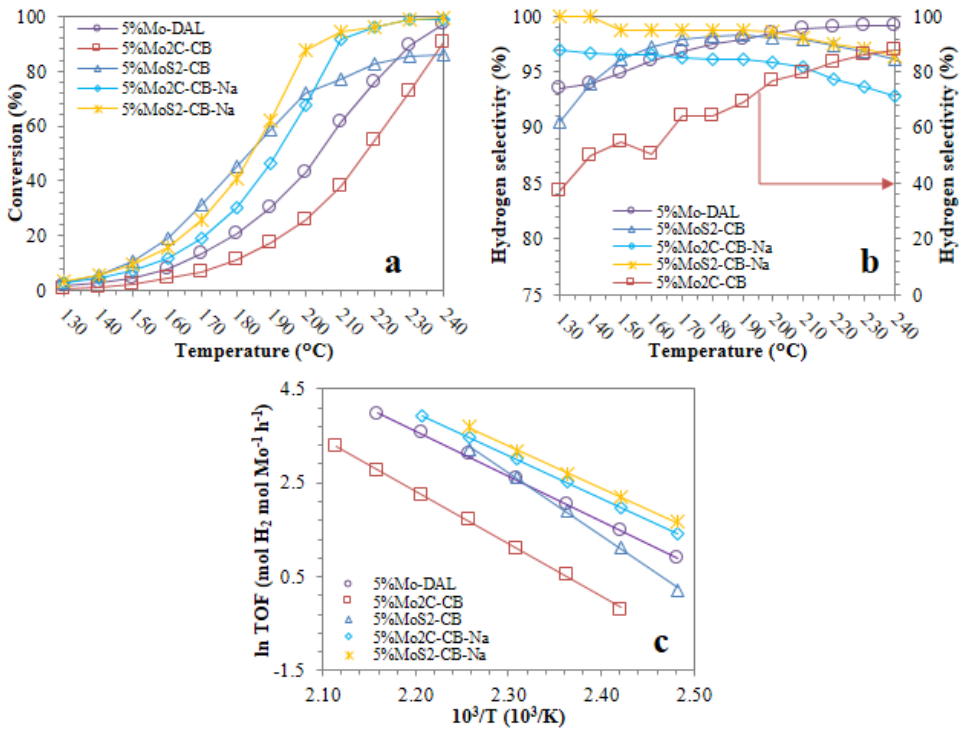

Figure 3.7 (a) The conversion profile (b) Hydrogen selectivity (c) Arrhenius plots of 5% Mo-DAL catalyst compared with the standard catalysts either without or with Na doping.

The 5 wt% of Mo loaded carbon black catalysts with two kinds of phases (Mo_2C and MoS_2-loaded) were prepared by the same procedures as for Mo-DAL and subsequent sulfurization. Successful formation of the β-Mo_2C and MoS_2 phases on the carbon black support was confirmed by XRD (Figure 3.6). The peaks at 2θ of 34.2°, 37.6°, and 39.4° observed for 5% Mo_2C-CB are ascribed to the Mo_2C phase (ICDD 00-011-0680), while those at 2θ of 14.1°, 33.3°, and 39.2° observed for 5% MoS_2-CB are attributed to the MoS_2 phase (ICDD 00-006-0097). The decomposition of formic acid with those catalysts was conducted in the same conditions as those for Mo-DAL catalysts (Figure 3.7). In the present conditions, 5% MoS_2-CB was superior to 5% Mo_2C-CB both in conversion of formic acid and selectivity to hydrogen at most of the temperature range. From this fact, it is obvious that S element presented in DAL was participated in improving

catalytic activity of Mo-DAL by the formation of more active MoS_2 species than β-Mo_2C. Our results are consistent to the previous report that MoS_2 nanoparticles supported on graphite was highly active for producing hydrogen from formic acid [14].

Addition effects of sodium were also investigated on the carbon black based catalysts. On the 5% Mo-DAL catalyst, formation of sodium formate was confirmed by XRD after the formic acid decomposition reaction (Figure 3.8). This result indicated that Na_2S originally contained in the pyrolyzed DAL reacted with formic acid to form sodium formate. Therefore, sodium formate was selected as a sodium source for examining addition effect of sodium. Sodium loaded catalysts, i.e. 5% Mo_2C-CB-Na and 5% MoS_2-CB-Na, were prepared just by mixing the parent Mo-CB catalysts (5% Mo_2C-CB and 5% MoS_2-CB) with sodium formate. The molar ratio of Mo:Na was adjusted to 1:9. The sodium added catalysts of 5% Mo_2C-CB-Na and 5% MoS_2-CB-Na exhibited much improved activity in the formic acid decomposition (Figure 3.7), while more drastic improvement was observed on the Mo_2C loaded catalyst than the MoS_2 loaded one. Jia et al. [17] also reported that the activity and stability of catalysts were improved when alkali metal ions were doped on Pd/C catalysts. The improvement was probably caused by two reasons. One is that basic sodium species provided absorption sites of the acidic reactant of formic acid on the catalysts [33]. The other one is that basic sodium species promote the dissociation of formic acid to form more reactive formate [17]. This was confirmed by the observation of XRD peaks corresponding to sodium hydrogen diformate at 2θ of 10.6°, 13.6°, 14.2°, and 35.4° (ICDD 01-075-7325) on spent DAL-based catalysts (Figure 3.8).

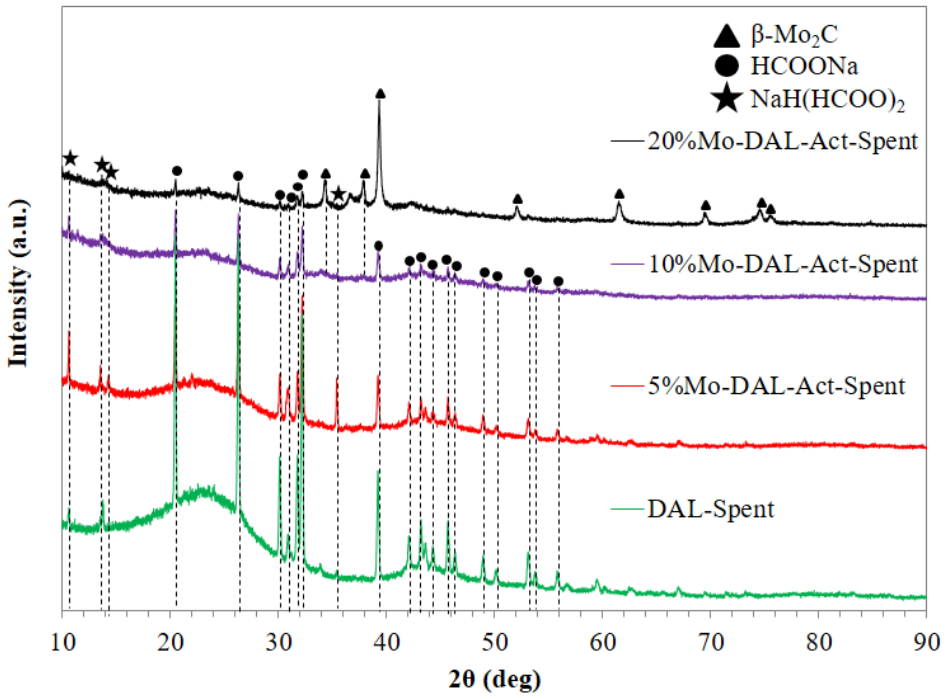

Figure 3.8 XRD patterns of DAL-based catalysts after catalytic performance test.

To get insights of catalytically active sites on the Mo-DAL catalysts, the activation energies on both DAL and carbon black based catalysts were compared (Table 3.2). Sodium undoped catalysts of 5% Mo_2C-CB and 5% MoS_2-CB showed relatively high activation energies of 92.7, 117.1 kJ·mol^{-1}, respectively. On the other hand, the sodium doped catalysts of 5% Mo_2C-CB-Na and 5% MoS_2-CB-Na showed lower activation energies of 76.1 and 74.6 kJ·mol^{-1}, respectively. This comparison also clearly shows that the catalytic activity of molybdenum species was effectively improved by sodium doping. Meanwhile, the activation energies observed for 5, 10, and 20% Mo-DAL catalysts were in the range of 75-84 kJ·mol^{-1}. The observed range is quite close to those for the sodium-doped catalysts, clearly indicating that sodium promoted Mo species were the active sites on the Mo-DAL catalysts.

3.3.4. Durability test for 20% Mo-DAL catalyst.

The stability of the Mo-DAL catalysts was investigated on the 20% Mo-DAL catalyst since this catalyst exhibited the highest catalytic activity among all the Mo-DAL catalysts (Figure 3.5). The durability test was conducted at 220 °C with a WHSV of 4 h^{-1}. The catalytic activity of 20% Mo-DAL was maintained at least for 50 h without significant dropping of its catalytic activity (Figure 3.9). Moreover, the hydrogen selectivity was also maintained well. The averaged values for formic acid conversion and hydrogen selectivity for 50 h reached 97.4 and 99.2%, respectively. The XRD patterns of the 20% Mo-DAL catalysts before and after long-term stability test are shown in Figure 3.10. The peaks attributed to β-Mo_2C, which is the main catalytic component on this catalyst, retained well even after the durability test, although the peaks attributed to sodium formate and sodium hydrogen diformate were newly appeared after the reaction. This result indicates that the catalytically active β-Mo_2C species did not suffer degradation and agglomeration, which led to reduce activity, on the DAL support.

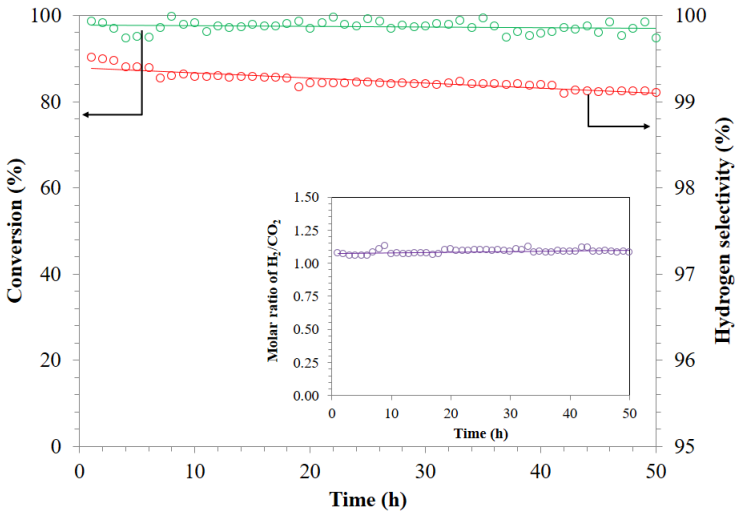

Figure 3.9 Long-term stability test of 20% Mo-DAL at 220 °C for 50 h. The inset shows molar ratio of H_2/CO_2 during stability test.

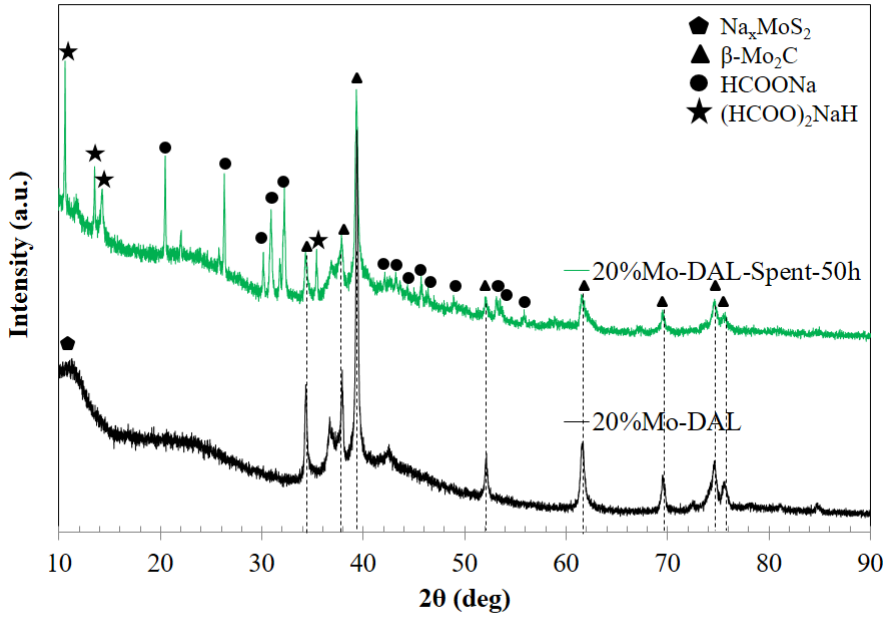

Figure 3.10 XRD patterns of 20% Mo-DAL catalyst before and after stability test for 50 hours.

3.3.5. Comparison of Mo-DAL catalysts with other reported ones.

Catalytic activity of Mo-DAL catalysts are compared to the other reported catalysts to elucidate how greener our catalysts are (Table 3.3). Although the precious metal catalysts show excellent catalytic performances even at lower reaction temperature than that for Mo-DAL, their prices are more than 50 times higher than Mo-DAL. Therefore, their wide implementation of precious metal catalysts for society is more difficult than of Mo-DAL. In the comparison among the non-precious metal catalysts, there are some cheaper catalysts existed, however, their catalytic performances especially the selectivity to hydrogen are not high enough for the purpose of hydrogen supply to PEFCs. According to those comparisons, it is demonstrated that the active and greener Mo-based catalysts for selective hydrogen production from formic acid even by using the cheap and wasted lignin as a catalyst precursor is feasible.

Table 3.3. Comparison of price and catalytic performance of non-precious and precious metal based catalysts

Catalyst	Price[a] ($USD.kg^{-1}$) [34,35]	WHSV[d] (h^{-1})	Temp. Optimum (°C)	Conv. (%)	H_2 Selectivity (%)	Ref.
α-Fe_2O_3	0.8[c]	8.5	200	24.1	83.4	[25]
5% Mo-DAL	2[b]	4	240	97.3	99.2	This Work
20% Mo-DAL	8[b]	4	220	98.0	99.4	This Work
α-MoC_{1-x}	39[b]	4	250	95.0	91.0	[27]
$Mg_{1.0}Mo_{99.0}C_{1-x}$	38.6[b]	4	200	93.0	95.0	[28]
9% MoS_2/graphite	3.5[b]	46.7	235	92.0	42.0	[14]
2% Pt/Norit	513	11.4	200	≥99.9	98.6	[24]
1% Au/SiO_2	415	11.4	250	≥99.9	99.5	[22]
2.5% Au/Al_2O_3	1038	50.3	150	≥99.9	≥99.9	[23]
1% Pd/C	437	36.6	130	≥99.9	≥99.9	[17]

[a]Prices of catalysts are calculated as follows: (prices of raw metals) × (loading amounts on catalysts). In this calculation, prices of support materials are excluded, [b]Price of Mo is calculated as follows: (Ratio of molecular weight of MoO_3/Mo) × (price of MoO_3), [c]Estimated as Fe_2O_3 industrial grade price, [d]Formic acid mass flow toward catalyst weight.

3.4. Conclusions

In this work, utilization of cheap and wasted lignin was attempted as a precursor of catalysts. A simple two-step preparation that is constituted by wet-impregnation of molybdenum species followed by pyrolysis process afforded the highly active, selective, durable and green catalysts for selective hydrogen production from formic acid. In comparison of DAL-based catalysts with standard carbon-based ones, the presence of sulfur and sodium species on the DAL support was suggested to be beneficial for improving catalytic activity and stability of parent molybdenum species. Especially, the 20% Mo-DAL catalyst showed remarkable durability in formic acid conversion and selectivity to hydrogen at least for 50 h. It is expected that this work provides a new viewpoint to utilize waste dealkaline lignin as a precursor of low-cost, effective and sustainable molybdenum-based catalysts for selective hydrogen production from formic acid.

References

[1] C. Li, X. Zhao, A. Wang, G.W. Huber, T. Zhang, Catalytic Transformation of Lignin for the Production of Chemicals and Fuels, Chemical Reviews, 115 (2015) 11559-11624.

[2] N. Mahmood, Z. Yuan, J. Schmidt, C.C. Xu, Hydrolytic depolymerization of hydrolysis lignin: Effects of catalysts and solvents, Bioresource Technology, 190 (2015) 416-419.

[3] A.K. Deepa, P.L. Dhepe, Lignin Depolymerization into Aromatic Monomers over Solid Acid Catalysts, ACS Catalysis, 5 (2015) 365-379.

[4] I. Kurnia, S. Karnjanakom, A. Bayu, A. Yoshida, J. Rizkiana, T. Prakoso, G. Guan, A. Abudula, *In-situ* catalytic upgrading of bio-oil derived from fast pyrolysis of lignin over high aluminum zeolites, Fuel Processing Technology, 167 (2017) 730-737.

[5] P.R. Patwardhan, R.C. Brown, B.H. Shanks, Understanding the fast pyrolysis of lignin, ChemSusChem, 4 (2011) 1629-1636.

[6] Y.Y. Wang, L.L. Ling, H. Jiang, Selective hydrogenation of lignin to produce chemical commodities by using a biochar supported Ni-Mo_2C catalyst obtained from biomass, Green Chemistry, 18 (2016) 4032-4041.

[7] I. Barrera-Martínez, N. Guzmán, E. Peña, T. Vázquez, R. Cerón-Camacho, J. Folch, J. Aburto, J.A.H. Salazar, Ozonolysis of alkaline lignin and sugarcane bagasse: Structural changes and their effect on saccharification, Biomass and Bioenergy, 94 (2016) 167-172.

[8] W. He, W. Gao, P. Fatehi, Oxidation of kraft lignin with hydrogen peroxide and its application as a dispersant for kaolin suspensions, ACS Sustainable Chemistry and Engineering, 5 (2017) 10597-10605.

[9] A. Yuliestyan, M. García-Morales, E. Moreno, V. Carrera, P. Partal, Assessment of modified lignin cationic emulsifier for bitumen emulsions used in road paving, Materials and Design, 131 (2017) 242-251.

[10] M.R. Snowdon, A.K. Mohanty, M. Misra, A study of carbonized lignin as an alternative to carbon black, ACS Sustainable Chemistry and Engineering, 2 (2014) 1257-1263.

[11] N. Meek, D. Penumadu, O. Hosseinaei, D. Harper, S. Young, T. Rials, Synthesis and characterization of lignin carbon fiber and composites, Composites Science and Technology, 137 (2016) 60-68.

[12] J. Pang, W. Zhang, J. Zhang, G. Cao, M. Han, Y. Yang, Facile and sustainable synthesis of sodium lignosulfonate derived hierarchical porous carbons for supercapacitors with high volumetric energy densities, Green Chemistry, 19 (2017) 3916-3926.

[13] J.S. Lee, T.H. Hyun, Metal Carbides, in: I.T. Horvath (Ed.), John Wiley & Sons, Ltd, New York, 2003, pp. 1-4.

[14] V.O. Koroteev, D.A. Bulushev, A.L. Chuvilin, A.V. Okotrub, L.G. Bulusheva, Nanometer-sized MoS_2 clusters on graphene flakes for catalytic formic acid decomposition, ACS Catalysis, 4 (2014) 3950-3956.

[15] J.S. Choi, G. Bugli, G. Djéga-Mariadassou, Influence of the degree of carburization on the density of sites and hydrogenating activity of molybdenum carbides, Journal of Catalysis, 193 (2000) 238-247.

[16] Y. Ma, G. Guan, X. Hao, J. Cao, A. Abudula, Molybdenum carbide as alternative catalyst for hydrogen production – A review, Renewable and Sustainable Energy Reviews, 75 (2017) 1101-1129.

[17] L. Jia, D.A. Bulushev, S. Beloshapkin, J.R.H. Ross, Hydrogen production from formic acid vapour over a Pd/C catalyst promoted by potassium salts: Evidence for participation of buffer-like solution in the pores of the catalyst, Applied Catalysis B: Environmental, 160-161 (2014) 35-43.

[18] A.K. Singh, S. Singh, A. Kumar, Hydrogen energy future with formic acid: A renewable chemical hydrogen storage system, Catalysis Science and Technology, 6 (2016) 12-40.

[19] F. Joó, Breakthroughs in hydrogen storage-formic acid as a sustainable storage material for hydrogen, ChemSusChem, 1 (2008) 805-808.

[20] J. Eppinger, K.W. Huang, Formic Acid as a Hydrogen Energy Carrier, ACS Energy Letters, 2 (2017) 188-195.

[21] M. Zacharska, A.L. Chuvilin, V.V. Kriventsov, S. Beloshapkin, M. Estrada, A. Simakov, D.A. Bulushev, Support effect for nanosized Au catalysts in hydrogen production from formic acid decomposition, Catalysis Science and Technology, 6 (2016) 6853-6860.

[22] A. Gazsi, T. Bánsági, F. Solymosi, Decomposition and reforming of formic acid on supported Au catalysts: Production of CO-free H_2, Journal of Physical Chemistry C, 115 (2011) 15459-15466.

[23] D.A. Bulushev, M. Zacharska, Y. Guo, S. Beloshapkin, A. Simakov, CO-free hydrogen production from decomposition of formic acid over Au/Al_2O_3 catalysts doped with potassium ions, Catalysis Communications, 92 (2017) 86-89.

[24] F. Solymosi, Á. Koós, N. Liliom, I. Ugrai, Production of CO-free H_2 from formic acid. A comparative study of the catalytic behavior of Pt metals on a carbon support, Journal of Catalysis, 279 (2011) 213-219.

[25] S.A. Halawy, S.S. Al-Shihry, M.A. Mohamed, Gas-phase decomposition of formic acid over α-Fe2O3 catalysts, Catalysis Letters, 48 (1997) 247-251.

[26] G. Patermarakis, The parallel dehydrative and dehydrogenative catalytic action of γ-Al_2O_3 pure and doped by MgO: Kinetics, selectivity, time dependence of catalytic behaviour, mechanisms and interpretations, Applied Catalysis A: General, 252 (2003) 231-241.

[27] J. Cao, J. Wang, Y. Ma, X. Li, P. Xiaokaiti, X. Hao, A. Abudula, G. Guan, Hydrogen production from formic acid over morphology-controllable molybdenum carbide catalysts, Journal of Alloys and Compounds, 735 (2018) 1463-1471.

[28] J. Wang, J. Cao, Y. Ma, X. Li, P. Xiaokaiti, X. Hao, T. Yu, A. Abudula, G. Guan, Decomposition of formic acid for hydrogen production over metal doped nanosheet-like MoC_{1-x} catalysts, Energy Conversion and Management, 147 (2017) 166-173.

[29] M. Li, Z. Wu, Z. Wang, S. Yu, Y. Zhu, B. Nan, Y. Shi, Y. Gu, H. Liu, Y. Tang, Z. Lu, Facile synthesis of ultrathin MoS_2/C nanosheets for use in sodium-ion batteries, RSC Advances, 7 (2017) 285-289.

[30] Y. Ma, G. Guan, P. Phanthong, X. Li, J. Cao, X. Hao, Z. Wang, A. Abudula, Steam reforming of methanol for hydrogen production over nanostructured wire-like molybdenum carbide catalyst, International Journal of Hydrogen Energy, 39 (2014) 18803-18811.

[31] L. Lange, W. Triebel, Sulfides, Polysulfides, and Sulfanes, in, Wiley-VCH, Weinheim, German, 2000, pp. 7-9.

[32] S. Hao, X. Shen, M. Tian, R. Yu, L. Chen, Reversible conversion of MoS_2 upon sodium extraction, Nano Energy, 41 (2017) 217-224.

[33] R.C. Baetzold, G.A. Somorjai, Preexponential factors in surface reactions, Journal of Catalysis, 45 (1976) 94-105.

[34] Commodity and Metal Price, in.

[35] Iron Oxide Pigments, in.

Chapter 4 Hydrolysis of Cellulose and Woody Biomass over Sustainable Weak-Acid Carbon Catalysts from Alkaline Lignin

4.1. Introduction

In the **Chapter 3**, the new insight to utilize waste dealkaline lignin as a catalyst precursor due to the presence of sodium and sulfur species from the lignosulfonate process. Furthermore, the lignosulfonate process would be modified by the introducing of sulfonate functional group in the stucture of lignin, as described in **Chapter 1**. Therefore, considering the sulfonated and oxygenated functional groups, the lignin could be used for the preparation of carbon acid catalysts for conversion of lignocellulosic biomass. The conversion of lignocellulosic biomass to fuels and chemicals has attracted great attention for implementing a sustainable society by large scale application of the abundance and renewable biomass resource [1,2]. Glucose and xylose are two main monomeric sugars derived from cellulose and hemicellulose, respectively, which can serve as the feedstock containing C6 and C5 compounds for downstream biorefinery processes [3-5]. Hydrolysis of cellulose to glucose typically requires mineral acids or enzymes, and in order to improve the reaction rate (Scheme 4.1), some special solvents such as ionic liquids are necessary to dissolve the water-insoluble cellulose, achieving a homogeneous reaction system [6-9]. However, such a way could produce a large amount of wastewater and increase the operation cost [10,11].

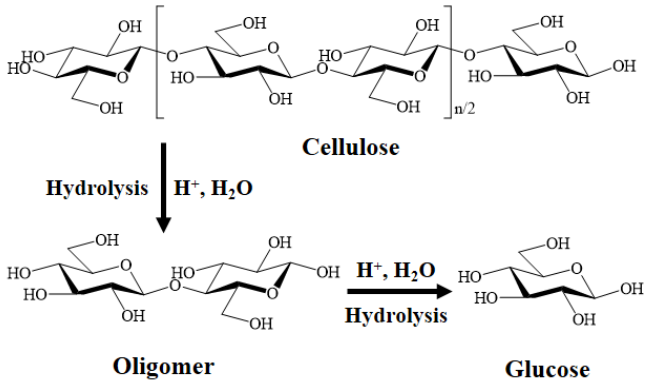

Scheme 4.1 Hydrolysis reaction of cellulose over homogeneous acid catalyst

Recently, various heterogeneous acid catalysts such as metal oxides [12], insoluble heteropolyacid [13], immobilized sulfonic acid on zeolite [14], zeolite-magnetic materials [15], and carbon-based acid catalysts [16-22] have been developed to substitute the homogeneous catalysts for the conversion of lignocellulose. In particular, heterogeneous carbon catalysts exhibited have high activity in the hydrolysis of cellulose and hemicellulose [17-20,23]. It is found that the polyaromatic structure of carbon can adsorb glucans through CH-π interactions [24-29], and the acidic functional groups on the surface of the carbon catalyst could bond with the cellulose chains, resulting in the activation of the β-1,4-glycosidic bonds to cleave [10]. Various methods such as oxidation and sulfonation with concentrated chemical solutions, e.g., HNO_3, H_2O_2, $KMnO_4$, and H_2SO_4 have been employed to generate such acidic functional groups on the carbon catalysts [21-23,30-32]. However, the energy consumption for the synthesis of the carbon materials such as carbon black and graphite is generally high, and the catalyst preparation process is complex [33-35]. Moreover, in order to increase the surface area of the carbon catalysts, the treatment by highly corrosive alkaline hydroxides is always required so that a large amount of wastewater is generated in the post-treatment process. Recently, to solve such issues, through simple air oxidation of lignocellulose and lignin residue, a reusable weakly acidic carbon catalyst was cost-effectively obtained

for the depolymerisation of lignocellulose [36]. It provides an environmental friendly and low-cost way to produce catalysts in the biorefinery.

About 70 MTon per year of lignosulfonate lignin is estimated to be produced as the waste from pulp and paper industries [37]. Effective utilization of the wasted lignosulfonate lignin has attracted great attention in recent years. Various thermochemical conversion processes such as pyrolysis and hydrothermal processing ways have been tried to convert it to high value-added chemicals [38-40]. However, a large amount of char is always produced finally since the lignin is a kind of thermo-stable polymeric compound and hardly to be decomposed. Consequently, many researchers considered to transfer the lignin derivatives to functional carbon materials including dispersant [41], emulsifier [42], carbon fiber [43], precursor catalysts material [44], electrode materials in supercapacitor [45], and carbon black [33].

Considering the sulfonated and oxygenated functional groups are rich on the surface of the lignosulfonate lignin, it could be used for the preparation of weak-acid carbon catalysts. In this work, a try was performed to synthesize the weak-acid carbon catalysts from alkaline lignin (AL) by thermal pyrolysis followed by a washing treatment process. The acidity and compositions of carbon catalyst were characterized by Boehm titration, acid-base back titration of NaCl method, elemental analysis, and fourier-transform infrared spectroscopy (FTIR). The alkaline lignin pyrolysis behaviors were analyzed by using a thermogravimetric analyzer (TGA) and a temperature-programmed desorption mass spectrometer (TPD-MS), and the effect of pyrolysis temperature on the acidity amount in the weak-acid carbon catalysts was investigated. The obtained catalysts were applied for the hydrolysis of cellulose and woody biomass for the selective production of monomeric sugars such as glucose and xylose. Various carbon catalysts derived from this way were screened and the hydrolysis conditions were optimized. It is expected to

provide a new way to utilize the wasted alkaline lignin as the source to prepare the weak-acid catalysts for the effective conversion of lignocellulosic biomass and their derivatives.

4.2. Materials and methods

4.2.1. Alkaline lignin characterization

Alkaline lignin (AL) (Tokyo Chemical Industry Co., Ltd, Japan) was used as a source for the preparation of carbon catalysts. The proximate and ultimate analysis results for alkaline lignin are shown at Table 4.1. The thermal degradation of alkaline lignin was analyzed by a thermogravimetric analyzer (DTG-60H, Shimadzu, Japan) with a heating rate of 10 °C/min in a temperature range of 50-850 °C (Δ = 50 °C) under nitrogen atmosphere. The decomposition compositions were detected by a temperature-programmed desorption mass spectrometer (TPD-MS, BEL-CAT-A, Japan), in which the sample was pre-treated at 100 °C for 10 min at first and then heated to 800 °C with a heating rate of 10 °C/min under helium atmosphere.

Table 4.1. Proximate and ultimate analysis of alkaline lignin.

Proximate analysis (wt %)				Ultimate analysis[c] (wt %)			
Moisture[a]	Volatile Matter	Fixed Carbon	Ash Content[b]	C	H	N	S
3.5	28.7	48.3	19.5	50.4	4.7	0.1	2.9

[a]determined by moisture balance; [b]determined from the residual weight after calcination at 800 °C for 2 h in air; [c]determined by CHNS elemental analysis.

4.2.2. Synthesis of AL-derived carbon catalysts

5 g of AL was located in a fixed-bed quartz reactor and heated up to the designed temperature (i.e., 350, 400, 450, 500 °C in this study) with a heating rate 5 °C/min under a 50 cm^3/min of argon gas flow and then the temperature was maintained for 1 h. The obtained product was treated by 40 ml of 1 M HCl to remove the residual inorganic impurities completely, and subsequently washed by deionized (DI) water until pH reached 6-7 and finally, washed by ethanol to wash out organic-soluble compounds in the product and dried in a vacuum oven at 80 °C for 18 h. Hereafter, the obtained AL-derived carbon catalysts are denoted as AL-Py-X, where X represents the pyrolysis temperature (i.e., 350, 400, 450, 500 °C). The elemental compositions (C, H, N, and S) in the obtained carbon catalysts were analyzed by an elemental analyzer (Vario EL cube, Elementar, German). Meanwhile, all the carbon catalysts were also characterized by the acid-base back titration of NaCl solution method to determine sulfonic functional groups [46], Boehm titration with different degrees of bases including NaOH, $NaHCO_3$ and Na_2CO_3 [47], and FTIR spectroscopy (FTIR 4200, Jasco, Japan).

4.2.3. Hydrolysis reaction

In this study, the microcrystalline cellulose was purchased from Alfa Aesar (Lot No. 10179415) with the degree of polymerization and crystalinity of 216 and 80.8%, respectivelly. Prior to use, the cellulose was ball-milled to decrease the crystallinity and used as the feedstock with the ball-milled Japanese cedar wood. The ball-milling was performed in a planetary ball mill (LP-1, Ito Seisakusho, Japan) at 300 rpm for 6 h, in which 1.6 g of microcrystalline cellulose or Japanese cedar wood powder with 64 g of zirconia balls with a size of 10 mm were put in a zirconia pot (80

cm^3). Meanwhile, the microcrystalline cellulose or Japanese cedar wood was also ball-milled with the obtained carbon catalysts together using the same ball-milling condition for comparison.

Hydrolysis reaction was carried out in an autoclave reactor (BR-25, BERGHOF, Germany). In brief, 100 mg of ball-milled cellulose or Japanese cedar wood, 100 mg of carbon catalyst, and 15 ml of DI water (or with 0.012 wt% HCl) were added into the reactor. Nitrogen was passed through the reactor with a flow rate of 50 cm^3/min for 10 min before the hydrolysis reaction started. The reactor was heated to 210 °C in 60 min and then directly cooled down to 30 °C in an ice bath for 40 min (Figure 4.1). Then, the reaction mixture was separated by using a PTFE membrane filter (1 μm). Afterward, the liquid product was diluted with DI water and analyzed by using a Shimadzu Prominence HPLC equipped with a RID-10A detector and an oven (CTO-20A) operated at 40 °C. A Supelco gel C610-H column (300 × 7.8 mm, Sigma) and 0.05 wt% H_3PO_4 solution were used as the column and eluent, respectively. The amounts of products were determined by an external standard method. Conversion of cellulose was determined based on the weight difference of the solid phase before and after the reaction. In addition, cellulose and hemicellulose compositions of Japanese cedar wood were 40.9% and 24.8%, respectively [48].

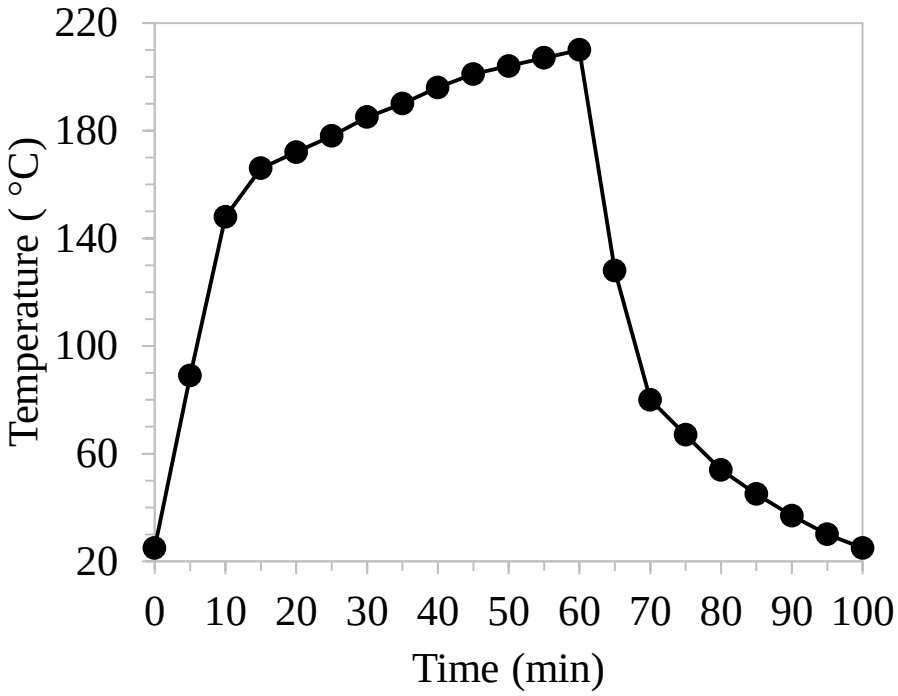

Figure 4.1 The temperature profile in the reactor during the cellulose and biomass hydrolysis with a process of heating to 210 °C in 60 min and then directly cooling down to 30 °C

4.3. Results and discussion

4.3.1. Characterization of AL-derived carbon catalysts

Table 4.2 shows the characteristrics of the obtained carbon catalysts. Herein, the total acid amount was determined by both Boehm titration and acid-base back titration of NaCl methods. One can see that the total acid amount decreased in the obtained carbon catalysts by increasing of the pyrolysis temperature owing to the thermal decomposition of oxygenated functional groups, which corresponded to the decrease of acid amount of oxygenated functional groups (Table 4.2) and molar ratio of H/C with the increase in the pyrolysis temperature (Table 4.3). To elucidate the thermal degradation behavior of AL during the pyrolysis of it for the preparation of carbon catalyst,

TGA and TPD-MS analyses were performed. As shown in Figure 4.2, the thermal decomposition in the inert atmosphere occurred in a wide temperature range of 230-600 °C. Figure 4.3 shows the TPD-MS analysis result. Herein, the signals of CO_2 (*m/z* = 44), CO (*m/z* = 28), and H_2O (*m/z* = 18) indicated the decomposition of oxygenated functional groups such as carboxylic acids, lactones, phenol and carbonyl functional groups in AL which are contributed to the acidity of carbon catalysts [49], and the dehydration of hydroxyl groups in AL. These results were in accordance with those observed by FTIR analysis. As shown in Figure 4.4, the peak intensity of oxygenated functional groups such as C=O stretching (1690 cm^{-1}), O-H bending of carboxylate (1430 cm^{-1}), and C-O stretching of phenol/lactones (1210-1280 cm^{-1}) [49,50] decreased with the increase in the pyrolysis temperature. Meanwhile, the evolution of SO_2 signal (*m/z* = 64) in TPD-MS spectrum should be resulted from the sulfonic acid group in AL. This result was also confirmed by the FTIR analysis (Figure 4.4), in which the peak intensity of S=O stretching of SO_3H (1026 cm^{-1}) maintained unchanged for all the catalysts although the peak intensity of oxygenated functional groups decreased with the increase in the pyrolysis temperature. However, as shown in Table 4.2, the density of sulfonic acid groups decreased with the increase in pyrolysis temperature. Based on these results, it can be concluded that the existences of sulfonated functional groups and oxygenated functional groups in the AL-derived carbon catalysts affected the acidity. It should be noted that the phenolic hydroxyl groups, carboxyl groups, and SO_3H groups on the carbon material could enhance the cleave of hydrogen bonds and the β-1,4-glycosidic bonds in the adsorbed cellulose molecules [31]. However, not all of sulfur species are in the form of sulfonic functional groups related to the source of lignin from waste of pulp and paper industries. For example, thiols groups also exist on the structure of the lignin, however, its contribution to the acidity is difficult to be confirmed by both the Boehm titration and acid-base back titration of NaCl solution method.

Similar as the previous study [31], since the the pKa values of thiol group and phenol group are in the range of 10-11 [51,52], and those of carboxylic acid group and sulfonic acid functional group are in the range of 0.7-4.2 [52], they can be considered in the same groups as shown in Table 4.2 in the Boehm titration analysis [47]. One can see that the sulfonic acid functional groups contributed only a part in the total acid amount (Table 4.3). However, it should be noted that some of sulfur species inside the carbon catalysts cannot be detected by the acid-base back titration of NaCl solution method [31,53]. Thus, in this study, only the sulfonic functional groups on the surface of catalysts can be estimated.

Table 4.2. Characteristics of the obtained weak-acid carbon catalysts from AL.

Catalyst	Total acid amount (mmol/g)[a]	Density of each acid functional groups			
		Sulfonic groups (mmol/g)[b]	Carboxylic groups (mmol/g)[c]	Lactonic groups (mmol/g)[a]	Phenolic and thiol groups (mmol/g)[a]
AL-Py-350	0.82	0.10	0.50	0.07	0.15
AL-Py-400	0.15	0.09	0.02	0.01	0.03
AL-Py-450	0.13	0.08	0.02	0.01	0.02
AL-Py-500	0.11	0.06	0.04	0.00	0.01

[a]Boehm titration method with 0.01 M NaOH, 0.01 M $NaHCO_3$, and 0.01 M Na_2CO_3; [b]Estimated by acid-base back titration of 1 M NaCl method; [c]Estimated by the difference of Boehm titration method with 0.01 M $NaHCO_3$ and acid-base back titration of 1 M NaCl method.

Table 4.3 H/C and S/C molar ratios and surfur contens in the obtained weak-acid carbon catalysts based on CHNS elemental analysis method.

Catalysts	Molar ratio		Sulfur content
	H/C	S/C	(mmol/g)
AL-Py-350	0.675	0.030	0.26
AL-Py-400	0.562	0.033	0.30
AL-Py-450	0.519	0.047	0.43
AL-Py-500	0.393	0.071	0.64

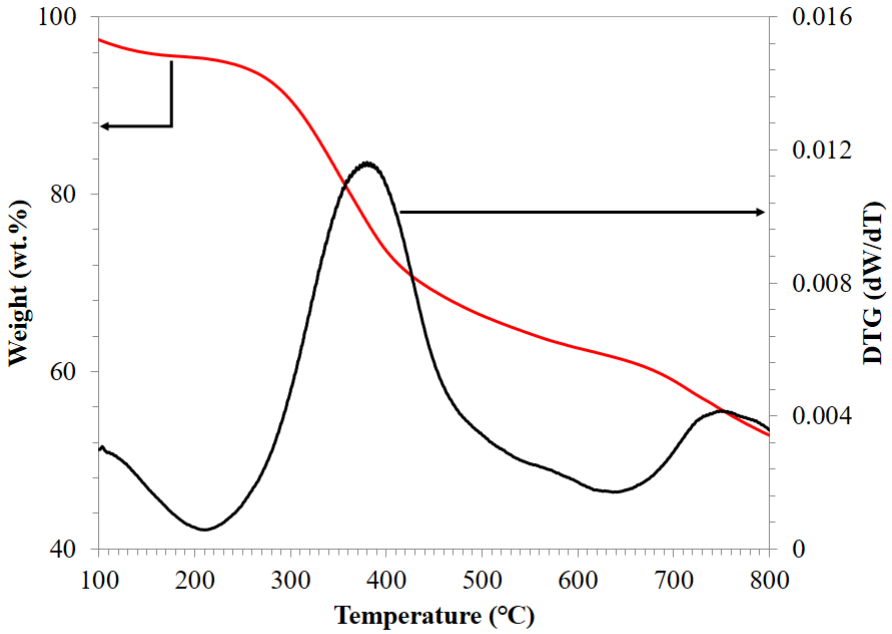

Figure 4.2. TGA and DTG profile of AL.

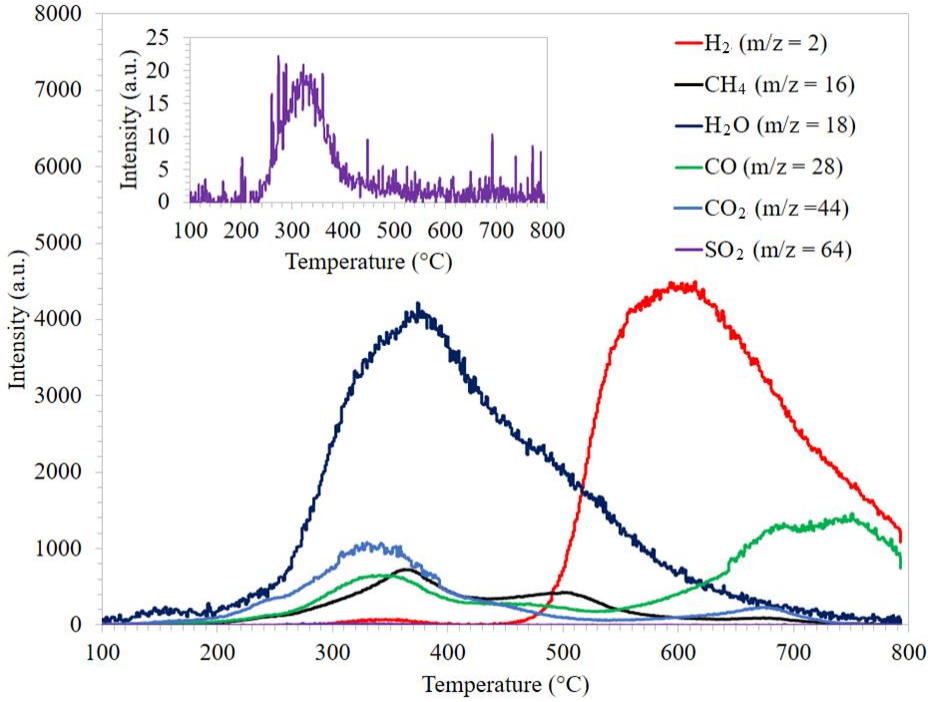

Figure 4.3. TPD-MS signal profiles of various gases during the decomposition of AL. H_2, *m/z* = 2; CH_4, *m/z* = 16; H_2O, *m/z* = 18; CO, *m/z* = 28; CO_2, *m/z* = 44. The inset: the signal of SO_2, *m/z* = 64.

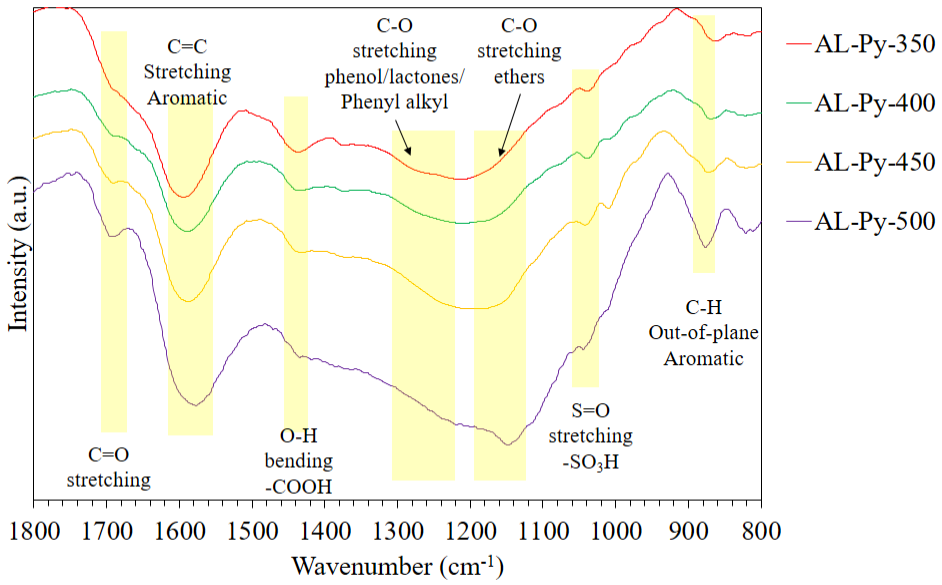

Figure 4.4. FTIR spectra of AL-derived carbon catalysts (weight ratio of KBr to sampel is 40:1).

4.3.2. Catalytic Performance

As stated in the experimental section, the original cellulose and Japanese cedar wood were ball-milled at first. This is for the reduction of the crystallinity degree of cellulose and avoid the effect of strong intermolecular hydrogen bonds and steric hindrance on the hydrolysis reaction on the solid-solid interfaces [54,55]. Moreover, it was reported that such a ball-milling treatment could also improve the reactivity of cellulose due to the decomposition of the crystalline structure of cellulose [56,57]. For the real woody biomass, cellulose and hemicellulose are encapsulated by lignin, and in this case, the ball-milling treatment can fracture the lignocellulose biomass structure to expose the cellulose and hemicellulose parts [58]. As indicated by the XRD patterns of ball-

milled crystalline cellulose and Japanese cedar wood (Figure 4.5), the crystallinity of cellulose and Japanese cedar wood decreased greatly, which should be benefit for the hydrolysis.

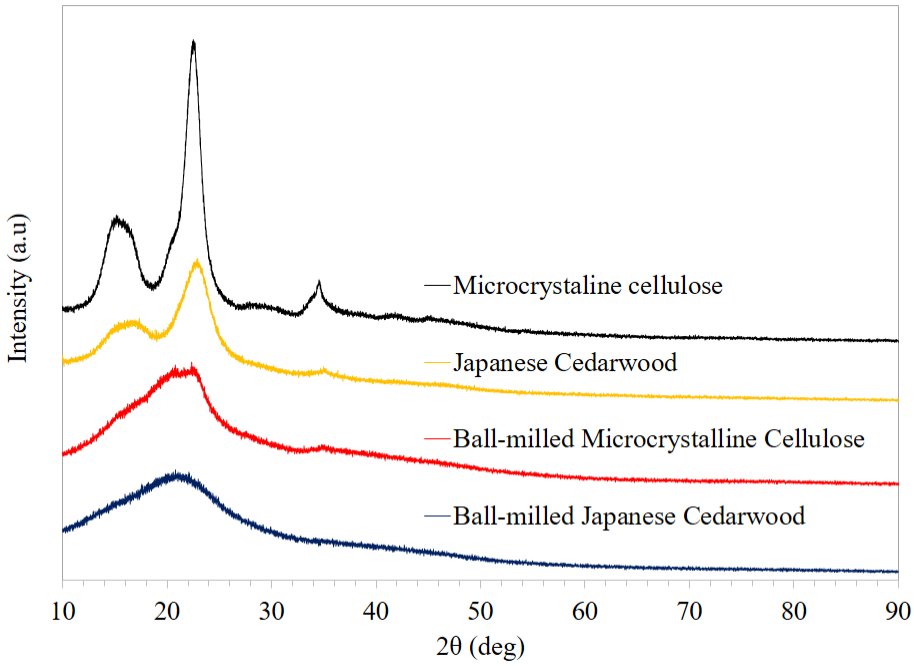

Figure 4.5 XRD patterns of microcrystalline cellulose and Japanese cedar wood before and after the ball-milling pre-treatment.

Table 4.4 Catalytic performances of the AL-derived carbon catalysts for the cellulose hydrolysis.[a]

Entry	Catalysts	Ball-milling of cellulose[b]	Medium	Conv. (%)	Yield (%)		Gluc. Sel. (%)
					Glucose[c]	Other products[d]	
1	None	Single	DI water	29.5	3.7	25.8	12.4
2	AL-Py-350	Single	DI water	45.5	12.2	33.3	26.8
3	AL-Py-400	Single	DI water	60.7	35.6	25.1	58.7
4	AL-Py-450	Single	DI water	70.8	46.3	24.5	65.3
5	AL-Py-500	Single	DI water	37.5	29.1	8.4	77.5
6	AL-Py-450	Single	0.012 wt% HCl	86.9	60.1	26.8	69.1
7	AL-Py-450	Mix	DI water	94.5	56.8	37.7	60.1
8	AL-Py-450	Mix	0.012 wt% HCl	96.1	69.8	26.3	72.6

[a]Heating to 210 ^{o}C in 60 min then directly cooling to 30 °C; Ratio of cellulose to catalyst (S/C = 1); [b]Single: only cellulose was ball-milled; Mix: ball-milling of cellulose with the AL-Py-450 carbon catalyst; [c]Based on quantification product from HPLC chromatogram; [d]The difference of conversion and standardized product.

In this study, the activity of AL-derived carbon catalysts was evaluated at a temperature of 210 °C by using the same weight amounts of the ball-milled cellulose and the catalyst (100 mg:100 mg) in DI water (Table 4.4, entries 2, 3, 4, and 5) at first. Obviously, the hydrolysis of ball-milled cellulose without catalyst gave a much lower conversion of 29.5% with a much lower glucose yield of 3.7% (entry 1) than those with the AL-derived carbon catalysts. Herein, among the obtained AL-derived carbon catalysts, AL-Py-450 carbon catalyst exhibited the highest activity with a ball-milled cellulose conversion of 70.8% and a glucose yield 46.3% (entry 4) even though the acid amount of it (0.13 mmol/g) was lower than those of AL-Py-350 (0.82 mmol/g) and AL-Py-400 (0.15 mmol/g) carbon catalysts. In contrast, although the AL-Py-350 carbon catalyst had a highest acid amount resulted from the more oxygenated functional groups in it, the ball-milled cellulose conversion was only 45.5% with a lower glucose yield of 12.2% (entry 2). Meanwhile, although the AL-Py-500 carbon catalyst had a highest proportion amount of carboxylic and sulfonated functional groups in it (Table 4.2) with an acid amount of 0.04 mmol/g and 0.06 mmol/g, respectively, it also showed lower catalytic activity with a ball-milled cellulose conversion of 35% and a glucose yield of 29.1% (entry 5). In addition, it is reported that the oxygenated functional groups were unstable at a temperature over 200 °C whereas the aryl SO_3H groups were stable for the xylose dehydration reaction over sulfonated graphene oxide (SGO) [59]. Herein, the synergetic effect of the oxygenated and sulfur functional groups on the AL-Py-450 carbon catalyst with suitable amounts and stability of both could be the main reason to achieve the highest performance.

The performance of AL-Py-450 carbon catalyst was also tested at different hydrolysis temperatures. As shown in Figure 4.6, the activity increased with the increase in hydrolysis temperature. Since our reaction system cannot work over 210 °C, the optimum hydrolysis temperature was not obtained in this study.

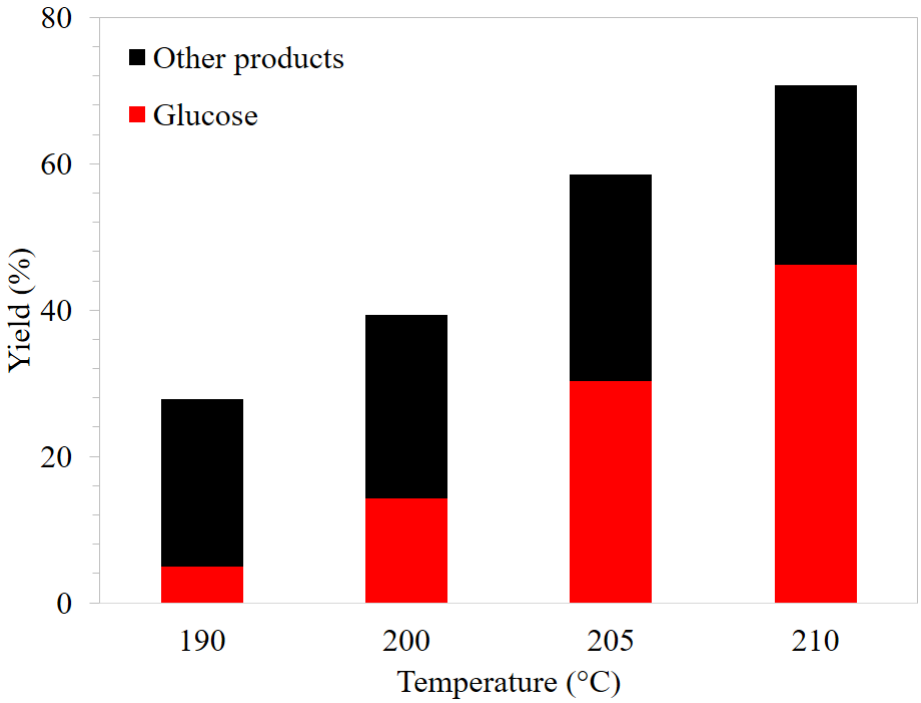

Figure 4.6. The catalytic performance of AL-Py-450 carbon catalyst in the hydrolysis of cellulose in a temperature range of 190-210 °C.

To increase the ball-milled cellulose conversion and the yield of monomeric sugars, the hydrolysis with the AL-Py-450 carbon catalyst was also performed in a mild acidic solution (0.012 wt% HCl, pH=2.5). Herein, the utilization of dilute HCl solution could avoid the corrosion of common stainless reactor or the generation of a large amount of wastewater [60]. Moreover, it is reported that the HCl was more effective than other mineral acids and organic acids for the cellulose hydrolysis [19]. As a result, in the presence of the dilute HCl, the cellulose conversion and glucose yield were effectively increased from 70.8% and 46.3% (Table 4.4, entry 4) to 86.9% and 60.1% (entry 6), respectively. This result indicated the synergistic effect between AL-Py-450 carbon catalyst and 0.012 wt% HCl in the hydrolysis of cellulose. It is reported that cellulose can

be hydrolyzed by carbon catalyst to produce oligosaccharides, which are further catalyzed by HCl into monomeric sugar [19]. Herein, the similar reaction route could occur. In addition, a try was performed to ball-mill the cellulose with the carbon catalyst powder to improve the contact area between them. It is found that the conversion and glucose yield were increased to 94.5% and 56.8%, respectively (entry 7), indicating that the contacting of reactants with the catalyst surface is important in the heterogeneous hydrolysis process. Furthermore, when the hydrolysis was conducted in the presence of trace of HCl in this case, the cellulose conversion and the glucose yield were increased as high as 96.1% and 69.8%, respectively (entry 8).

To confirm the effect of ball-milling on the catalyst characteristics, SEM analysis, acid-base back titration of NaCl method, and Boehm titration were conducted. As shown in Figure 4.7, as AL-Py-450 catalyst was ball-milled, the particle size was reduced to ca. 1 μm from 20-50 μm, which should be benefit for the contacting with the cellulose. However, the acid amount was not significantly increased when compared to the non-ball-milling catalyst (Table 4.5). It is reported that the ball-milling could preferably enhance the solid-solid reaction by increasing the contact area between cellulose and carbon catalysts [61]. In the present study, the similar result was also obtained.

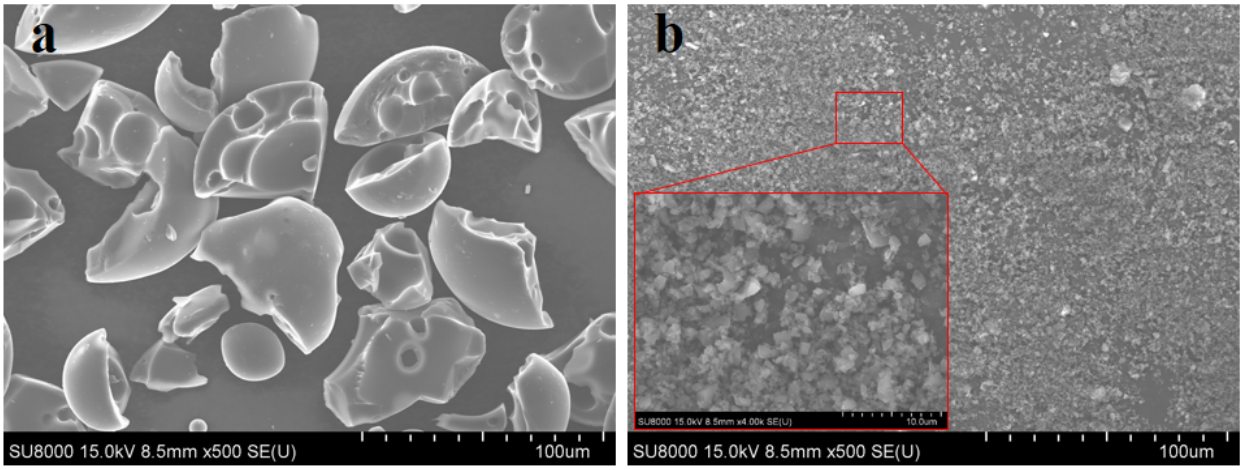

Figure 4.7 SEM images of AL-Py-450 catalyst (a) before and (b) after the ball-milling.

Table 4.5 Characteristics of AL-Py-450 before and after ball-milling.

Catalyst	Total acid amount (mmol/g)[a]	Densities of acid functional groups			
		Sulfonic groups (mmol/g)[b]	Carboxylic groups (mmol/g)[c]	Lactonic groups (mmol/g)[a]	Phenolic and thiol groups (mmol/g)[a]
AL-Py-450	0.13	0.07	0.03	0.01	0.02
AL-Py-450 BM 6 h	0.14	0.10	0.01	0.01	0.02

[a]Boehm titration method with 0.01 M NaOH, 0.01 M $NaHCO_3$, and 0.01 M Na_2CO_3; [b]Estimated by acid-base back titration of 1 M NaCl method; [c]Estimated by the difference results of Boehm titration method with 0.01 M $NaHCO_3$ and acid-base back titration of 1 M NaCl method.

4.3.3. Comparison of catalytic performance of AL-Py-450 carbon catalyst with other reported carbon catalysts in cellulose hydrolysis

Table 4.6 compares the catalytic activity of AL-Py-450 carbon catalyst with other reported carbon catalysts for the cellulose hydrolysis. Although the obtained AL-Py-450 carbon catalyst exhibited lower performance than some of the reported ones such as the activated carbon catalyst, it still has the following advantages: (i) The concentrated chemicals, e.g., H_2SO_4 [22,23,31], HNO_3 [23], and $KMnO_4$ [23], are unnecessary during the preparation stage; (ii) Lower energy consumption for preparation of such a carbon catalyst when comparing with carbon black [19], activated carbon [18-20], and graphite [23] since they always need high temperature and long carbonization time; (iii) Utilization of the wasted lignosulfonate lignin from pulp and paper industries as the carbon source, which provides a sustainable way to use the wastes as the catalysts in the biorefinery.

Table 4.6. Comparison of the catalytic activity of various carbon catalysts in the cellulose hydrolysis.

Carbon source	Catalyst Preparation	Substrate Pre-treatment	Reaction condition	Conv. (%)	Yield[f] (%)	Ref.
Activated carbon	Sulfonation	B/C[a,b] = 600; 60 rpm; 48 h	150 °C, 24 h	42.5	40.5	[22]
Cellulose	Carbonization and H_2SO_4 >96%; 150 °C	-	150 °C, 3 h	68	4	[31]
Graphene Oxide	Hummers method	-	150 °C; 24h	58.6	49.9	[23]
Nanoporous carbon	NaOCl; 25 °C; pH>12	-	150 °C; 24h followed by 180 °C; 3h	-	70	[18]
Carbon black	Activation of Carbon Black by KOH (1 : 3)	B/C[a,c]= 200; 60 rpm; 48 h	180 °C; 20 min[d]	98	88	[19]
Activated carbon	Air oxidation	B/C[a,c] = 40; 500 rpm; 2 h	180 °C; 20 min[d]	97	86	[20]
Alkaline lignin	Pyrolysis at 450 °C	B/C[a,c] = 40; 300 rpm; 6h	210 °C [d,e]	96.1	69.8	*This work*

[a]Weight ratio of ball in the mill to cellulose (B/C); [b]ball-milling pre-treatment of cellulose only; [c]Ball-milling of cellulose with catalysts; [d]in 0.012 wt% reaction medium; [e]Heating to 210 °C in 60 min and directly cooling to 30 °C; [f]Yield of glucose.

Table 4.7. Hydrolysis of Japanese cedar wood over AL-Py-450 carbon catalyst[a].

Ball-milling[b]	Catalyst	Medium	Yield (%)[d]	
			Glucose	Xylose
Single	None[c]	DI water	2.2	17.0
Mix	AL-Py-450	DI water	25.3	34.7
Mix	AL-Py-450	0.012 wt% HCl	47.1	40.3

[a]Heating to 210 °C in 60 min then directly cooling to 30 °C; Ratio of Japanese cedar wood to catalyst (S/C = 1); [b]Single: only biomass was ball-milled; Mix: ball-milling of biomass with the AL-Py-450 carbon catalyst; [c]Without AL-Py-450 carbon catalyst; [d]Based on quantification product from HPLC chromatogram.

4.3.4. Catalytic activity of AL-Py-450 in hydrolysis of real lignocellulosic biomass (Japanese cedar wood)

Japanese cedar wood was used to evaluate the catalytic ability of AL-Py-450 carbon catalyst in the hydrolysis of real lignocellulosic biomass (Table 4.7). Herein, AL-Py-450 carbon catalyst powder and Japanese cedar wood were ball-milled together before performing the hydrolysis reaction. For the comparison, hydrolysis of ball-milled Japanese cedar wood without the catalyst was performed at first, and only 2.2% and 17.0% of glucose and xylose were obtained respectively. When AL-Py-450 carbon catalyst was applied for the hydrolysis in DI water medium, the yields of glucose and xylose were increased to 25.3% and 34.7%, respectively, confirming that the AL-Py-450 carbon catalyst also had high activity for the hydrolysis of woody biomass. Furthermore,

in the presence of the trace of HCl, the yields of glucose and xylose were increased to 47.1% and 40.3%, respectively.

4.4. Conclusions

Alkaline lignin (AL) was successfully utilized as a source for the preparation of weak-acid carbon catalyst using a facile pyrolysis method with a washing process. It is found that the synergic effect of sulfur functional groups and oxygenated functional groups on the obtained carbon catalysts played an important role in catalysis of cellulose and biomass hydrolysis. Among the prepared AL-derived catalysts, the AL-Py-450 carbon catalyst exhibited the highest performance in the conversion of cellulose to glucose. Especially, by pre-ball-milling of cellulose or woody biomass with the catalysts and utilization of a low concentration of HCl in the reaction system, the conversion and product yields were greatly increased. It is expected that this work could provide a new perspective to utilize the wasted alkaline lignin as a source to prepare the weak-acid catalysts for the hydrolysis reactions.

References

[1] J.N. Chheda, G.W. Huber, J.A. Dumesic, Liquid-phase catalytic processing of biomass-derived oxygenated hydrocarbons to fuels and chemicals, Angewandte Chemie - International Edition, 46 (2007) 7164-7183.

[2] H. Kobayashi, H. Ohta, A. Fukuoka, Conversion of lignocellulose into renewable chemicals by heterogeneous catalysis, Catalysis Science and Technology, 2 (2012) 869-883.

[3] H. Kobayashi, A. Fukuoka, Synthesis and utilisation of sugar compounds derived from lignocellulosic biomass, Green Chemistry, 15 (2013) 1740-1763.

[4] C.-H. Zhou, X. Xia, C.-X. Lin, D.-S. Tong, J. Beltramini, Catalytic conversion of lignocellulosic biomass to fine chemicals and fuels, Chemical Society Reviews, 40 (2011) 5588-5617.

[5] L.T. Mika, E. Cséfalvay, Á. Németh, Catalytic conversion of carbohydrates to initial platform chemicals: chemistry and sustainability, Chemical Reviews, 118 (2018) 505-613.

[6] M.E. Himmel, S.-Y. Ding, D.K. Johnson, W.S. Adney, M.R. Nimlos, J.W. Brady, T.D. Foust, Biomass recalcitrance: engineering plants and enzymes for biofuels production, Science, 315 (2007) 804-808.

[7] S. Kassaye, K.K. Pant, S. Jain, Synergistic effect of ionic liquid and dilute sulphuric acid in the hydrolysis of microcrystalline cellulose, Fuel Processing Technology, 148 (2016) 289-294.

[8] Y.-Y. Liu, J.-L. Xu, Y. Zhang, C.-Y. Liang, M.-C. He, Z.-H. Yuan, J. Xie, Reinforced alkali-pretreatment for enhancing enzymatic hydrolysis of sugarcane bagasse, Fuel Processing Technology, 143 (2016) 1-6.

[9] N.A.S. Ramli, N.A.S. Amin, Catalytic hydrolysis of cellulose and oil palm biomass in ionic liquid to reducing sugar for levulinic acid production, Fuel Processing Technology, 128 (2014) 490-498.

[10] A. Shrotri, H. Kobayashi, A. Fukuoka, Cellulose depolymerization over heterogeneous catalysts, Accounts of Chemical Research, 51 (2018) 761-768.

[11] N.R. Baral, A. Shah, Techno-economic analysis of utilization of stillage from a cellulosic biorefinery, Fuel Processing Technology, 166 (2017) 59-68.

[12] A. Takagaki, C. Tagusagawa, K. Domen, Glucose production from saccharides using layered transition metal oxide and exfoliated nanosheets as a water-tolerant solid acid catalyst, Chemical Communications, (2008) 5363-5365.

[13] J. Tian, C. Fang, M. Cheng, X. Wang, Hydrolysis of cellulose over $Cs_xH_{3-x}PW_{12}O_{40}$ (X = 1-3) heteropoly acid catalysts, Chemical Engineering and Technology, 34 (2011) 482-486.

[14] L. Zhou, Z. Liu, M. Shi, S. Du, Y. Su, X. Yang, J. Xu, Sulfonated hierarchical H-USY zeolite for efficient hydrolysis of hemicellulose/cellulose, Carbohydrate Polymers, 98 (2013) 146-151.

[15] D.-M. Lai, L. Deng, Q.-X. Guo, Y. Fu, Hydrolysis of biomass by magnetic solid acid, Energy and Environmental Science, 4 (2011) 3552-3557.

[16] H.-X. Li, X. Zhang, Q. Wang, K. Zhang, Q. Cao, L.e. Jin, Preparation of the recycled and regenerated mesocarbon microbeads-based solid acid and its catalytic behaviors for hydrolysis of cellulose, Bioresource Technology, 270 (2018) 166-171.

[17] P.-W. Chung, A. Charmot, O.A. Olatunji-Ojo, K.A. Durkin, A. Katz, Hydrolysis catalysis of miscanthus xylan to xylose using weak-acid surface sites, ACS Catalysis, 4 (2014) 302-310.

[18] A.T. To, P.-W. Chung, A. Katz, Weak-acid sites catalyze the hydrolysis of crystalline cellulose to glucose in water: importance of post-synthetic functionalization of the carbon surface, Angewandte Chemie - International Edition, 54 (2015) 11050-11053.

[19] H. Kobayashi, M. Yabushita, T. Komanoya, K. Hara, I. Fujita, A. Fukuoka, High-yielding one-pot synthesis of glucose from cellulose using simple activated carbons and trace hydrochloric acid, ACS Catalysis, 3 (2013) 581-587.

[20] A. Shrotri, H. Kobayashi, A. Fukuoka, Air oxidation of activated carbon to synthesize a biomimetic catalyst for hydrolysis of cellulose, ChemSusChem, 9 (2016) 1299-1303.

[21] F. Shen, T. Guo, C. Bai, M. Qiu, X. Qi, Hydrolysis of cellulose with one-pot synthesized sulfonated carbonaceous solid acid, Fuel Processing Technology, 169 (2018) 244-247.

[22] A. Onda, T. Ochi, K. Yanagisawa, Selective hydrolysis of cellulose into glucose over solid acid catalysts, Green Chemistry, 10 (2008) 1033-1037.

[23] X. Zhao, J. Wang, C. Chen, Y. Huang, A. Wang, T. Zhang, Graphene oxide for cellulose hydrolysis: How it works as a highly active catalyst?, Chemical Communications, 50 (2014) 3439-3442.

[24] S. Tsuzuki, A. Fujii, Nature and physical origin of CH/π interaction: significant difference from conventional hydrogen bonds, Physical Chemistry Chemical Physics, 10 (2008) 2584-2594.

[25] P.-W. Chung, A. Charmot, T. Click, Y. Lin, Y. Bae, J.-W. Chu, A. Katz, Importance of internal porosity for glucan adsorption in mesoporous carbon materials, Langmuir, 31 (2015) 7288-7295.

[26] P.-W. Chung, A. Charmot, O.M. Gazit, A. Katz, Glucan adsorption on mesoporous carbon nanoparticles: effect of chain length and internal surface, Langmuir, 28 (2012) 15222-15232.

[27] P.-W. Chung, M. Yabushita, A.T. To, Y. Bae, J. Jankolovits, H. Kobayashi, A. Fukuoka, A. Katz, Long-chain glucan adsorption and depolymerization in zeolite-templated carbon catalysts, ACS Catalysis, 5 (2015) 6422-6425.

[28] M. Yabushita, H. Kobayashi, J.-Y. Hasegawa, K. Hara, A. Fukuoka, Entropically favored adsorption of cellulosic molecules onto carbon materials through hydrophobic functionalities, ChemSusChem, 7 (2014) 1443-1450.

[29] H. Kobayashi, A. Fukuoka, Development of solid catalyst solid substrate reactions for efficient utilization of biomass, Bulletin of the Chemical Society of Japan, 91 (2018) 29-43.

[30] X. Li, F. Shu, C. He, S. Liu, N. Leksawasdi, Q. Wang, W. Qi, M.A. Alam, Z. Yuan, Y. Gao, Preparation and investigation of highly selective solid acid catalysts with sodium lignosulfonate for hydrolysis of hemicellulose in corncob, RSC Advances, 8 (2018) 10922-10929.

[31] S. Suganuma, K. Nakajima, M. Kitano, D. Yamaguchi, H. Kato, S. Hayashi, M. Hara, Hydrolysis of cellulose by amorphous carbon bearing SO_3H, COOH, and OH groups, Journal of the american chemical society, 130 (2008) 12787-12793.

[32] A. Charmot, P.-W. Chung, A. Katz, Catalytic hydrolysis of cellulose to glucose using weak-acid surface sites on postsynthetically modified carbon, ACS Sustainable Chemistry and Engineering, 2 (2014) 2866-2872.

[33] M.R. Snowdon, A.K. Mohanty, M. Misra, A study of carbonized lignin as an alternative to carbon black, ACS Sustainable Chemistry and Engineering, 2 (2014) 1257-1263.

[34] J.M. Rosas, R. Berenguer, M.J. Valero-Romero, J. Rodríguez-Mirasol, T. Cordero, Preparation of different carbon materials by thermochemical conversion of lignin, Frontiers in Materials, 1 (2014) 1-17.

[35] J.i. Hayashi, A. Kazehaya, K. Muroyama, A.P. Watkinson, Preparation of activated carbon from lignin by chemical activation, Carbon, 38 (2000) 1873-1878.

[36] H. Kobayashi, H. Kaiki, A. Shrotri, K. Techikawara, A. Fukuoka, Hydrolysis of woody biomass by a biomass-derived reusable heterogeneous catalyst, Chemical Science, 7 (2016) 692-696.

[37] W.-J. Liu, H. Jiang, H.-Q. Yu, Thermochemical conversion of lignin to functional materials: a review and future directions, Green Chemistry, 17 (2015) 4888-4907.

[38] I. Kurnia, S. Karnjanakom, A. Bayu, A. Yoshida, J. Rizkiana, T. Prakoso, G. Guan, A. Abudula, *In-situ* catalytic upgrading of bio-oil derived from fast pyrolysis of lignin over high aluminum zeolites, Fuel Processing Technology, 167 (2017) 730-737.

[39] S.F. Hashmi, H. Meriö-Talvio, K.J. Hakonen, K. Ruuttunen, H. Sixta, Hydrothermolysis of organosolv lignin for the production of bio-oil rich in monoaromatic phenolic compounds, Fuel Processing Technology, 168 (2017) 74-83.

[40] M. Niu, Y. Hou, W. Wu, R. Yang, Degradation of lignin in $NaVO_3$-H_2SO_4 aqueous solution with oxygen, Fuel Processing Technology, 161 (2017) 295-303.

[41] W. He, W. Gao, P. Fatehi, Oxidation of kraft lignin with hydrogen peroxide and its application as a dispersant for kaolin suspensions, ACS Sustainable Chemistry and Engineering, 5 (2017) 10597-10605.

[42] A. Yuliestyan, M. García-Morales, E. Moreno, V. Carrera, P. Partal, Assessment of modified lignin cationic emulsifier for bitumen emulsions used in road paving, Materials and Design, 131 (2017) 242-251.

[43] N. Meek, D. Penumadu, O. Hosseinaei, D. Harper, S. Young, T. Rials, Synthesis and characterization of lignin carbon fiber and composites, Composites Science and Technology, 137 (2016) 60-68.

[44] I. Kurnia, A. Yoshida, Y.A. Situmorang, Y. Kasai, A. Abudula, G. Guan, Utilization of dealkaline lignin as a source of sodium-promoted MoS_2/Mo_2C hybrid catalysts for hydrogen production from formic acid, ACS Sustainable Chemistry & Engineering, 7 (2019) 8670-8677.

[45] J. Pang, W. Zhang, J. Zhang, G. Cao, M. Han, Y. Yang, Facile and sustainable synthesis of sodium lignosulfonate derived hierarchical porous carbons for supercapacitors with high volumetric energy densities, Green Chemistry, 19 (2017) 3916-3926.

[46] Y. Wu, Z. Fu, D. Yin, Q. Xu, F. Liu, C. Lu, L. Mao, Microwave-assisted hydrolysis of crystalline cellulose catalyzed by biomass char sulfonic acids, Green Chemistry, 12 (2010) 696-696.

[47] H.P. Boehm, Some aspects of the surface chemistry of carbon blacks and other carbons, Carbon, 32 (1994) 759-769.

[48] A. Yamaguchi, O. Sato, N. Mimura, Y. Hirosaki, H. Kobayashi, A. Fukuoka, M. Shirai, Direct production of sugar alcohols from wood chips using supported platinum catalysts in water, Catalysis Communications, 54 (2014) 22-26.

[49] J.L. Figueiredo, M.F.R. Pereira, M.M.A. Freitas, J.J.M. Órfão, Modification of the surface chemistry of activated carbons, Carbon, 37 (1999) 1379-1389.

[50] R.L. Shriner, C.K.F. Hermann, T.C. Morril, D.Y. Curtin, R.C. Fuson, The systematic identification of organic compounds, 8th ed., Jhon Wiley & Sons, Inc., Hoboken, NJ., 2004.

[51] Y. Zheng, W. Zheng, D. Zhu, H. Chang, Theoretical modeling of pKa's of thiol compounds in aqueous solution, New Journal of Chemistry, 43 (2019) 5239-5254.

[52] Dissociation constants of organic acids and bases, in: D.R. Lide (Ed.), CRC Press, Boca Raton, FL, 2005, pp. 46-56.

[53] P.P. Upare, J.W. Yoon, M.Y. Kim, H.Y. Kang, D.W. Hwang, Y.K. Hwang, H.H. Kung, J.S. Chang, Chemical conversion of biomass-derived hexose sugars to levulinic acid over sulfonic acid-functionalized graphene oxide catalysts, Green Chemistry, 15 (2013) 2935-2943.

[54] K. Mazeau, L. Heux, Molecular dynamics simulations of bulk native crystalline and amorphous structures of cellulose, The Journal of Physical Chemistry B, 107 (2003) 2394-2403.

[55] H. Chen, J. Liu, X. Chang, D. Chen, Y. Xue, P. Liu, H. Lin, S. Han, A review on the pretreatment of lignocellulose for high-value chemicals, Fuel Processing Technology, 160 (2017) 196-206.

[56] H. Kobayashi, Y. Ito, T. Komanoya, Y. Hosaka, P.L. Dhepe, K. Kasai, K. Hara, A. Fukuoka, Synthesis of sugar alcohols by hydrolytic hydrogenation of cellulose over supported metal catalysts, Green Chemistry, 13 (2011) 326-333.

[57] X. Chen, Y. Zhang, J. Mei, G. Zhao, Q. Lyu, X. Lyu, H. Lyu, L. Han, W. Xiao, Ball milling for cellulose depolymerization and alcoholysis to produce methyl levulinate at mild temperature, Fuel Processing Technology, 188 (2019) 129-136.

[58] R.G. Blair, Mechanical and combined chemical and mechanical treatment of biomass, in: Z. Fang, R.L. Smith Jr, X. Qi (Eds.), Springer, Dordecht, 2015, pp. 269-288.

[59] E. Lam, J.H. Chong, E. Majid, Y. Liu, S. Hrapovic, A.C.W. Leung, J.H.T. Luong, Carbocatalytic dehydration of xylose to furfural in water, Carbon, 50 (2012) 1033-1043.

[60] J. Geboers, S. Van de Vyver, K. Carpentier, P. Jacobs, B. Sels, Efficient hydrolytic hydrogenation of cellulose in the presence of Ru-loaded zeolites and trace amounts of mineral acid, Chemical Communications, 47 (2011) 5590-5592.

[61] M. Yabushita, H. Kobayashi, K. Hara, A. Fukuoka, Quantitative evaluation of ball-milling effects on the hydrolysis of cellulose catalysed by activated carbon, Catalysis Science and Technology, 4 (2014) 2312-2317.

Chapter 5 Synthesis of *p*-Menthane-3,8-diol over Lignin-Derived Carbon Catalysts

5.1. Introduction

The pyrolysis treatment of lignosulfonate lignin in the low temperature can maintain the acid functional groups of the lignin-derived carbon material well and further it is active for converting cellulose and lignocellulosic biomass to the glucose and xylose, as indicated in **Chapter 4**. Therefore, the utilization of lignin-derived carbon acid catalyst is worth investigating for synthesizing *p*-menthane-3,8-diol from cyclization-hydration reaction of citronellal, as mosquitoes repellent. Nowadays, 700 million people are infected by bacteria, viruses, or parasites transmitted by mosquitoes, and more than a million deaths every year [1]. It is reported that 438 thousand people deaths have been caused only by malaria, which is spreading by Anopheles mosquitoes [2]. Mosquitoes repellents are generally used for self-protection to control the spread of diseases by mosquitoes biting since it is a simple and effective way [3]. In general, it is applied in either lotion or spray states and directly coated on the skin. *N*,*N*-diethyl-*m*-methylbenzamide (DEET) is the most popular synthetic mosquitoes repellent, which can maintain a long protection time of about 5-6 hours. However, this synthetic active compound has some potential neuro-toxicity effects to human body such as insomnia, mood disturbance, and impaired cognitive function [4]. In comparison with DEET, *p*-menthane-3,8-diol (PMD) is one of a natural-derived mosquito repellent. Although its effect is slightly lower than DEET, it is non-toxic and non-irritant to human body. Thus, it has been received growing attention as a substitute of DEET [5].

The PMD can be synthesized through the acid-catalyzed cyclization-hydration of citronellal (Scheme 5.1). Recently, this reaction is mostly conducted by using homogeneous acid catalysts such as dilute H_2SO_4 [6-8], acetic acid [8], and citric acid [9]. However, such homogeneous

catalysts are difficult to be separated from the final product; furthermore, they are, also hardly to be reused. Recently, PMD was also synthesized via the citronellal cyclization hydration reaction using the pressurized carbon dioxide-water medium as the homogeneous acid catalyst [8]. However, high pressure (1 MPa) and high temperature (100 °C) are needed in this process so that the operation cost is high. To date, only a few studies used heterogeneous catalysts for the production of PMD via the citronellal cyclization-hydration reaction as the homogeneous acid catalyst. For example, H-ZSM 5 (with Si/Al molar ratio = 38) had ever been used as the heterogeneous catalyst, but the performance was not sufficiently high [8].

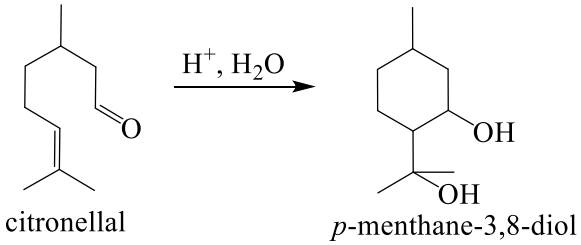

Scheme 5.1 Citronellal cyclization-hydration reaction to *p*-menthane-3,8-diol

Carbon-based solid acid catalysts have been used as the inexpensive catalysts to substitute the homogeneous catalysts for the conversions of various organic compounds such as esterification of fatty acid with alcohol [10,11], hydrolysis of cellulose [12-15], dehydration of xylose and fructose to 5-hydroxymethylfurfural [16,17]. To date, various methods such as oxidation by HNO_3, H_2O_2, or $KMnO_4$ and sulfonation with concentrated H_2SO_4, have been employed for the generation of acidic functional groups on the carbon catalysts [10,13-16]. However, preparation of some carbon-based materials such as carbon black and graphite consumes huge energy [18-20]. Meanwhile, in order to increase the surface area of carbon materials, the strong alkaline hydroxide is generally required which would generate a large amount of wastewater in the post-treatment process. To

solve such issues, recently, a simple way by air oxidation of lignocellulose residue was used to prepare a reusable carbon catalyst for the lignocellulose depolymerization [21]. It provides a sustainable and inexpensive route to produce carbon-based acid catalysts in the organic compound conversion.

Annually, about 70 MTon of lignosulfonate lignin is generated as the waste from pulp and paper industries [22]. It is urgent issue to effectively use the lignosulfonate lignin. Thermochemical efforts such as pyrolysis and hydrothermal processing have been employed to convert lignin to high value-added chemicals [23-25]. Nevertheless, since lignin is a kind of thermo-stable polymeric compound, which is too rigid to be decomposed, a large amount of char is always remained in the final products, which could be further converted to functional carbon materials such as carbon black [18], activated carbon [26], carbon fiber [27], electrode materials of supercapacitor [28], catalyst precursor materials [29,30], and carbon catalyst [31]. In our previous study, it is found that the existence of sulfonated and oxygenated functional groups on the surface of the lignosulfonate lignin is benefit for the preparation of carbon catalysts [31].

In this work, the carbon catalysts were prepared from the alkaline lignin (AL) by a simple pyrolysis method followed by an acid solution treatment process as our previous study [31]. Since the acid properties of AL-derived carbon catalysts prepared with different pyrolysis temperatures have been characterized by Boehm titration, acid-base back titration of NaCl method, elemental analysis, and Fourier-transform infrared spectroscopy (FTIR) in our previous work [31]. Herein, XPS analysis was further applied to elucidate the states of acid functional groups in the AL-derived carbon catalysts, and meanwhile Raman spectroscopy was used to evaluate the effect of temperature on the degree of graphitization of AL-derived carbon catalysts. Furthermore, the obtained catalysts were applied for the synthesis of PMD via the citronellal cyclization-hydration

reaction. It is expected to provide a new perspective to utilize waste alkaline lignin as the source of catalysts for the effective production of PMD without harsh chemical modification and high energy consumption.

5.2. Materials and methods

5.2.1. Materials

(±)-Citronellal was purchased from Wako Chemicals Co., Ltd., Japan (Lot No. ECN5193). (-)-Citronellal (Lot No. P6FXO) and isopulegol (Lot: No. G6Q2C) were supplied from Tokyo Chemical Industry Co., Ltd, Japan (TCI). All chemicals were used without further purification. Alkaline lignin (AL) from TCI was used as a source for the preparation of carbon catalysts. The proximate and ultimate analysis results for alkaline lignin have been reported in our previous study [31]. Carbon black (Vulcan XC 72R, CABOT Corp., USA) and H-USY (HSZ-330, Si/Al = 6, TOSOH Corp., Japan) were also used as the solid weak acid catalysts for comparison. High-grade H_2SO_4 and anhydrous citric acid were purchased from Wako Chemicals Co., Ltd., Japan for the preparation of 0.25 wt% H_2SO_4 and 7 wt% citric acid, respectively as the homogeneous acid catalysts.

5.2.2. Preparation of the AL-derived Weak-Acid Carbon Catalysts

AL-derived carbon catalysts were prepared by the thermal pyrolysis of AL at different temperatures followed by an acid solution treatment process [31]. In brief, 5 g of AL was put into a fixed-bed quartz reactor and heated up to the final pyrolysis temperature (i.e., 300, 350, 400, 450, and 500 °C in this work) with a heating rate of 5 °C/min under a 50 cm^3/min of argon flow and

then maintained at the final temperature for 1 h. The obtained solid was treated by 40 mL of 1 M HCl to remove the residual inorganic impurities, and subsequently washed by deionized (DI) water until pH 6-7 and finally, washed by ethanol to wash out organic soluble compound on the surface of carbon, and then dried in a vacuum oven at 80 °C for 18 h. Hereafter, those catalysts are denoted as AL-Py-X, where X represents the pyrolysis temperature ((i.e., 300, 350, 400, 450, and 500 °C).

The obtained AL-derived carbon catalysts had been characterized by Boehm titration and acid-base back titration of NaCl method to determine the specific acid amount in our previous study [31]. Herein, all catalysts were further characterized by XPS analysis (VG Scientific ESCALab 250i-XL, UK) and Raman spectroscopy. The thermal degradation of AL-derived carbon catalysts were detected by a temperature-programmed desorption (TPD, BEL-Cat, Japan) equipped with a mass spectrometer (MS, BEL-Mass, Japan), in which the sample was pre-treated at 100 °C for 10 min at first and then heated to 800 °C with a heating rate of 10 °C/min under helium atmosphere.

5.2.3. Catalytic Performance

The cyclization-hydration of citronellal to PMD was conducted in a screw-capped tube reactor coupled with a magnetic stirrer and a temperature controller (Personal Organic Synthesizer Zodiac CCX, Eyela, Japan). In brief, (±)-Citronellal (0.2 g), solid catalyst (0.1 g), and DI water (5 g) were introduced into a screw-capped tube reactor and heated at 50 °C for 1-24 h. After the reaction, the reactor was cooled down in an ice bath. The water phase was separated by decantation at first, and then 10 mL of ethanol was added to the oil-solid fraction and shaken by a vortex shaker for the extraction of the product. Thereafter, the suspension was filtered by a PTFE membrane filter (0.1 μm, Advantec), and the filtrate was transferred to a vial bottle (10 ml) containing 1 g of anhydrous sodium sulfate.

The product solution was analyzed by a *gas chromatography/mass spectrometry system* (GC-MS, GC-2010 plus for GC, QP-2010 for MS, Shimadzu, Japan) with a Zebron ZB-WAXplus capillary column (30 m × 0.25mm × 0.25 μm, Phenomenex, USA). In brief, 0.5 μL of product solution was injected into the GC-MS by using an auto-injector with an injector temperature of 300 °C. The column temperature was programmed as follows: initially, the temperature was kept at 60 °C for 2 min and then heated up to 250 °C with a heating rate of 10 °C/min and held at 250 °C for 14 min. The mass spectra of products were identified by NIST 11 mass spectrum library. The amounts of products were determined by the standard external method. Note that the standard of *p*-menthane-3,8-diol was prepared based on the reported work [9], and the purity was determined by ^{1}H-NMR (Figure 5.1). The conversion of (±)-citronellal, PMD selectivity, and PMD yield were calculated by using equations 5.1, 5.2, and 5.3, respectively, as follow:

Equation 5.1 Conversion calculation of citronellal

$$\text{Conversion}_{t=n}\ (\%) = \frac{mol\ citronellal_{t=0} - mol\ citronellal_{t=n}}{mol\ citronellal_{t=0}} \times 100$$

Equation 5.2 Selectivity calculation of PMD

$$\text{PMD selectivity}_{t=n}\ (\%) = \frac{mol\ PMD_{t=n}}{(mol\ isopulegol + mol\ PMD + mol\ dimer)_{t=n}} \times 100$$

Equation 5.3 Yield calculation of PMD

$$\text{PMD yield}_{t=n}(\%) = \frac{PMD\ selectivity_{t=n}\ (\%)\ \times\ Conversion_{t=n}\ (\%)}{100}$$

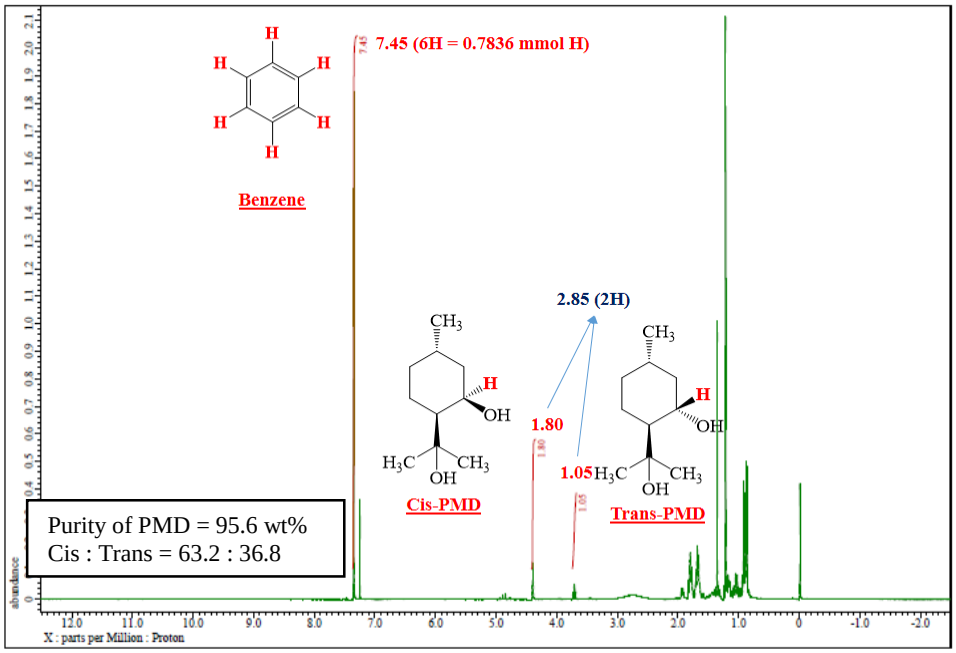

Figure 5.1 Characterization of standard PMD by 1H-NMR ($W_{benzene}$ = 10.2 mg; W_{sample} = 54 mg)

5.3. Results and discussion

5.3.1. Characterization of AL-Derived Carbon Catalysts

In our previous study [31], it is found that the total acid amount in the obtained catalyst decreased with the increase in the pyrolysis temperature. Herein, the thermal decomposition of oxygenated functional groups could result in the decrease of acid amount, which was confirmed by C1s XPS spectra. As shown in Figure 5.2 (a), the peak intensities ascribable to the oxygenated functional groups including C-O-C/C-O-H of ether/hydroxyl groups (286 eV) and O-C=O of carboxyl group (288.9 eV), decreased with the increase in the pyrolysis temperature. Furthermore, as also indicated in Table 5.1, the atomic ratio of O/C decreased with the increase in the pyrolysis temperature. It should be noted that the oxygenated functional groups have contribution to the

acidity of carbon catalysts. These results are also agreement with the TPD-MS analysis results of AL-derived carbon catalysts, as presented in Figure 5.3. The signals intensities of CO_2 (*m/z* = 44), CO (*m/z* = 28), and H_2O (*m/z* = 18), which are ascribable to the thermal decomposition of oxygenated functional groups, i.e., carboxylic acid, lactones, phenol, and carbonyl functional groups, decreased with the increase in the pyrolysis temperature. Meanwhile, the S2p XPS spectra show three peaks which are ascribable to thiol (164 eV), thiophene (165.2 eV), and sulfonated functional groups (168 eV) (Figure 5.2 (b)). These results confirmed our previously reported work [31], further indicating the presence of thiol and thiophene functional groups in the AL-derived carbon catalysts. That is, both sulfur functional group and sulfonated functional group existed in the catalysts, which are related to the lignin source from the wastes of pulp and paper industries. In general, the thiol and thiophene functional groups are classified as the same group as the phenol group since the pKa value of them are in the same range of 10-11 [32,33]. Based on these analysis results, it can be concluded that the existences of oxygenated functional groups and sulfur functional groups in the AL-derived carbon catalysts should be the main factors to affect the acidity. In our previous study, it is found that the oxygenated functional groups and sulfur functional groups in the AL-derived carbon catalysts were active for the hydrolysis of cellulose and Japanese cedar wood to produce monomeric sugars such as glucose and xylose [31].

Table 5.1 Calculated atomic percentages from XPS analysis.

Catalyst	Atomic percentage[a] (At. %)			Atomic ratio (mol/mol)	
	C1s	O1s	S2p	O/C	S/C
AL-Py-300	62.26	37.16	0.58	0.597	0.009
AL-Py-350	65.05	34.37	0.58	0.528	0.009
AL-Py-400	65.55	33.59	0.86	0.512	0.013
AL-Py-450	70.70	28.47	0.83	0.403	0.012
AL-Py-500	73.74	25.43	0.83	0.345	0.011

[a]based on C1s, O1s, and S2p XPS spectra

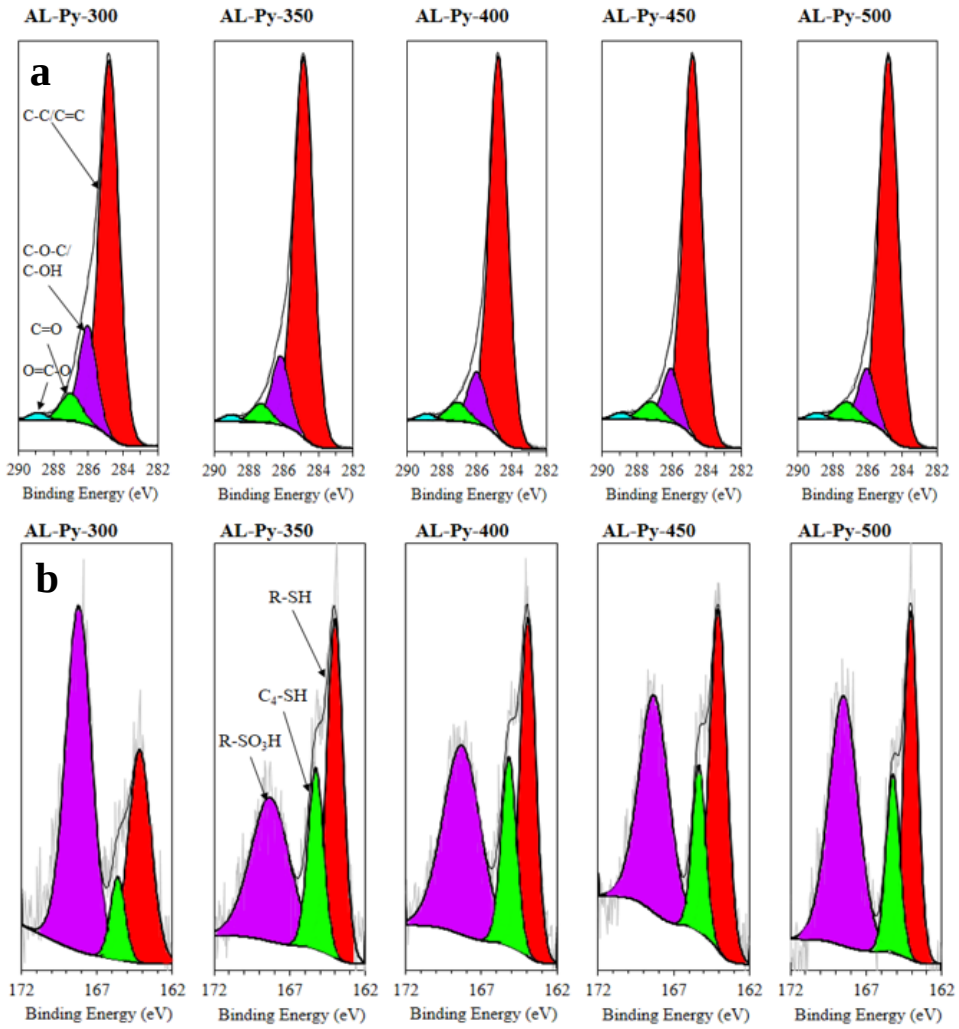

Figure 5.2. (a) C1s and (b) S2p XPS spectra of AL-derived weak-acid carbon catalysts.

Raman spectroscopy was also employed to elucidate the degree of graphitization of carbon material in the prepared AL-derived carbon catalysts by comparison of the ratios between two peaks D-band and G-band (I_D/I_G) [18]. As shown in Figure 5.4, two peaks at 1400 cm^{-1} (D-band) and 1605 cm^{-1} (G-band) were obviously observed for all catalysts, and the ratio of I_D/I_G gradually increased with the increase in the pyrolysis temperature, indicating that a higher proportion of the disordered graphite structure was formed at a higher pyrolysis temperature.

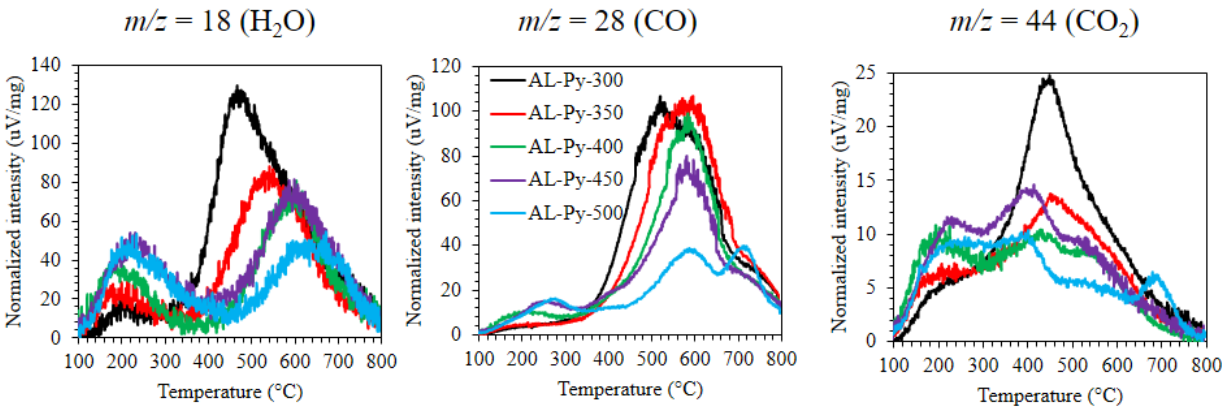

Figure 5.3. TPD-MS signal profiles during the decomposition of AL under helium atmosphere.

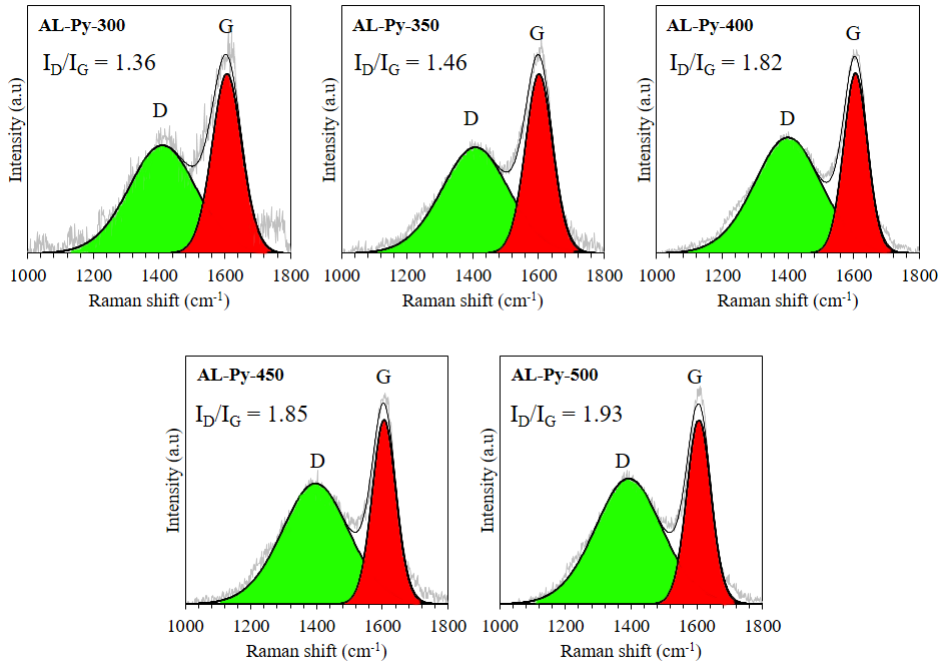

Figure 5.4. Raman spectra of AL-derived weak-acid carbon catalysts.

5.3.2. PMD Synthesis on AL-Derived Carbon Catalyst

Table 5.2. Catalytic Performances of the Solid Acid Catalysts for the Cyclization-Hydration of (±)-Citronellal.[a]

Entry	Catalysts	Conv. (%)	Yieldb (%)		
			Isopulegol	PMD	Dimer
1	AL-Py-300	99	48	37	14
2	AL-Py-350	98	44	48	6
3	AL-Py-400	98	11	84	3
4	AL-Py-450	97	12	83	3
5	AL-Py-500	97	9	86	2

[a]weight ratio of (±)-citronellal to catalyst (S/C = 2); weight ratio of water to (±)-citronellal (W/S = 25); reaction temp.: 50 °C; reaction time: 24 h; [b]yield of the sum of isomers.

In this work, the activity of AL-derived carbon catalysts for the cyclization-hydration of (±)-citronellal to the PMD was evaluated at a temperature of 50 °C, which is similar to the reported work with the optimum temperature condition [6,9]. The results are summarized in Table 5.2 (entries 1-5). One can see that the conversion of the citronellal decreased with the increase of pyrolysis temperature for the preparation of catalyst, which corresponds to the decrease of the total acid amount in the catalysts. It is reported that the rate of cyclization-hydration of citronellal would be affected by the acid concentration [6,9]. As a result, among the obtained AL-derived carbon

catalysts, AL-Py-300 exhibited the highest activity with a citronellal conversion as high as 99 %. However, the yield toward PMD was low (37 %) (entry 1) with high yields of byproducts, i.e., 48 % for isopulegol and 14 % for dimer product, respectively. In contrast, a high yield of PMD with low yields of byproducts was obtained when AL-Py-500 was employed (entry 5). That is, the yield toward PMD was as high as 86 % with low yields of isopulegol (9 %) and dimer product (2 %). It should be noted that the AL-Py-500 had the lowest acid amount (0.11 mmol/g) among all AL-derived weak acid carbon catalysts (e.g. AL-Py-300 has acid amount of 1.25 mmol/g) [31]. These results indicate that lower acid amount is suitable for producing PMD from citronellal. Similar selectivity change is reported on the PMD synthesis catalyzed by aqueous sulfuric acid. PMD was more selectively produced when using a lower concentration of sulfuric acid (0.25 wt% H_2SO_4) at 50 °C for 11 h, while isopulegol and dimer were dominated with a higher concentration of sulfuric acid (10 wt% H_2SO_4) at 35 °C for 4 h [6]. It is probably related to the reaction mechanisms. The paper about the cyclization of citronellal with a Lewis acid catalyst reported that isopulegol is formed by the concerted reaction of ring-closure and deprotonation from the methyl group on the C1 position, in which the intra-molecular hydrogen bonding between the carbonyl oxygen atom and the hydrogen atom connecting to the carbon atom on the C1 position directs this reaction (Scheme 5.2) [34]. Based on this reported assumption, weaker acidity or fewer acid amount is not enough to polarize the carbonyl oxygen atom to form this intra-molecular hydrogen bonding, and instead the positively charged carbon atom on the C2 position during the ring-closure was attacked by water molecule to form PMD. In this proposed reaction pathway, the intermediates toward the isopulegol and PMD formation are different. Actually, when isopulegol was used as a reactant instead of citronellal, none of PMD was formed in the presence of the AL-Py-500 catalyst as well as 7 wt% of citric acid and 0.25 wt% of sulfonic acid, indicating that isopulegol is not an

intermediate product for PMD formation in the current reaction conditions (Table 5.3, entries 3-5), although isopulegol was proposed to be an intermediate in the other report [8]. The time course of the citronellal reaction with the AL-Py-500 catalyst also supports our proposed reaction pathway that isopulegol is not an intermediate (Figure 5.5). If isopulegol is an intermediate, isopulegol starts to form at early stage of the reaction, and then its amount will be reduced by converting to PMD. However, as shown in Figure 5.5, PMD started to increase at 3h of the reaction while isopulegol amount had no obvious change after the first 3 h of the reaction.

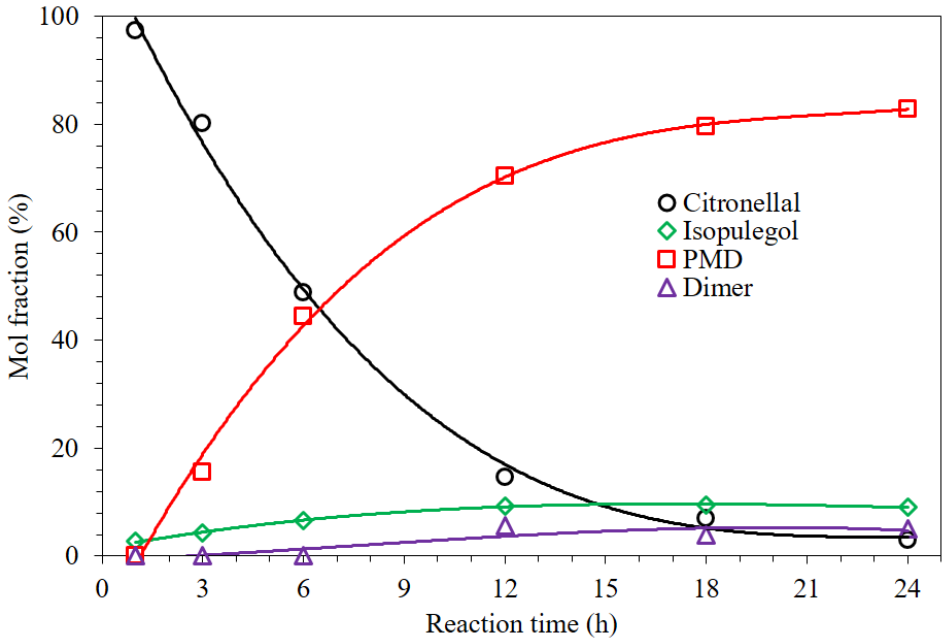

Figure 5.5 Reaction profile of cyclization-hydration of (±)-citronellal over the AL-Py-500 catalyst with the conditions of S/C = 2 and W/S = 25 at 50 °C.

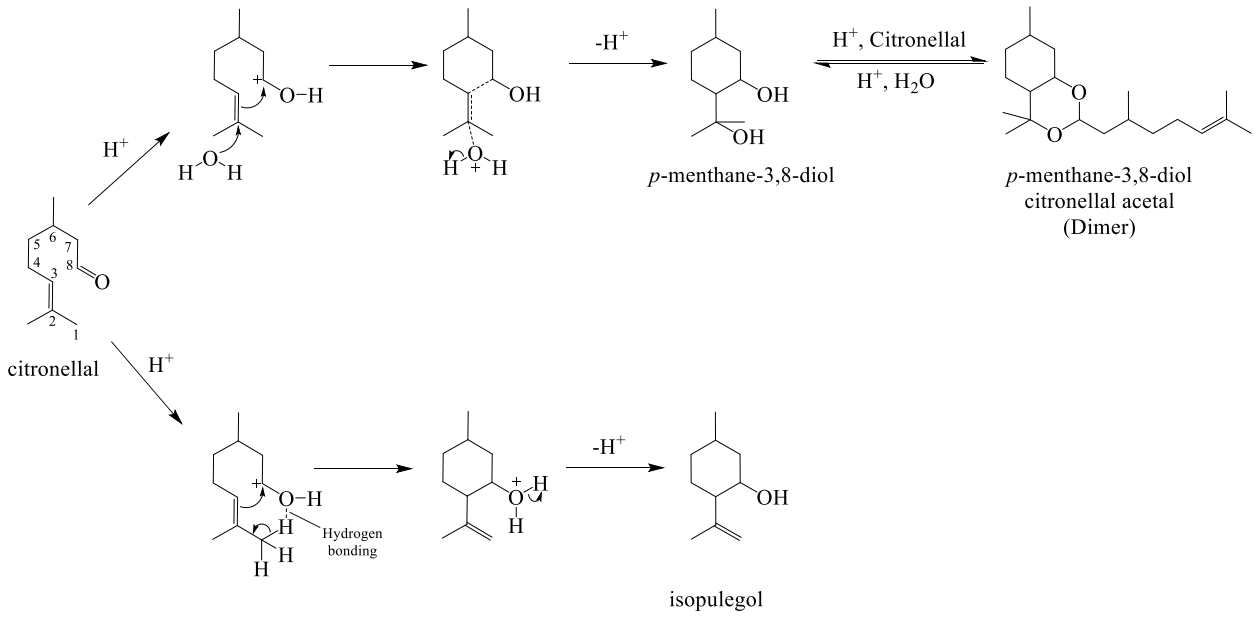

Scheme 5.2 Proposed reaction mechanism in the cyclization-hydration of citronellal to PMD.

Table 5.3 Catalytic Performance of the AL-Py-500 Catalyst for Cyclization-Hydration Reaction using Different Substrates.

Entry	Substrates	Conv. (%)	Yield[d] (mol %)		
			Isopulegol	PMD	Dimer
1[a]	(±)-Citronellal	97	9	86	2
2[a]	(-)-Citronellal	98	4	94	<0.1
3[a]	Isopulegol	<0.1	>99.9	<0.1.	<0.1.
4[b]	Isopulegol	<0.1	>99.9	<0.1.	<0.1.
5[c]	Isopulegol	<0.1	>99.9	<0.1.	<0.1.

[a]weight ratio of substrate to AL-Py-500 catalyst (S/C = 2); weight ratio of water to substrate (W/S = 25); reaction temp.: 50 ° C; reaction time: 24 h; [b]Reaction using 0.25 wt% H_2SO_4 and isopulegol with a weight ratio of 1:1 for 12 h reaction; [c]Reaction using 7 wt% citric acid and isopulegol with a weight ratio of 5:3 for 15 h reaction; [d]yield of the sum of isomers.

Meanwhile, the yield of PMD was improved to 94 % when (-)-citronellal was used as the substrate (Table 6.3, entry 2). Herein, the employed (-)-citronellal had a high enantiomeric purity with an optical rotation of $[\alpha]_D^{20}$ = - 16.2° which is identical to the reported value for the standard one ($[\alpha]_D^{20}$ = - 16.2°) [35],[35] and the employed (±)-citronellal was the mixture of enantiomers with an optical rotation of $[\alpha]_D^{20}$ = + 11°. Thus, the yield of PMD should be affected by the enantiomeric

purity of the reactant. This result is consistent with the reported work [8], in which the yield of PMD was improved when *S*-(-)-citronellal was used instead of the (±)-citronellal.

5.3.3. Comparison of Catalytic Activity of AL-Py-500 Catalyst with Other Catalysts

For comparison, the cyclization-hydration of (±)-citronellal was also performed using other two commercial solid catalysts, i.e., carbon black (CB) and H-USY (Table 5.4). One can see that the conversion of (±)-citronellal over H-USY catalyst (70 %) was much lower than that over the AL-Py-500 catalyst (97 %) although the acid amount of H-USY (0.61 mmol/g) was higher. In addition, the selectivity was preferred to the isopulegol with a yield of 43 %. It is reported that H-USY (Si/Al = 6) has both Brønsted and Lewis acid sites [36], in which the Lewis acid function could direct the cyclization to isopulegol [37]. In comparison, the commercial CB with a lower acid amount (0.06 mmol/g) exhibited higher selectivity toward PMD than the H-USY. Herein, it is considered that the oxygenated functional groups, especially carboxylic functional groups on the CB, provided the Brønsted acid sites (Table 5.5), which catalyzed the cyclization-hydration of citronellal to produce PMD. However, the conversion of (±)-citronellal (53 %) as well as the yield towards PMD (46 %) over CB were lower than those over the AL-Py-500 catalyst (97 % and 86 %, respectively), which should be related to the lower carboxylic functional groups proportion on CB (0.02 mmol/g). Thus, the AL-derived carbon catalysts are more suitable for the cyclization-hydration of citronellal to PMD.

Table 5.4 Comparison of The Catalytic Activity of AL-Py-500 Catalyst with Other Catalysts

Catalyst type	Catalyst	Reaction condition	Conv. (%)	Selectivity[a] (%)	Ref.
Homogeneous	0.25 wt% H_2SO_4	50 °C; 11 h	98	92	[6]
	7 wt% Citric acid	50 °C; 15 h	82	79	[9]
	CO_2-H_2O	7.5 MPa; 100 °C; 11 h	97	85	[8]
Heterogeneous	ZSM-5	100 °C; 2 h	48	73	[8]
	H-USY	50 °C; 24 h	70	37	This work
	Carbon Black	50 °C; 24 h	53	87	This work
	AL-Py-500	50°C; 24 h	97	89	This work

[a]the sum of PMD isomers

Table 5.5 Characterizations of commercial acid catalysts.

Catalyst	Total acid amount (mmol/g)[a]	Density of each acid functional group[b]		
		Carboxylic group (mmol/g)	Lactonic group (mmol/g)	Phenolic group (mmol/g)
CB	0.06	0.02	0.03	0.01
H-USY (Si/Al = 6)	0.61	-	-	-

[a]Acid-base back titration method with 0.01 M NaOH; [b]Boehm titration method with 0.01 M NaOH, 0.01 M $NaHCO_3$, and 0.01 M Na_2CO_3

Also in the comparison with homogeneous acid catalysts, the AL-Py-500 catalyst exhibited the most excellent class of catalytic performance, although H_2SO_4 (0.25 wt%) showed just slightly higher conversion and selectivity. Considering the easy separation and reusability of the AL-Py-500 catalyst, it should be a promising catalyst for the PMD production. In particular, this catalyst can be made from the wasted lignosulfonate lignin, which provided a sustainable way to use the wastes as the catalysts in the organic synthesis.

5.3.4. Reusability of AL-Py-500 Catalyst

The reusability of the AL-Py-500 catalyst was also investigated, in which the reaction was performed at 50 °C for 24 h with S/C = 2 and W/S = 25. As shown in Figure 4, the catalytic activity decreased to some extent, and the conversion decreased from 97 % (fresh) to 73 % (3rd cycle),

corresponding to the decrease of total acid amount in the catalyst (Table 5.6). Nevertheless, the selectivity toward PMD maintained almost unchanged for at least 3 reuse cycles. Thus, the AL-Py-500 catalyst can be considered as a stable solid acid catalyst for the cyclization-hydration of citronellal to PMD.

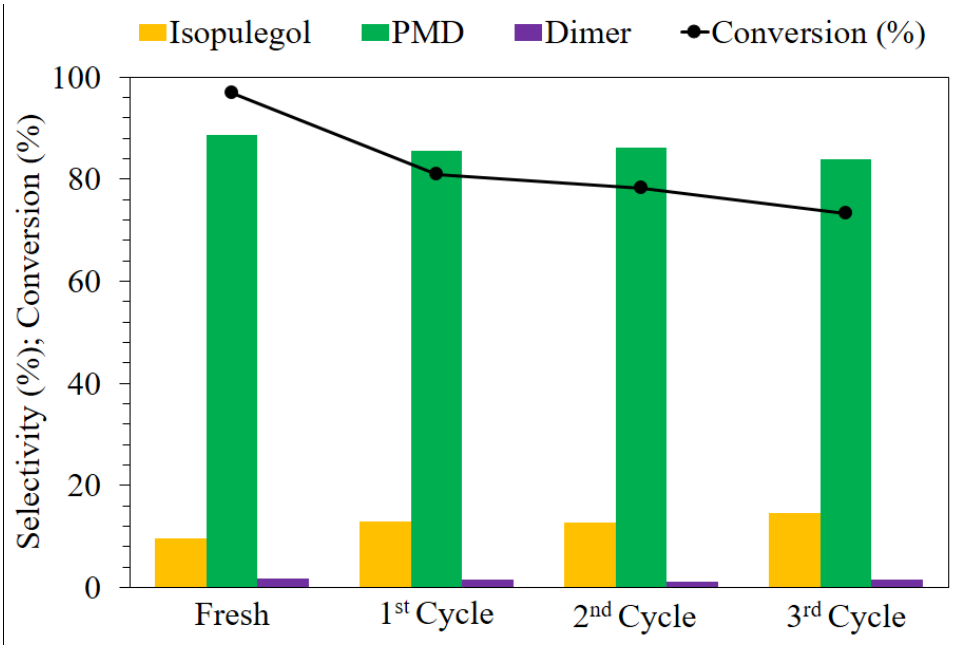

Figure 5.6 Reusability of the AL-Py-500 catalyst for the cyclization-hydration reaction of (±)-citronellal.

Table 5.6 Characterization of the fresh and spent AL-Py-500 catalyst.

Cycle number	Total acid amount (mmol/g)[a]	Density of each acid functional group			
		Sulfonic groups (mmol/g)[b]	Carboxylic groups (mmol/g)[a]	Lactonic groups (mmol/g)[a]	Phenolic and thiol groups (mmol/g)[a]
Fresh[1]	0.11	0.06	0.04	0.00	0.01
1st	0.09	0.04	0.04	0.00	0.01
2nd	0.08	0.03	0.04	0.00	0.01
3rd	0.06	0.03	0.03	0.00	0.00

[a]Boehm titration method with 0.01 M NaOH, 0.01 M $NaHCO_3$, and 0.01 M Na_2CO_3; [b]Estimated by acid-base back titration of 1 M NaCl method; [c]Estimated by the difference of Boehm titration method with 0.01 M $NaHCO_3$ and acid-base back titration of 1 M NaCl method.

5.4. Conclusions

AL-derived carbon catalysts were simply prepared and successfully used for cyclization-hydration of citronellal to PMD. Among the AL-derived carbon catalysts, AL-Py-500 with the lowest acid amount (0.11 mmol/g) resulted in the highest PMD yield of 86 % with low yields of isopulegol (9 %) and dimer product (2 %). As reported on the homogeneous catalyst of sulfuric acid, the formation of PMD preferred over the catalysts with fewer acid amount or weaker acid sites, while stronger acid sites produces isopulegol. Although the performance of AL-Py-500 was

slightly lower than the homogeneous catalyst of 0.25 wt% H_2SO_4, it can be easily separated and reused, which will reduce the PMD production cost and avoid environmental pollution. Especially, the wasted lignosulfonate lignin from pulp and paper industries can be effectively applied as the carbon source for the catalyst preparation, which provides a sustainable way to use the wastes in the organic synthesis.

References

[1] H. Caraballo, K. King, Emergency Department Management Of Mosquito-Borne Illness: Malaria, Dengue, And West Nile Virus, Emergency medicine practice, 5 (2014) 1-23.

[2] WHO | World Health Organization, WHO, (2016).

[3] J. Drapeau, Insect Repellents Based on para-Menthane-3,8-diol, in, 2017.

[4] R. Tice, B. Brevard, N,N-Diethyl-m-toluamide (DEET), Intergrated Laboratory Systems, North Carolina, 1999.

[5] M.F. Maia, S.J. Moore, Plant-based insect repellents : a review of their efficacy , development and testing PMD from lemon eucalyptus (Corymbia citriodora) extract, Malaria Journal, 10 (2011) 1-15.

[6] Y. Yuasa, H. Tsuruta, Y. Yuasa, A Practical and Efficient Synthesis of *p*-Menthane-3,8-diols, Organic Process Research & Development, 4 (2002) 159-161.

[7] H.E. Zimmerman, J. English Jr, Stereoisomerism of Isopulegol Hydrates and Some Analogous 1,3-Diols, Journal of the american chemical society, 75 (1953) 2367-2370.

[8] H. Cheng, X. Meng, R. Liu, Y. Hao, Y. Yu, S. Cai, F. Zhao, Cyclization of citronellal to p-menthane-3,8-diols in water and carbon dioxide, Green Chemistry, 11 (2009) 1227-1231.

[9] J. Drapeau, M. Rossano, D. Touraud, U. Obermayr, M. Geier, A. Rose, W. Kunz, Green synthesis of para-Menthane-3,8-diol from Eucalyptus citriodora: Application for repellent products, Comptes Rendus Chimie, 14 (2011) 629-635.

[10] H. Liu, J. Chen, L. Chen, Y. Xu, X. Guo, D. Fang, Carbon Nanotube-Based Solid Sulfonic Acids as Catalysts for Production of Fatty Acid Methyl Ester via Transesterification and Esterification, ACS Sustainable Chemistry and Engineering, 4 (2016) 3140-3150.

[11] M. Hara, Biodiesel production by amorphous carbon bearing SO_3H, COOH and phenolic OH groups, a solid Brønsted acid catalyst, Topics in Catalysis, 53 (2010) 805-810.

[12] A. Shrotri, H. Kobayashi, A. Fukuoka, Air oxidation of activated carbon to synthesize a biomimetic catalyst for hydrolysis of cellulose, ChemSusChem, 9 (2016) 1299-1303.

[13] A.T. To, P.-W. Chung, A. Katz, Weak-acid sites catalyze the hydrolysis of crystalline cellulose to glucose in water: importance of post-synthetic functionalization of the carbon surface, Angewandte Chemie - International Edition, 54 (2015) 11050-11053.

[14] S. Suganuma, K. Nakajima, M. Kitano, D. Yamaguchi, H. Kato, S. Hayashi, M. Hara, Hydrolysis of cellulose by amorphous carbon bearing SO_3H, COOH, and OH groups, Journal of the american chemical society, 130 (2008) 12787-12793.

[15] A. Charmot, P.-W. Chung, A. Katz, Catalytic hydrolysis of cellulose to glucose using weak-acid surface sites on postsynthetically modified carbon, ACS Sustainable Chemistry and Engineering, 2 (2014) 2866-2872.

[16] R. Liu, J. Chen, X. Huang, L. Chen, L. Ma, X. Li, Conversion of fructose into 5-hydroxymethylfurfural and alkyl levulinates catalyzed by sulfonic acid-functionalized carbon materials, Green Chemistry, 15 (2013) 2895-2903.

[17] E. Lam, J.H. Chong, E. Majid, Y. Liu, S. Hrapovic, A.C.W. Leung, J.H.T. Luong, Carbocatalytic dehydration of xylose to furfural in water, Carbon, 50 (2012) 1033-1043.

[18] M.R. Snowdon, A.K. Mohanty, M. Misra, A study of carbonized lignin as an alternative to carbon black, ACS Sustainable Chemistry and Engineering, 2 (2014) 1257-1263.

[19] J.M. Rosas, R. Berenguer, M.J. Valero-Romero, J. Rodríguez-Mirasol, T. Cordero, Preparation of different carbon materials by thermochemical conversion of lignin, Frontiers in Materials, 1 (2014) 1-17.

[20] J.i. Hayashi, A. Kazehaya, K. Muroyama, A.P. Watkinson, Preparation of activated carbon from lignin by chemical activation, Carbon, 38 (2000) 1873-1878.

[21] H. Kobayashi, H. Kaiki, A. Shrotri, K. Techikawara, A. Fukuoka, Hydrolysis of woody biomass by a biomass-derived reusable heterogeneous catalyst, Chemical Science, 7 (2016) 692-696.

[22] W.-J. Liu, H. Jiang, H.-Q. Yu, Thermochemical conversion of lignin to functional materials: a review and future directions, Green Chemistry, 17 (2015) 4888-4907.

[23] I. Kurnia, S. Karnjanakom, A. Bayu, A. Yoshida, J. Rizkiana, T. Prakoso, G. Guan, A. Abudula, *In-situ* catalytic upgrading of bio-oil derived from fast pyrolysis of lignin over high aluminum zeolites, Fuel Processing Technology, 167 (2017) 730-737.

[24] S.F. Hashmi, H. Meriö-Talvio, K.J. Hakonen, K. Ruuttunen, H. Sixta, Hydrothermolysis of organosolv lignin for the production of bio-oil rich in monoaromatic phenolic compounds, Fuel Processing Technology, 168 (2017) 74-83.

[25] K.Y. Nandiwale, A.M. Danby, A. Ramanathan, R.V. Chaudhari, B. Subramaniam, Zirconium-Incorporated Mesoporous Silicates Show Remarkable Lignin Depolymerization Activity, ACS Sustainable Chemistry and Engineering, 5 (2017) 7155-7164.

[26] C. Rodríguez Correa, M. Stollovsky, T. Hehr, Y. Rauscher, B. Rolli, A. Kruse, Influence of the Carbonization Process on Activated Carbon Properties from Lignin and Lignin-Rich Biomasses, ACS Sustainable Chemistry and Engineering, 5 (2017) 8222-8233.

[27] N. Meek, D. Penumadu, O. Hosseinaei, D. Harper, S. Young, T. Rials, Synthesis and characterization of lignin carbon fiber and composites, Composites Science and Technology, 137 (2016) 60-68.

[28] J. Pang, W. Zhang, J. Zhang, G. Cao, M. Han, Y. Yang, Facile and sustainable synthesis of sodium lignosulfonate derived hierarchical porous carbons for supercapacitors with high volumetric energy densities, Green Chemistry, 19 (2017) 3916-3926.

[29] I. Kurnia, A. Yoshida, Y.A. Situmorang, Y. Kasai, A. Abudula, G. Guan, Utilization of dealkaline lignin as a source of sodium-promoted MoS_2/Mo_2C hybrid catalysts for hydrogen production from formic acid, ACS Sustainable Chemistry & Engineering, 7 (2019) 8670-8677.

[30] N. Srisasiwimon, S. Chuangchote, N. Laosiripojana, T. Sagawa, TiO_2/Lignin-Based Carbon Composited Photocatalysts for Enhanced Photocatalytic Conversion of Lignin to High Value Chemicals, ACS Sustainable Chemistry and Engineering, 6 (2018) 13968-13976.

[31] I. Kurnia, A. Yoshida, N. Chaihad, A. Bayu, Y. Kasai, A. Abudula, G. Guan, Hydrolysis of cellulose and woody biomass over sustainable weak-acid carbon catalysts from alkaline lignin, Fuel Processing Technology, 196 (2019) 106175-106175.

[32] Y. Zheng, W. Zheng, D. Zhu, H. Chang, Theoretical modeling of pKa's of thiol compounds in aqueous solution, New Journal of Chemistry, 43 (2019) 5239-5254.

[33] Dissociation constants of organic acids and bases, in: D.R. Lide (Ed.), CRC Press, Boca Raton, FL, 2005, pp. 46-56.

[34] M. Vandichel, F. Vermoortele, S. Cottenie, D.E. De Vos, M. Waroquier, V. Van Speybroeck, Insight in the activity and diastereoselectivity of various Lewis acid catalysts for the citronellal cyclization, Journal of Catalysis, 305 (2013) 118-129.

[35] T. Yamamoto, H. Ujihara, S. Watanabe, M. Harada, H. Matsuda, T. Hagiwara, Synthesis and odor of optically active trans-2,2,6-trimethylcyclohexyl methyl ketones and their related compounds, Tetrahedron, 59 (2003) 517-524.

[36] R.M. West, M.S. Holm, S. Saravanamurugan, J. Xiong, Z. Beversdorf, E. Taarning, C.H. Christensen, Zeolite H-USY for the production of lactic acid and methyl lactate from C_3-sugars, Journal of Catalysis, 269 (2010) 122-130.

[37] A. Corma, M. Renz, Sn-Beta zeolite as diastereoselective water-resistant heterogeneous Lewis-acid catalyst for carbon–carbon bond formation in the intramolecular carbonyl–ene reaction, Chemical Communications, 4 (2004) 550-551.

Chapter 6 Conclusions and Future Perspectives

Lignin is an important component of biomass and the largest renewable aromatic source for chemicals, fuels, and functional materials. The largest commercial lignin product is from the pulp and paper industries. The utilization of lignin wastes would solve the environmental issues related to the reduction of environmental impacts of the paper-making process. Various thermochemical processes for the converting of lignosulfonate lignin into high-value-added chemical and material have been developed. Catalytic upgrading of bio-oil derived from lignin is a way to get high-value-added chemicals and fuels. Many researches employed *Py*-GC-MS to screen the catalysts during the catalytic pyrolysis and catalytic upgrading process. However, the ratio of catalyst-to-biomass in *Py*-GC-MS was too high and simultaneously the coke and char products cannot be distinguished since they were mixed with the catalyst together in the final product. We have presented the laboratory scale of catalytic upgrading bio-oil derived from lignin by using five types of high aluminum zeolites i.e., H-Ferrierite, H-Mordenite, H-ZSM-5, H-Beta and H-USY zeolites with the lower ratio of catalyst loading ratio compared to the *Py*-GC-MS process. It is found that the channel structure, pore sizes and acidity of zeolite had great effect on the product distribution, coke formation, and deoxygenation. Among the high aluminum zeolites, H-ZSM-5 showed the highest performance to produce the high yield of aromatic hydrocarbon. Furthermore, the modification of H-ZSM-5 catalyst by metal doping on the structure of ZSM-5 structure like Mo-incorporated ZSM-5, should be considered to improve catalytic activity, selectivity, and stability of catalytic upgrading of lignin bio-oil. In addition, since reductive gaseous will be produced, i.e. CO, CH_4, and H_2 under the high temperature and would activate the molybdenum species to improve catalytic activity of the H-ZSM-5 catalyst. However, one-step catalytic pyrolysis process is not

really effective for converting lignin to fuel or chemicals, since the low yield of monomeric product. To improve the yield, some pretreatment processes such as mechanical, chemical, physio-chemical or biological pretreatment are generally needed since these ways could enhance the decomposition of the polymeric lignin. Especially, those pretreated lignins could be processed at lower temperatures in the catalytic pyrolysis process to get larger amount of bio-oil from lignin. Furthermore, the bio-oil product could be treated by catalytic hydroprocessing to obtain more monomeric products, which can be used as high-quality fuels or chemicals. In this case, it is very important to develop non-precious metal catalysts for catalytic hydroprocessing in the future.

The problem that we found on the fast pyrolysis of lignosulfonate lignin is the high amount of char in the final product (52.2 wt.%). However, it can be utilized as the alternative of functional carbon material such as catalyst precursors or carbon acid catalysts material. Thus, the utilization of lignisulfonate lignin is not only limited by the lignin conversion to the fuel and chemical products. In our research, lignosulfonate lignin or dealkaline lignin (DAL) contains carbon (C), sulfur (S), and some sodium metal species as impurities, and we utilized it as precursor to prepare MoS_2/Mo_2C based catalysts (Mo-DAL) and also promoted the catalytic activity for the hydrogen production from the formic acid decomposition. The comparison study of the catalytic performance of the Mo-DAL catalyst with the carbon black-based one (Mo_2C-CB) revealed that the Mo-DAL catalyst exhibited superior activity to the Mo_2C-CB catalyst, since multiple kinds of active sites such as Na-intercalated MoS_2, MoS_2, and β-Mo_2C were formed on the Mo-DAL catalysts, which should be worth to investigating since the MoS_2 and β-Mo_2C can be widely applied in hydogen production by using the steam reforming of biomass and steam reforming of metanol, or used for battery, supercapacitor, and water-spliting. Furthermore, the introducing nitrogen source such as melamine for the synthesis nitrogen-doped carbon supported catalysts

should be attractive for promotion of the catalytic activity of lignin-derived catalysts for hydrogen production process.

Meanwhile, the nature structure of neutralized lignosulfonate lignin (alkaline lignin, pH 10) contains the phenolic hydroxyl groups, carboxyl groups, and SO_3H groups. In our research, a low-cost and sustainable weak-acid carbon catalysts were prepared from alkaline lignin (AL) by low temperature pyrolysis of AL to keep the acid functional groups followed by an acid solution treatment process to remove alkaline metal impurities. The sustainable carbon catalysts derived from alkaline lignin (AL) shows a high activity for cellulose hydrolysis to produce glucose and also for cyclization-hydration of citronellal to produce *p*-menthane-3,8-diol. However, the selectivity contribution of various acid sites groups (oxygenated functional group and sulfur functional group) on alkaline lignin-derived carbon catalysts are still unclear in the cyclization-hydration of citronellal to produce *p*-menthane-3,8-diol. Further, the confirmation of each specific acid functional group on carbon catalyst toward product selectivity of the cyclization-hydration of citronellal are necessary to known. In addition, the low surface area of AL-derived carbon acid catalyst is needed to improve. In preparation method, the additional treatment of AL with melamine and formaldehyde could increase the surface area of the carbon catalyst due to the formation of cross-link between lignin, melamine, and formaldehyde, which is worth to investigating in the future. Meanwhile, since the presence of acid sites on the AL-derived carbon catalysts, the utilization of AL-derived carbon catalysts for other reactions related to biorefinery processes such as isomerization, esterification, dehydration, and hydration should be considered.

List of Publication

List of publication in SCI journals:

1. **Irwan Kurnia**, Akihiro Yoshida, Nichaboon Chaihad, Asep Bayu, Yutaka Kasai, Abuliti Abudula, and Guoqing Guan, Hydrolysis of Cellulose and Woody Biomass over Sustainable Weak-Acid Carbon Catalysts from Alkaline Lignin, *Fuel Processing Technology*, 196 (2019) 106175.
2. **Irwan Kurnia**, Akihiro Yoshida, Yohanes Andre Situmorang, Yutaka Kasai, Abuliti Abudula, and Guoqing Guan, Utilization of Dealkaline Lignin as a Source of Sodium-Promoted MoS_2/Mo_2C Hybrid Catalysts for Hydrogen Production from Formic Acid, *ACS Sustainable Chemistry & Engineering*, 7 (2019) 8670–8677.
3. **Irwan Kurnia**, Surachai Karnjanakom, Asep Bayu, Akihiro Yoshida, Jenny Rizkiana, Tirto Prakoso, Abuliti Abudula, and Guoqing Guan, *In-situ* catalytic upgrading of bio-oil derived from fast pyrolysis of lignin over high aluminum zeolites, *Fuel Processing Technology*, 167 (2017) 730-737.
4. Nichaboon Chaihad, **Irwan Kurnia**, Akihiro Yoshida, Chuichi Watanabe, Koji Tei, Prasert Reubroycharoen, Yutaka Kasai, Abuliti Abudula, and Guoqing Guan, Catalytic pyrolysis of wasted fishing net over calcined scallop shells: Analyical Py-GC/MS study, *Journal of Analytical and Applied Pyrolysis*, (2019) 104750.
5. Nichaboon Chaihad, Surachai Karnjanakom, **Irwan Kurnia**, Akihiro Yoshida, Abuliti Abudula, Prasert Reubroycharoen, and Guoqing Guan, *In-situ* catalytic upgrading of bio-oils derived from fast pyrolysis of cellulose, hemicellulose, and lignin over various zeolites, *Journal of the Japan Institute of Energy*, 98 (2019), 254-258.

6. Nichaboon Chaihad, Surachai Karnjanakom, **Irwan Kurnia**, Akihiro Yoshida, Abuliti Abudula, Prasert Reubroycharoen, and Guoqing Guan, Catalytic upgrading of bio-oils over high-alumina zeolites, *Renewable Energy*, 136 (2019) 1304-1310.
7. Surachai Karnjanakom, Akihiro Yoshida, Asep Bayu, **Irwan Kurnia**, Xiaogang Hao,Panya Maneechakr, Abuliti Abudula, and Guoqing Guan, Bifunctional Mg-Cu-Loaded β-Zeolite: High Selectivity for the Conversion of Furfural into Monoaromatic Compounds, *ChemCatChem*, 10 (2018) 3564-3575.
8. Surachai Karnjanakom, Akihiro Yoshida, Wahyu Bambang Widayatno, Asep Bayu, **Irwan Kurnia**, Xiaogang Hao, Panya Maneechakr, Abuliti Abudula, and Guoqing Guan, Selective deoxygenation of carboxylic acids to BTXs over Cu/β-zeolite prepared by ethylene glycol-assisted impregnation, *Catalysis Communications*, 110 (2018) 33-37.

List of papers presented in conferences:

International Conferences:

1. **Irwan Kurnia**, Akihiro Yoshida, AbulitiAbudula, Guoqing Guan, Formic Acid Decomposition for Hydrogen Production over Molybdenum Based Catalyst Supported on Lignin-derived Carbons, *The 8th Tokyo Conference on Advanced Catalytic Science and Technology (TOCAT8),* Yokohama, Japan, Aug.5-10, 2018.
2. **Irwan Kurnia**, Surachai Karnjanakom, Asep Bayu, Akihiro Yoshida, Katsuki Kusakabe, Abuliti Abudula, Guoqing Guan, Catalytic upgrading of bio-oil from fast pyrolysis of lignin over high aluminum zeolites, *The 30th International Symposium on Chemical Engineering* at KAIST, Daejeon, South Korea, Dec.1-3, 2017.
3. Nichaboon Chaihad, Surachai Karnjanakom, **Irwan Kurnia**, Akihiro Yoshida, Abuliti Abudula, Prasert Reubroycharoen, Guoqing Guan, Catalytic Upgrading of Bio-Oils Derived from Cellulose, Hemicellulose, Lignin and Sunflower Stalk over Various Zeolites, *5th Asian Conference for Biomass Science* at Tohoku University, Jan. 17, 2018, Sendai, Japan.

Domestic Conferences:

1. **Irwan Kurnia**、Yohanes Andre Situmorang、吉田 曉弘、阿布 里提、官 国清、 葛西 裕、Synthesis p-menthane-3,8-diol over sustainable acid carbon catalysts derived from alkaline lignin. *化学工学会第84年会*、芝浦工業大学、東京 2019 年 3 月 13-15 日.
2. Zhongliang Yu, **Irwan Kurnia**, Xiaowei An, Akihiro Yoshida, Abuliti Abudula, Guoqing Guan, Selective dehydration of formic acid with Mo_2N catalysts at low temperatures, *第122回触媒討論会* in 北海道教育大学、函館、2018 年 9 月 26−28 日.

3. **Irwan Kurnia**, 吉田 暁弘, 阿布 里提, 官国清, リグニンを炭素源として製造したモリブデン触媒上でのギ酸分解反応, *化学工学会第 83 年会*, 関西大学千里山キャンパス, 大阪, 2018 年 3 月 13－15 日。
4. **Irwan Kurnia**, 吉田曉弘, 于涛, 阿布里提, 葛西裕, 官国清, Formic acid decomposition for hydrogen production over molybdenum carbide prepared by using lignin as the carbon source, 第 13 回バイオマス科学会議, 東北大学, 仙台, 2018 年 1 月 17-18 日.
5. **Irwan Kurnia**, Akihiro Yoshida, Abuliti Abudula, Guoqing Guan, Catalytic upgrading of bio-oil derived from lignin over metal-modified ZSM-5 zeolites, *平成 29 年度化学系学協会東北大会*,岩手大学,盛岡市, 2017 年 9 月 16－17 日.
6. **Irwan Kurnia**, Akihiro Yoshida, Abuliti Abudula, Guoqing Guan, Catalytic upgrading of bio-oil derived from lignin over metal-modified ZSM-5 zeolites, *H29 年度 4 校交流会*, 八戸市,2017 年 9 月 15 日.
7. **Irwan Kurnia**, Abudukeranmu Abulikem, 吉田曉弘, 阿布里提,官国清, 高アルミニウムゼオライトを用いたリグニン由来のバイオオイルの脱酸素化, *第 26 回日本エネルギー学会大会*,名古屋ウィンクあいち, 2017 年 8 月 1 日－8 月 2 日.

Curriculum Vitae

Personal Details

Full Name : Irwan Kurnia

Nationality : Indonesian

Education Background

Period	Name of School/University	Location	Major
Apr 2017 - Mar 2020	Hirosaki University	Hirosaki, Japan	Safety System Engineering
Aug 2011 – June 2013	Institut Teknologi Bandung	Bandung, Indonesia	Chemical Engineering
Aug 2005 – July 2009	Padjadjaran University	Jatinangor, Indonesia	Chemistry

Industrial Work Experiences

Period	Name of Company	Address	Position
Jan 2010 - Mar 2011	PT. Kao Indonesia Chemicals	Jl. Raya Tambun KM. 42 Bekasi 17510, Indonesia	Research and Development (Synthesis & Functional Surfactant)
May 2014 – Aug 2015	PT. Indesso Aroma	Jl. Alternatif Cibubur-Cileungsi KM. 9, Indonesia	Research and Development (Scale-up & Synthesis of Essential Oil Derivative)

Academic Work Experiences

Period	Institutions	Address	Position
Sept 2008 - Mar 2009	Organic Chemistry Laboratory	Padjadjaran University, Indonesia	Academic Assistant
Nov 2013 - Jan 2014	Chemical Engineering Program	Institut Teknologi Bandung, Indonesia	Academic Assistant Mass & Energy Balance (Dr. Tirto Prakoso)
Feb 2014 – Apr 2014	Oil & Fat Laboratory	Institut Teknologi Bandung, Indonesia	Academic Assistant for Laboratory Practice (Dr. Tirto Prakoso)
July 2013 – Apr 2014	Oil & Fat Laboratory	Institut Teknologi Bandung, Indonesia	Researcher , Commissioning & Start-Up Staff • Biodiesel from Waste Cooking Oil PT. Pertamina Hulu Energi ONWJ Project • Extraction Carotenoid from CPO PT. Pupuk Kaltim Project
Oct 2015 – Jan 2016	Chemical Engineering Program	Institut Teknologi Bandung, Indonesia	Academic Assistant for New Department of Bioenergy and Chemurgy
Oct 2015 – July 2016	Chemical Engineering Program	Institut Teknologi Bandung, Indonesia	Academic Assistant for ABET Certification

Scholarship

Period	Sponsor	Purpose
Oct 2016 - Mar 2019	Ministry of Education, Culture, Sports, Science and Technology (MEXT) (Monbukagakusho), Japanese Government	Study for PhD course